University of Crete
Department of Computer Science

FO.R.T.H.
Institute of Computer Science

Location Sensing via Sparse and Low Rank Signal Models

Sofia Nikitaki

A thesis submitted for the degree of Doctor of Philosophy

Heraklion, July 2014

UNIVERSITY OF CRETE
DEPARTMENT OF COMPUTER SCIENCE

Location Sensing via Sparse and Low Rank Signal Models

Dissertation submitted by

Sofia Nikitaki

in partial fulfillment of the requirements for the
Doctor of Philosophy degree in Computer Science

Author: _____
Sofia Nikitaki

Examination Committee: _____
Panagiotis Tsakalides, Professor - Advisor, Dept. of Computer Sc., Univ. of Crete

_____
Apostolos Traganitis, Professor, Dept. of Computer Sc., Univ. of Crete

_____
Maria Papadopouli, Associate Professor, Dept. of Computer Sc., Univ. of Crete

_____
Athanasios Mouchtaris, Assistant Professor, Dept. of Computer Sc., Univ. of Crete

_____
George Tsihrintzis, Professor, Dep. of Computer Sc. Univ. of Piraeus

_____
Baltasar Beferull-Lozano, Associate Professor, Universidad de Valencia

_____
Kristof Van Laerhoven, Research Group Leader, Tech. Univ. of Darmstadt

Depart. approval: _____
Panos Traxanias, Professor, Chairman of the Department

Heraklion, July 2014

...to my dancing partner in life

Acknowledgements

First and foremost I would like to express my deepest thanks to my advisor Prof. Panagiotis Tsakalides for the continuous support during my Ph.D study and research, for his guidance and motivation. Prof. Tsakalides encouraged me to grow as a researcher, he gave me the opportunity to develop my own individuality by supporting me to work and collaborate with different institutes. He is a great mentor.

I would like to thank the members of the Phd committee Prof. Maria Papadopouli and Prof. Athanasios Mouchtaris for the useful discussions and suggestions the last four years. Moreover, I would like to thank Dr. Kristof Van Laerhoven and the Embedded Sensing Systems group at the Technical University of Darmstadt for their hospitality and for providing their hardware and valuable insights during the last part of my Phd.

Additionally, especial thanks to Dr. Gregory Tsagkatakis for the productive discussions and his contributions the last two years. Moreover, I would like to thank all the members of the Telecommunications Networks Laboratory and Signal Processing Laboratory at FORTH. Specifically I would like to thank Dr. Stefano Papadakis for his contribution in the experimental setup in the premises of ICS-FORTH.

Of course no acknowledgements would be complete without thanking my parents, Dimitris and Aggeliki. Both have instilled any admirable qualities in me, provided me with self-respect and personal strength. Moreover, I would like to thank my big sister Vicky, who always boosts my confidence and makes me smile.

Last, I must acknowledge with tremendous and deep thanks Kostas. His love, patience and support helped me all these years.

Abstract

Location and mobility management are major functions and essential features for seamless and ubiquitous environments. Self-organizing sensor networks, health care monitoring, personal tracking and context dependent information services are some of the potential applications. Received signal strength (RSS) fingerprinting is a highly accurate location technique that has the major advantage of exploiting already existing infrastructure to avoid additional deployment costs. Fingerprint based localization systems adopt a calibration phase in order to create signature maps that represent the physical space by capturing the variations of the dynamic nature of indoor propagation. These maps, or fingerprints, are compared to the RSS at the runtime phase in order to perform localization.

This thesis explores the notion of sparsity and reformulates the problem of user localization as a sparse approximation problem. The proposed fingerprint-based localization techniques adopt the Compressed Sensing (CS) framework, which provides a new paradigm for recovering signals being sparse in some basis by means of a limited amount of randomly received measurements. Specifically, exploiting the observation that the base stations receive correlated signals from the mobile devices, we propose two CS-based algorithms: a centralized and a decentralized one. According to the centralized Jointly CS scheme all local runtime measurements received from the mobile device are sent to a central unit to perform location estimation. On the contrary, the decentralized scheme builds upon gossip consensus based approaches to distribute decision estimations in the network.

Although fingerprint CS-based systems achieve high accuracy, issues that concern both the calibration and the location estimation phases can potentially limit the accuracy and scalability of these systems. Concerning the automation of the calibration phase required by fingerprint based systems, we propose a wireless localization and laser-scanner assisted Fingerprinting system that provides autonomous signature map generation. During the location estimation phase, the system mitigates the existing problems adopting a Bayesian formal-

ism that incorporates a sparsity prior and dynamically determines the sufficient number of runtime measurements required for accurate positioning.

Further challenges related to typical fingerprint-based schemes arise since it is implicitly assumed that communication occurs over the same frequency channel during the training and the runtime phases. When this assumption is violated, the mismatches between training and runtime fingerprints can significantly deteriorate the localization performance. Additionally, the exhaustive calibration procedure required during training limits the scalability of this class of methods, especially in the case where no additional hardware is utilized. To address these limitations, we propose a novel fingerprint collection technique without the need of additional hardware that significantly reduces the calibration time by pseudo-random channel sampling. The sub-sampled signature map is reconstructed as an instance of the Matrix Completion problem.

Finally, we propose a reduced effort recalibration technique for fingerprint-based indoor positioning systems. The proposed method exploits the dynamic characteristics of an indoor environment and considers that a sub-set of measurements may explicitly depend on past measurements. Particularly, we minimize the number of RSS fingerprints by performing pseudo-random sub-sampling in space. The proposed framework exploits the spatial correlation structure of the RSS fingerprints while considering prior information provided from previously observed measurements, to reconstruct the signature map.

Extended abstract in Greek

Η εκτίμηση της θέσης ενός χρήστη και η διαχείριση της κινητικότητας του αποτελούν βασικά χαρακτηριστικά για τη δημιουργία έξυπνων χώρων. Τα έξυπνα δίκτυα αισθητήρων με ικανότητα αυτό-οργάνωσης, η παρακολούθηση ασθενών και η περιήγηση σε εσωτερικούς ή εξωτερικούς χώρους είναι ορισμένες από τις εφαρμογές που απαιτούν την ικανότητα για εύρεση θέσης. Τεχνικές εντοπισμού θέσης που χρησιμοποιούν την ένταση του λαμβανόμενου σήματος μιας κινητής συσκευής σε κάποιο δεδομένο χώρο έχουν το σημαντικό πλεονέκτημα ότι εκμεταλλεύονται τις ήδη υφιστάμενες υποδομές και αποφεύγουν το πρόσθετο κόστος εγκατάστασης νέου εξοπλισμού. Τα συστήματα εντοπισμού θέσης με βάση μετρήσεις της έντασης σήματος υιοθετούν μια αρχική διαδικασία εκπαίδευσης προκειμένου να δημιουργήσουν χάρτες υπογραφών έντασης σήματος που αντιπροσωπεύουν το φυσικό χώρο και καταγράφουν τις διακυμάνσεις του δυναμικού χαρακτήρα της διάδοσης σήματος. Στη συνέχεια, κατά τη φάση της εκτίμησης θέσης, οι χάρτες αυτοί χρησιμοποιούνται ως βάσεις σύγκρισης με τις τρέχουσες μετρήσεις έντασης σήματος ώστε να εντοπιστεί ο χρήστης.

Σε αυτή τη διατριβή, διερευνάται η έννοια της αραιότητας της θέσης του χρήστη στο χώρο ώστε το πρόβλημα εκτίμησης θέσης να μοντελοποιηθεί ως ένα πρόβλημα αραιής προσέγγισης. Οι προτεινόμενες τεχνικές εντοπισμού βασίζονται στα ίχνη του λαμβανόμενου σήματος κι υιοθετούν τεχνικές συμπιεσμένης δειγματοληψίας (*compressed sensing*). Οι τεχνικές συμπιεσμένης δειγματοληψίας παρέχουν ένα νέο πρότυπο για την ανάκτηση σημάτων που είναι αραιά σε κάποια βάση, μέσω ενός περιορισμένου πλήθους τυχαία λαμβανομένων μετρήσεων. Συγκεκριμένα, αξιοποιώντας την παρατήρηση ότι οι σταθμοί βάσης λαμβάνουν συσχετισμένα σήματα από τις κινητές συσκευές, προτείνουμε δύο αλγορίθμους: έναν κεντρικό και έναν κατανεμημένο. Σύμφωνα με τον κεντρικό αλγόριθμο όλες οι τοπικές μετρήσεις που λαμβάνονται από την κινητή συσκευή αποστέλλονται σε μία κεντρική μονάδα ώστε να εκτιμηθεί η θέση του χρήστη. Αντίθετα,

το κατανεμημένο σύστημα βασίζεται σε αλγορίθμους κοινής συναίνεσης για τη διανομή των εκτιμήσεων θέσης σε όλο το δίκτυο.

Τα συστήματα που χρησιμοποιούν χάρτες έντασης σήματος και υιοθετούν τεχνικές συμπιεσμένης δειγματοληψίας επιτυγχάνουν υψηλή ακρίβεια. Ωστόσο, παρουσιάζουν θέματα τα οποία μπορούν δυνητικά να περιορίσουν την ακρίβεια και την επεκτασιμότητα τους. Για να επιταχύνουμε την διαδικασία εκπαίδευσης, προτείνουμε την αυτοματοποίηση της μέσω ενός συστήματος που χρησιμοποιεί λέιζερ σαρωτή για τη λήψη ιχνών έντασης σήματος στο χώρο. Κατά τη διάρκεια της εκτίμησης θέσης, το σύστημα μας υλοποιεί μία Μπεϋζιανή τεχνική όπου η υπόθεση αραιού σήματος ανάγεται στη μοντελοποίηση της στατιστικής κατανομής του μέσω μιας εκ των προτέρων κατανομής πιθανότητας καθορίζοντας δυναμικά τον επαρκή αριθμό των μετρήσεων που απαιτούνται για την ακριβή εκτίμηση θέσης του χρήστη.

Υπάρχοντα συστήματα που βασίζονται σε ίχνη σήματος υποθέτουν ότι η κινητή συσκευή επικοινωνεί στο ίδιο κανάλι συχνότητας κατά τη διάρκεια των φάσεων εκπαίδευσης και εκτίμησης. Όταν αυτή η υπόθεση παραβιάζεται, οι αναντιστοιχίες μεταξύ των χαρτών έντασης σήματος των φάσεων εκπαίδευσης και εκτίμησης μπορεί να επιδεινώσει σημαντικά την απόδοση. Επιπρόσθετα, σε δυναμικά περιβάλλοντα απαιτείται μία εξαντλητική διαδικασία βαθμονόμησης κατά τη διάρκεια της φάσης εκπαίδευσης γεγονός που περιορίζει την εφαρμογή αυτών των μεθόδων, ιδιαίτερα στην περίπτωση όπου δεν χρησιμοποιείται επιπρόσθετος εξοπλισμός.

Για την αντιμετώπιση αυτών των περιορισμών, προτείνουμε μια νέα τεχνική συλλογής ιχνών έντασης σήματος που βασίζεται στη ψευδοτυχαία δειγματοληψία καναλιού η οποία μειώνει σημαντικά το χρόνο εκπαίδευσης. Σε αυτή τη περίπτωση, ο λαμβανόμενος υπό-δειγματοληπτημένος χάρτης ιχνών σήματος αναδομείται μέσω τεχνικών συμπλήρωσης πίνακα (*matrix completion*) χαμηλής τάξης. Η προτεινόμενη μέθοδος αξιοποιεί τα δυναμικά χαρακτηριστικά του περιβάλλοντος και θεωρεί ότι πρόσφατες μετρήσεις συσχετίζονται άμεσα με παρελθοντικές μετρήσεις. Πιο συγκεκριμένα, βελτιστοποιούμε τη διαδικασία δειγματοληψίας υιοθετώντας ψευδοτυχαία υποδειγματοληψία στο χώρο. Η προτεινόμενη τεχνική εκμεταλλεύεται τη συσχέτιση των λαμβανόμενων σημάτων στο χώρο εξετάζοντας παράλληλα προηγούμενες πληροφορίες που παρέχονται από παρελθοντικές μετρήσεις ώστε να ανακατασκευάσει τον υπό-δειγματοληπτημένο χάρτη ιχνών.

Contents

List of Figures

List of Tables

Chapter 1

Introduction

The father of ubiquitous computing, M. Weiser, pioneered in 1993 the idea of exploiting location information in order to create a new user experience. During the last 20 years astonishing progress has been made in wireless communication and technological developments. In particular, the innovative technological developments in the sensing capabilities of smart phones have redefined the notion of location awareness and mobile computing. Pervasive and ubiquitous computing requires location and mobility management for mobile devices in order to provide location dependent context.

Location awareness is essential for defining and documenting the mobile Internet and the associated infrastructure enabling location-based services. The pillar of the future internet, the Internet of Things (IoT), depends on location information sharing to support a future ambient lifestyle where everything and everyone could be interconnected everywhere and every time. According to [1], in February 2012, almost three-quarters (74%) of the smart phone owners used their devices for directions queries and other location-related information (up from 55% in May 2011). Mobile aware devices play an important role in the fields on emergency response, disaster management, environmental sampling and location marketing.

Indoor positioning systems have become very popular in recent years as a great percentage of our everyday life evolves indoors. Great advantages of satellite based positioning systems, such as Global Positioning System (GPS) [2], COMPASS [3] and Galileo [4], have been operated for personal navigation the last few years. Although satellite based localization systems have attracted various outdoor applications, its accuracy in indoor environments is considerably reduced due to the lack of the desirable line-of-sight (LoS). The inability of radio signals to penetrate most buildings leads to the so-called urban canyon effect, where GPS efficiency is expunged as the satellite signals suffer from multi-path reflections. Additionally, wireless phone service providers supply a different wide-area location technology that utilizes cell tower observations of smart phones for position estimation. Specifically, Europe and US governments require the providers to locate emergency phone calls to within

100m. To meet this constraint, providers utilize a variety of techniques, including sophisticated signal propagation models and augmentation of handsets with GPS.

In the last year, the research community has focused its attention to determine systems that do not require any additional hardware. From a network perspective, IEEE 802.11 is the dominant local wireless networking standard, as more and more 802.11-compatible access points (APs) are installed in a large number of buildings. This extensive deployment and availability of infrastructure make the IEEE 802.11 appealing for positioning purposes. Furthermore, by leveraging the spatial proximity of APs in an area, installation cost can be significantly reduced [5].

1.1 Measuring principles and positioning algorithms

A typical localization scenario involves a set of Base Stations (BSs) placed at known positions and a Mobile Station (MS) that needs to be located. The BSs can be network enabled devices such as wireless mesh routers, wireless Access Points (AP), and sensor nodes, while the MS is a mobile device, such as a smartphone. The actual localization can be performed either at a central unit or at the mobile device. Certain localization schemes utilize the information from the BSs and require the MS to compute its own position, while other schemes utilize information from the MS to compute the location of the user remotely at the Localization Server (LS) [6]. (c.f Figure 1.1)

A critical issue regarding the design of localization schemes is the type and the characteristics of the measurements that are going to be used in the task. According to the wireless communication protocol, communication packets are exchanged between the MS and the APs. Considering the physical waveforms of the exchanged packets, signal metrics are extracted to estimate the physical distance between the transmitter and the receiver. Typically, the efficiency of location estimation depends on the range of the measurement technique.

The distance between the receiver and the transmitter can be derived by multiplying the radio signal velocity and the travel time. Particularly, the time of arrival (TOA) based systems extract the distance information with respect to at least three received signals. Time difference of arrival (TDOA) systems, as opposed to TOA, utilize the time range difference between multiple signals to extract the distance information. Time based systems require synchronization of the measurement unit and additional hardware for time-stamp labeling of the transmitting signal (c.f Figure 1.2(a)).

Measuring the power of the received signals, the so-called Received Signal Strength (RSS), provides an abundant, reliable, and straightforward source of data. Naturally, the power, and therefore the RSS, are affected by various factors in the propagation medium, the most significant of which is the distance between the transmitter and the receiver (c.f Figure 1.2(b)). While one could simply compare the power of the received signal with the known transmission power in order to extract distance information, the layout and dynamics of physical spaces make the problem dramatically more challenging, as signal power

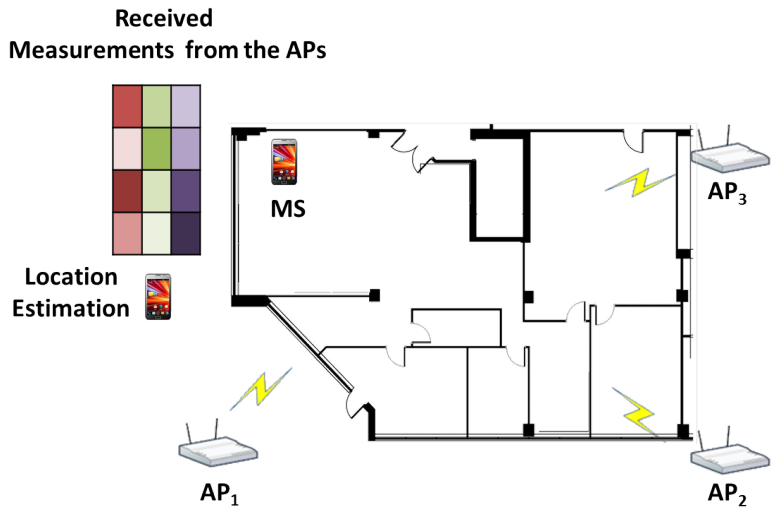

(a)

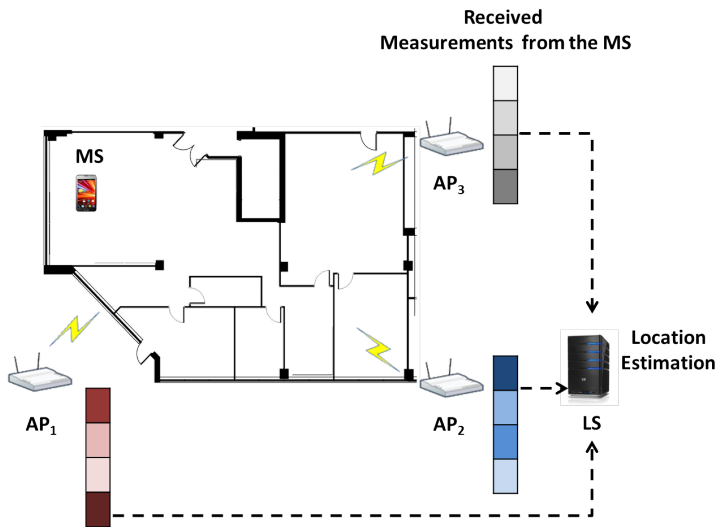

(b)

FIGURE 1.1: (a) Local location sensing. The mobile device captures the measurements transmitted from the access points and performs location estimation. (b) Remote location sensing. The location server estimates remotely the location of the user.

attenuation is heavily dependent on obstacles such as walls and people. For this purpose, theoretical and empirical path loss models are utilized to calculate the signal path loss due to propagation. (RSS)-based methods, as opposed to traditional time of arrival exploit the ex-

isting wireless infrastructure and avoid the additional cost of deploying localization-specific hardware.

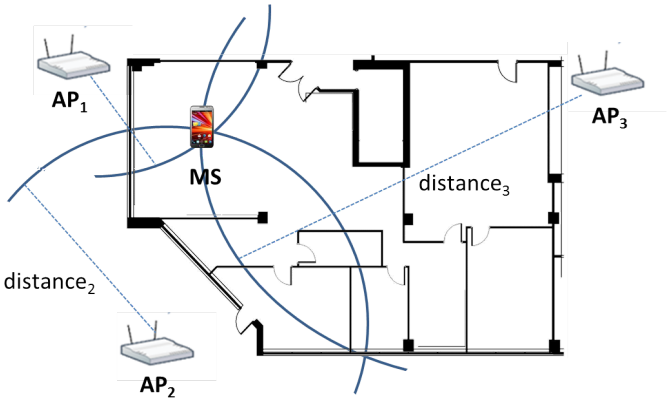

(a)

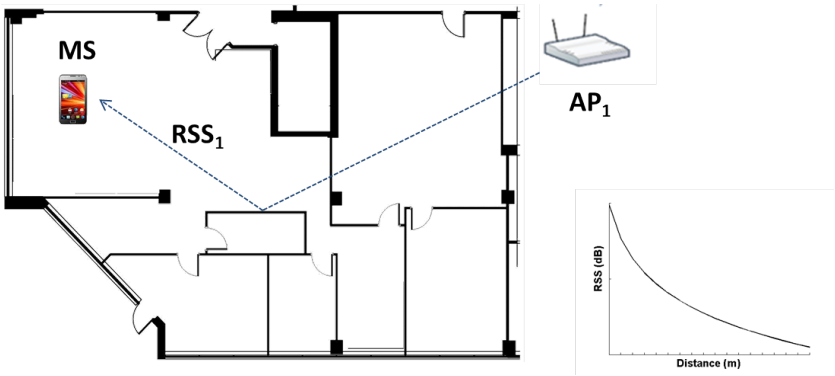

(b)

FIGURE 1.2: (a) Location estimation based on TDOA (b) Location estimation based on RSS.

In addition to the type of measurements, the efficient processing of the data using a robust localization algorithm is equally important. *Triangulation* and *scene analysis* are the two principal techniques for location sensing. Triangulation or *distance-based* methods estimate the position of the mobile user by computing its distance from at least three reference points [7, 8, 9, 10]. The RSS measurements are translated to distance by applying theoretical or empirical path-loss models. The main challenge arising in these systems is the difficulty to formulate a reliable pathloss model due to multipath, fading, shadowing, and the presence of countless objects (*e.g.*, walls, obstacles, floor layout, and moving objects), significantly deviating from the ideal LoS conditions. As a consequence, distance-based

methods typically exhibit large localization errors.

To address this difficulty, *scene analysis* or *fingerprinting* techniques build training or signature maps to represent the physical space by capturing the variations of the dynamic nature of indoor propagation [11]. To build a training map, an extensive calibration process is mandatory, where RSS fingerprints are collected at every possible location [12, 13]. Although fingerprint-based systems achieve high performance in terms of localization, the time and effort required during the training phase remain a major disadvantage. Naturally, training will be even more expensive and time consuming in multi-channel wireless environments, where a signature map will consist of representative fingerprints at each possible spatial position and for every operational frequency. Furthermore, for accurate positioning, a recalibration procedure is mandatory every time that environmental changes occur in the area of interest.

1.2 Performance Metrics

The performance benchmarks associated with localization systems, such as accuracy, precision, complexity, scalability, robustness and cost are essential criteria that determine the effectiveness of the system. Naturally, the accuracy of a system, typically measured by the mean location error, is the important user requirement. The accuracy or the area of uncertainty is reported as the error distance, typically in Euclidean space, between the estimated and the actual location of the mobile station. The higher the accuracy the better the localization system; however there is often a tradeoff between the desired location error and other characteristics. Location precision is an essential measure of the robustness of the positioning system as it reveals the variation in its performance over many trials. The cumulative distribution functions (CDF) of the location error is the commonly adopted metric for validating the effectiveness of the system.

The complexity of the system depends on the hardware, the software and various operation factors. Performing the localization at the LS offers various benefits including lower power consumption at the mobile device and the ability to perform computationally demanding high level reasoning. This is important since, in spite of improvements in energy consumption, battery capacity grows slowly and power management is still a challenge in mobile computing. Moreover, remote location estimation facilitates the installation, maintenance, and management of the service.

Additionally to the low complexity, robust indoor localization systems function with high accuracy to different communication channels, non-stationary environments, incomplete runtime measurements and damaged hardware. Moreover, the scalability of a system ensures accurate positioning performance in cases of a large indoor application area. Positioning performance degradates as the distance between the mobile device and the AP increases and thus an adequate number of APs must be considered in order to ensure wireless coverage of the area.

Dynamic indoor environmental changes may affect the localization performance. Adaptiveness is defined as the effectiveness of the localization system to cope with unpredictable changes. An adaptive system that provides better localization accuracy will prevent the need for repeating the exhaustive and highly (costed) expensive calibration. The cost of a positioning system can emanate from the use of extra infrastructure, additional bandwidth, money, lifetime, weight, energy, and nature of deployed technology. The cost may include installation and survey time during the deployment period.

1.3 Location based applications

The rapid expansion of wireless networks combined with the high penetration of mobile devices has led positioning systems to become very popular nowadays. Localization is one of the key aspects of any wireless network as it enables a vast array of services; most notably in context-aware applications and in enhancing network protocols.

Context-aware applications introduce information concerning the operating environment, such as location, activity of people, and/or the presence/state of other devices. Specifically, location based services, location sensitive content delivery, direction finding, asset tracking, teleporting, robotics, emergency notification, environment monitoring, vehicle tracking and mapping depend on knowing the locations of sensor nodes. Additionally, location-based routing protocols can save significant energy by eliminating the need for route discovery and improve caching behavior for location dependent requests. Naturally, GPS supports these applications. However, enabling GPS receivers in every node or manually configuring locations is not only cost ineffective for most sensor network applications but also practically impossible for indoor environment applications.

Furthermore, software protocols for service robots that perform tasks such as basic patient care in nursing homes, maintenance and security in office buildings, and food and concierge service in restaurants and hotels always require localization. Finding the location of robots in indoor environments is crucial in many applications. Robots equipped with RFIDs and laser range finders allow visually impaired individuals to navigate in unfamiliar indoor environments and interact with the robotic guide via speech, sound, and wearable keyboards. A great example in housekeeping applications is the iRobot Roomba which is an automated vacuum cleaning robot for domestic use. The robot creates a map of the room as it moves by using feedback from a variety of bumper and optical sensors. All of these applications require an accurate mechanism for position estimation.

Moreover, sensor's location information can be utilized in order to achieve efficient network coverage. The effective detection of weak points in a sensor field can be utilized for future deployment suggestions or reconfiguration schemes that improve the overall quality of service. Additional use cases include military and civilian applications which exploit location information to track assets in indoor environments. Moreover, direction finding and guided tour services are important applications for indoor localization. The first is used

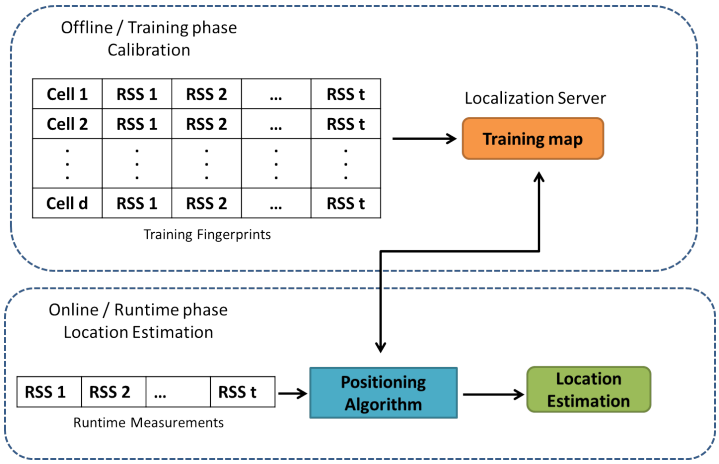

FIGURE 1.3: Fingerprint based techniques

to find the direction and route between two points, while the latter provides information that can be displayed on a device carried by a user based on the device's current location. Call forwarding, determining the location of an event as well as location-based routing can benefit from a robust localization system.

In general, localization is a technology that has the potential to augment and unlock advances on several other fronts (e.g., scalability, cooperation, low energy solutions) that will pave the way towards this paradigm shift.

1.4 State of the Art Fingerprint Based Localization Systems

Location information is essential for providing a rich experience to mobile users and is generating a growing interest in the development of fingerprint-based localization systems. The localization process typically involves two phases: an *offline/training* phase where RSS fingerprints are collected at different locations in the target area and an *online/runtime* phase where received RSS measurements are compared with the training fingerprints to perform localization (c.f. Figure 1.3). In the following, we describe current state of the art methods adopted by localization schemes.

1.4.1 Training phase: Calibration Techniques

Fingerprint-based systems must allocate considerable resources, effort, and time in order to construct the signature map resulting in issues that are particularly prominent in dynamically changing environments where recalibration is mandatory. As a consequence, researchers

have strived to develop training techniques that attempt to shorten the calibration phase of fingerprint-based systems [14].

Authors in [15] propose a training procedure where the whole area is divided into rooms, thereby limiting the possible locations to room-level granularity. This approach minimizes training time at the expense of less precise location estimates. Other localization protocols adopt data interpolation methods to complete the training map using fingerprints taken at a small number of training points [16]. The interpolation is based on either intuitive guidelines or on linear regression techniques [17]. Recently, a Compressed Sensing-based training technique was proposed [18] that exploits the sparse nature of the RSS readings in the frequency domain to estimate the radio map from a small number of random measurements. More specifically, training measurements are collected from randomly selected positions and the central unit reconstructs the signature map per AP via a sparsity seeking convex optimization procedure. A limitation of this approach is that reconstruction is performed independently for each AP and consequently the correlation among various APs is not taken into account.

To reduce the maintenance effort of the training phase, in [19] the signature map is estimated dynamically based on the runtime observations. To achieve this goal, neighbouring APs exchange RSS measurements during the runtime phase in order to update the signature map via a Gaussian Process regression model. Similarly, our proposed system is based on the measurements received at the APs. However, the calibration effort is reduced via channel sub-sampling and the inherent correlation structure of the sampled RSS fingerprints is considered for recovering the unobserved measurements.

To balance the performance degradation associated with a shortened calibration phase, the authors in [20] propose a hybrid generative/discriminative learning method that requires a small number of labeled samples and utilizes unlabeled samples to recover additional information for the target region area. Recently *crowdsourcing* approaches to the training phase have been proposed. They promise to significantly decrease the inherent training effort [21], however they still face the problem of manual fingerprint map building.

1.4.2 Runtime Phase: Localization techniques

The majority of localization techniques can be classified in three categories with respect to the runtime phase: *deterministic*, *probabilistic*, and *spatial sparsity*-based.

Radar [12] is a deterministic indoor positioning system which combines signal strength measurements with specific signal propagation models to provide accurate location estimates. Position estimation is performed by the k-Nearest Neighbour in Signal Space algorithm (NNSS), which employs signature maps that combine signal strength measurements acquired during the training phase at different positions of the mobile device [16, 12]. The signal-strength measurements received during the runtime phase are compared with the reference map to acquire the positions of the k nearest neighbors, *i.e.*, the ones with the smaller

distances in the signal space. The estimated position is given by the average of the coordinates of these neighbors according to:

$$L_q = (\sum_{i1}^{D} |\boldsymbol{y}_r - \boldsymbol{y}_t|^q)^{1/q}, \tag{1.1}$$

where $\boldsymbol{y}_r \in \mathbb{R}^P$ is the runtime measurement vector, $\boldsymbol{y}_t \in \mathbb{R}^P$ is the fingerprint vector, P is the number of APs and D in the number of possible positions of the user in the ground plane. In cases where q is equal to one or two we consider the Manhattan distance or the Euclidean distance, respectively. As position estimation $\boldsymbol{x}$ we consider the centroid of the coordinates of K points that have the minimum L_q. The weighted scheme of KNN, the K weighted nearest neighbor (WKNN) is considered when we compute the centroid of the K weighted points.

Authors in [22] introduce a localization system that generates statistical-based fingerprints by exploiting the measurements sent by the APs at the mobile device. A weighted confidence interval based algorithm is utilized in order to estimate the location of the user. [**?**] presents a localization algorithm based on the second-order spatial correlations among the RSSI measurements transmitted from various APs. The system compares the data at the unknown position with the data of each cell by using the Kullback–Leibler Divergence (KLD) between their corresponding probability densities.

The main idea in the probabilistic approach is to compute the conditional PDF of a certain possible cell c_i where $i = 1, \ldots, D$ of the mobile user given measurements $\boldsymbol{y}$[23]. Using the Bayes' rule we get:

$$p(c_i|\boldsymbol{y}) = \frac{p(\boldsymbol{y}|c_i)p(c_i)}{p(\boldsymbol{y})} \tag{1.2}$$

where $p(\boldsymbol{y}|c_i)$ is the likelihood, $p(c_i)$ is the prior, and $p(\boldsymbol{y})$ is a normalizing constant. We suppose that there is no a priori information about the position and all positions c_i are equally likely. Assuming the conditional independence of the measurements from all the APs, the conditional probability in (1.2) is

$$p(\boldsymbol{y}|c_i) = \prod_{k1}^{P} p(y_k|c_i). \tag{1.3}$$

Bayesian probabilistic methods search for the maximum likelihood estimator of position (MLE), given as:

$$\widehat{c} = \arg\max p(\boldsymbol{y}|c_i). \tag{1.4}$$

The position estimation can also be given as an area confidence: for example a set of cells c_i, such that $\sum_i p(c_i) > P_{th}$, where P_{th} is a threshold probability[24]. In cases where it is considered necessary, the symbolic location c_i can be translated to a common coordinate

system.

Another popular localization scheme is the Compass system [25] which utilizes the IEEE 802.11 infrastructure and digital compasses to achieve low cost localization services. Compass uses signal strength fingerprints and a probabilistic approach to determine the position of the user. Horus [26] is a map-based system, which considers different causes for the wireless channel variations and utilises them for location sensing. Horus employs a stochastic description of the signature map and performs localization via a maximum likelihood based approach. Within the probabilistic framework, Bayesian classification has been naturally adopted to address the localization problem [23], [27]. The Bayesian estimator is a stochastic approach that computes the conditional distribution of a certain user position given the runtime signal strength measurements. Authors in [28] transform the information of the received measurements into principal components (PCs) and adopt a probabilistic approach based on PCs in order to perform maximum likelihood localization.

Moreover, distance-based gossip algorithms that consider a propagation model, have been proposed for distributed localization of energy sources in sensor networks. In [29], the estimated position is computed by averaging the locations of the BSs that are closest to the target, while providing lower weights to the base stations that are further from the target. While, in [29] the positions of the BSs are considered known, the authors in [30] propose a distributed gossip localization algorithm that aims to reduce the number of BSs with known locations. The authors in [31] propose a distributed distance-based signal strength localization protocol for wireless mesh networks. The two-phase localization algorithm builds a relative coordinate system and applies a mass-spring approach for the optimization of the MS location in the second phase. Finally, the commercial MeshNetwork Positioning system (MPS) leverages the patented position location methods built into mesh network quadrature division multiple access (QDMA) radio technology [32].

Authors in [33] minimize the location error by utilizing high dimensional fingerprints for each operation frequency and transmitted signal power at each possible location. Although their approach optimizes the accuracy of already existing techniques, an exhaustive training phase is required.

Positioning techniques based on spatial sparsity are based on the observation that the mobile user's location is sparse over the ground plane, *i.e.*, the MS can only be in one location at each given time. Particularly, the MS location can be represented in a sparse vector where the index of the non-zero component indicates the corresponding cell where the MS is located. In [34], we reformulated the localization problem as a sparse approximation problem based on the *Compressed Sensing* (CS) theory that provides a new paradigm for recovering sparse signals by solving an l_1 minimization problem [35, 36]. Moreover, in [37] we proposed a centralized localization protocol based on Jointly Compressed Sensing in order to exploit the intra- and inter- signal correlations present in the RSS measurements. Along similar lines, the authors in [18] applied the theory of CS in order to minimize the

number of the APs needed for accurate position estimation. In another recent work [38], indoor localization was also approached via the CS framework. The localization algorithm presented in [38] is based on the measurements transmitted from the APs, while it requires the MS to interact with a central unit that estimates its position. Under this scenario, CS theory is utilized in order to minimize the number of measurements exchanged with the central unit. Overall, all the related initial studies suggest that the CS framework improves the localization performance while minimizing the measurements transmitted in the network.

1.5 Contribution of the thesis

This dissertation comprises different techniques in order to provide efficient, adaptive and accurate indoor localization estimations based on recently introduced sparse approximation and low-rank matrix recovery techniques. Compressed sensing provides novel framework for recovering signals being sparse in some basis by means of a limited amount of random incoherent projections. Additionally, low-rank matrix recovery is a field in its infancy that serves as a new paradigm for reconstructing low rank data matrices from a small number of randomly sampled entries. Thus, taking advantage of sparsity aware signal processing and low-rank matrix theory we introduce indoor wireless local area network fingerprint based approaches that utilize Received Signal Strength measurements.

Initially, we introduce two fingerprint-based localization algorithms based on Compressed Sensing that exploit the intra- and inter- signal correlation structures of the received measurements at the based stations. The key idea is to exploit the common structure of the signal ensemble in order to reduce the amount of exchanged network data required for accurate localization. To this aim, we apply a centralized and decentralized compressed sensing protocol. The centralized approach considers the runtime measurements received at the BSs and offers accurate position estimation as a fraction of the measurements needed by current state-of-the-art methods. According to our centralized localization protocol, all local samples are sent to a central unit for sparse signal recovery. The decentralized version of the algorithm considers the spatial correlations among the received measurements at the base stations to provide global accurate position estimation, while reducing significantly the amount of measurements exchanged among the BSs and required for accurate positioning. To this aim we exploit the common structure of the received measurements to design a gossip-based algorithm in order to alleviate the effects of radio channel-induced signal variations on the estimation accuracy.

While fingerprint based systems achieve high accuracy, their major problem is the exhaustive training phase as it requires substantial cost and labour. For this purpose we introduce WoLF, a wireless localization and laser-scanner assisted fingerprinting system that solves this problem by automating the way indoor fingerprinting maps are generated. WoLF creates high resolution maps while WiFi localization on the generated high resolution maps can be performed by sparse reconstruction which exploits the peculiarities imposed by the

physical characteristics of indoor environments. WoLF applies a sparse Bayesian learning (SBL) approach in order to find the position of the mobile user and dynamically determine the sufficient number of APs required for accurate positioning.

It is interestingly observed that already existed fingerprint-based schemes implicitly assume that communication occurs over the same frequency channel during the training and the runtime phases. However, when this assumption is violated, the mismatches between training and runtime fingerprints can significantly deteriorate the localization performance. Additionally, the exhaustive calibration procedure required during training limits the scalability of this class of methods. To address these difficulties we propose a novel, scalable, multi-channel fingerprint-based indoor localization system that employs modern mathematical concepts based on the Sparse Representations and Matrix Completion theories. Particularly we investigate the channel changes on the fingerprint characteristics and the effects of channel mismatch on state-of-the-art localization schemes. The proposed a novel fingerprint collection technique significantly reduces the calibration time, by formulating the map construction as an instance of the Matrix Completion problem. During location estimation, we propose a frequency-aware sparse Bayesian learning technique.

Concluding the thesis, we provide a dynamic recalibration technique for fingerprint based systems that dynamically adapts to the environmental changes while minimizing the recalibration effort required in fingerprint based systems. Our key observation is that in non-stationary indoor environments, the training measurements are constantly changing over time while the subsequent measurements may explicitly depend on past observations. Thus, we exploit the spatio-temporal corruptions of the training fingerprints to reduce the training phase effort by reconstructing the signature map from fewer measurements.

Concluding, the main contributions of this thesis are:

- The design of indoor fingerprint-based localization algorithms based on Jointly Compressed Sensing that provide efficient location estimation while minimizing the number of measurements exchanged in the wireless network. The proposed localization approaches are implemented in a centralized and decentralized version.

- The design of a Wireless localization and Laser-scanner assisted Fingerprinting system that provides autonomous signature map generation during the calibration phase and for location estimation adopts a Sparse Bayesian Learning approach.

- The design of a robust to changes in channel frequency indoor localization system that introduces a reduced effort calibration phase. The recovery of partial fingerprints is formulated as an instance of the Matrix Completion theory.

- The design of an adaptive reduced effort recalibration technique for fingerprint based localization algorithms based on Dynamic Matrix Completion.

This thesis is structured as follows. Chapter 2 first introduces the basic principles in Compressed Sensing inspired by the inherent sparsity appeared in the localization problem. In the following, the appropriate background for Matrix Completion framework is provided, motivated by the need to recover the low-rank signature maps generated during the training phase of fingerprint based localization systems. Chapter 3 presents the proposed centralized and decentralized indoor localization algorithms based on the principles of Jointly Compressed Sensing, along with a set of experimental results based on real data collected in the premises of a research institute. Chapter 4 introduces WoLF, a sparsity based wireless localization and laser-scanner assisted Fingerprinting system. Experimental results with data collected in a university building validate WoLF in terms of localization accuracy under actual environmental conditions. Chapter 5 presents a multi-channel indoor localization system that adopts a reduced effort calibration phase. Experimental evaluation on real data highlights the performance of the proposed framework in terms of reconstruction error and localization accuracy. Chapter 6 introduces an adaptive recalibration algorithm for fingerprint based localization systems. Analytical studies and simulations are provided to evaluate the performance of the proposed technique in terms of reconstruction and location error. Finally in Chapters 7 and 8 we present the conclusions and the future work directions, respectively.

Chapter 2

Background Theory

Compressed Sensing and Matrix Completion have recently gained great attention as they provide interesting theoretical guarantees, as well as practical applications across fields. The rapidly developing field of sparse signal recovery is already changing the way engineers think about data acquisition and reconstruction. In this section, we review the basic principles in CS and MC theory required for understanding the proposed algorithms introduced in the following chapters.

2.1 Linear systems

Searching for the solution of a linear system of equations arises in most of engineer sciences. Particularly, consider a full-rank matrix $\boldsymbol{\Phi} \in \mathbb{R}^{J\times D}$ which is in same sense 'random', for example a matrix with i.i.d. Gaussian entries. Denote the vector $\boldsymbol{y} \in \mathbb{R}^{J\times 1}$ with $J < D$ and an unknown signal $\boldsymbol{b} \in \mathbb{R}^{D\times 1}$ that can be expressed via the ensemble:

$$\boldsymbol{y} = \boldsymbol{\Phi} \cdot \boldsymbol{b}. \tag{2.1}$$

The vector $\boldsymbol{y}$ can be described as a vector of *observations* or *linear measurements* of the unknown signal $\boldsymbol{b}$ in terms of the matrix $\boldsymbol{\Phi}$(c.f. Figure 2.1).

In the dimension of the signal $\boldsymbol{b}$ is less than the dimension of $\boldsymbol{\Phi}$, that is if $J < D$, the system (2.1) results in an underdetermined linear system of equations, where the number of observations is less than the number of the unknowns. In case where $J = D$, the system (2.1) is referred to as a determined system. Note that in this case $\boldsymbol{\Phi}$ is a square matrix. Finally, the system is called overdetermined if $J > D$.

If the system is determined, (2.1) is a standard linear system and the solution is unique if $\boldsymbol{\Phi}$ is nonsingular, $\boldsymbol{b} = \boldsymbol{\Phi}^{-1}\boldsymbol{y}$. In the overdetermined case, and if $\boldsymbol{\Phi}$ is nonsingular the solution $\boldsymbol{b}$ of (2.1) is the error vector $\boldsymbol{\Phi b} - \boldsymbol{y}$ with the smallest $l2-$norm. This is the standard

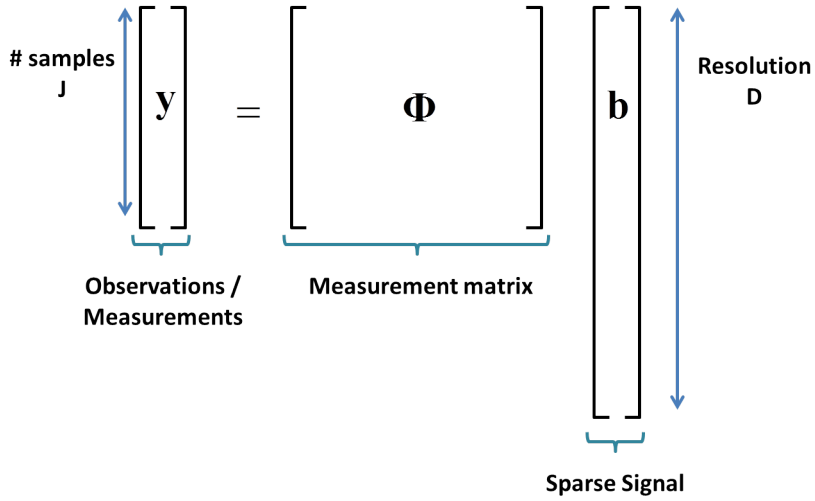

FIGURE 2.1: Sparse sensing process with a full-rank matrix $\boldsymbol{\Phi}$. The vector $\boldsymbol{b}$ is sparse with resolution D. The vector of observations y holds J measurements, where $J < D$.

least-squares method and results to the solution of the optimization problem: $\min_{\boldsymbol{b}} \|\boldsymbol{\Phi b} - \boldsymbol{y}\|_2$. When $\boldsymbol{\Phi}$ is singular the following optimization problem can be solved using standard least squares methods.

$$\hat{\boldsymbol{b}} = \arg\min\{\|\boldsymbol{b}\|_2, \quad \boldsymbol{b} \in S\}, \tag{2.2}$$

where

$$S := \{\boldsymbol{b} \in \mathbb{R}^D, \ \|\boldsymbol{\Phi}\hat{\boldsymbol{b}} - \boldsymbol{y}\|_2 = \min_{\boldsymbol{b}} \|\boldsymbol{\Phi b} - \boldsymbol{y}\|\} \tag{2.3}$$

The solution can be found using the pseudo inverse or using the singular value decomposition.

If the case of an underdetermined system elementary linear algebra tells us that $\boldsymbol{b}$ is not uniquely recoverable from $\boldsymbol{y}$. This occurs as the system (2.1) leads to an infinite set of feasible solutions (c.f. Figure 2.2(b)). Interestingly enough, searching for a sparse solution and given that sensing matrix $\boldsymbol{\Phi}$ possesses some properties a unique solution is feasible. This is the well known Sparse Solution Problem.

2.2 Low-dimensional signals

A great amount of applications in signal processing and communication can be found where the signals of interest are represented as a linear combination of a few elements of a known basis or dictionary. When this representation occurs the signal is called *sparse*. Specifically, sparse signal models capture the fact that in many systems high-dimensional signals

contain relatively smaller amount of information compared to their dimensions. Following *Occams'razor* principle, among the various number of signal representation sparsity is the best one, as is the most straightforward.

Sparse Signals

Sparsity has been exploited in various areas of applied mathematics, computer science and engineering for a variety of applications in wireless communications, astronomy, biology and many others.

Mathematically, a signal $\boldsymbol{b}$ is called K-sparse if its ℓ_0 norm is equal to K, where $K \ll D$. Particularly, the ℓ_0 norm is defined as the number of non-zero components in a vector according to:

$$\|\boldsymbol{b}\|_0 := \left\{ \sum_k |b(k)|^0 \quad : b(k) \neq 0 \right\}. \tag{2.4}$$

A traditional example in image processing is the wavelet decomposition that divides the image into low- and high-frequency components. The high- frequency components are sparse and capture most of the information. In coding theory, information is transmitted in a coded block in which a small fraction of the entries may be corrupted with noise. Thus, the received data contain a small number of damaged data and thus the error is said to be sparse. This sparsity allows the correction of gross errors. In positioning problems the main objective is to estimate the user's location which is unique in the area of ground plane. Consequently, the position of the user is said to be sparse in space.

Compressible Signals

An interesting observation is that in the real-world signals tend to be compressible rather than sparse. Compressible signals are approximated by sparse signals as their coefficients decay rapidly when sorted in order of decreasing magnitude. Particularly, there exist classes of signals such that the coefficients obey a power law decay and thus in this case they are highly compressible [39]. Particularly, if we sort the coefficients b_i of $\boldsymbol{b} \in \mathbb{R}^D$ such that $|b_1| \geq |b_2| \geq \ldots \geq |b_D|$, then a power law is followed if there are constants $C, r > 0$ such that:

$$|b_i| \leq C i^{-r}. \tag{2.5}$$

Large values of r results in more compressible signals.

Low-rank matrices

Low-rank matrices are a popular class of matrices, where their rank is much lower than their dimension. Particularly, consider the singular value decomposition (SVD) of a matrix $\boldsymbol{\Psi} \in \mathbb{R}^{J \times D}$ of rank r

$$\boldsymbol{\Psi} = \sum_i \sigma_{i \in [r]} u_i v_i^{\star}, \tag{2.6}$$

where $\sigma_1, \ldots, \sigma_r \geq 0$ are the singular values, and $u_1, \ldots, u_r \in \mathbb{R}^J$, $v_1, \ldots, v_r \in \mathbb{R}^D$ are the corresponding singular vectors. A matrix is called low-rank when a small number of the singular values is non-zero. Informally, the property of having a low-rank property is

the *noncommutative analogue* of sparsity. Particularly, instead of utilizing all the number of elements used to construct the signal, only the number of nonsingular values are constructed. Low-rank matrices arise in a variety of real-word problems. For example, in geolocation the matrix of pairwise distances between the sensor typically has rank 2 or 3, according to the dimensions of the space. Moreover, in recommendation systems, such as *Netflix*, matrices are utilized in order to indicate users preferences over a list of items. The premise behind these systems is that there is only a small number of factors influencing the preferences and that a user's preference vector is determined by how each factor applies to that user. Thus, these matrices hold a low-rank property.

2.3 Sparse representations

The potential of *exploiting sparsity* in signal processing is attracting great attention in the last years. Especially considerable attention has been focused on the Sparse Solution Problem (SSP) where sparse vectors in high dimensions can be recovered from what was previously believed to be incomplete information. The unknown signal of interest $\boldsymbol{b} \in \mathbb{R}^D$; it is assumed to be K-sparse.

The SSP can be expressed as the optimization problem:

$$\min_{\boldsymbol{b}} \|\boldsymbol{b}\|_0 \quad \text{subject to } \boldsymbol{y} = \boldsymbol{\Phi}\boldsymbol{b}. \tag{2.7}$$

However, the ℓ_0 norm is a discrete norm and thus minimizing (2.7) is NP-hard, requiring an exhaustive combination of all $\binom{D}{K}$ possible locations of the non-zero components of $\boldsymbol{b}$ [40].

One avenue for translating this problem into something more tractable is to replace the ℓ_0 norm with its optimal or tightest convex relaxation, the ℓ_1 norm. The ℓ_1 norm returns larger costs to non-sparse solutions and thus determines more efficiently the sparse vector. (c.f. Figure 2.2(s)) The use of ℓ_1 minimization to promote sparsity has a long history starting back from 1938 where Beurling proposed a method for recovering signal only from partial information of its Fourier transform. Later on in 1970's and early 1980's the use of ℓ_1 minimization in large problems became practical with the explosion of computing power. Additionally, ℓ_1 minimization received considerable attention in statistics literature as a method for variable selection in regression, the famous Lasso. In the following paragraphs we discuss algorithms for the effective recovery of the sparse vector $\boldsymbol{b}$.

Specifically, we consider the following optimization problem:

$$\min_{\boldsymbol{b}} \|\boldsymbol{b}\|_1 \quad \text{subject to } \boldsymbol{y} = \boldsymbol{\Phi}\boldsymbol{b}, \tag{2.8}$$

where the $\ell_1 := \sum_j |b_j|$.

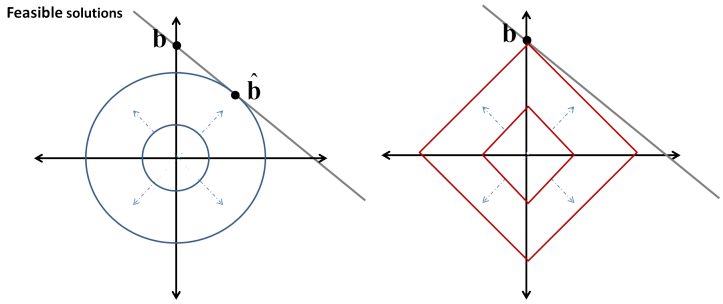

FIGURE 2.2: (a) ℓ_2 and (b) ℓ_1 norm cost functions in case where $\boldsymbol{b} = (b_1, b_2)^T$ is a $2D$ vector. The ℓ_1 returns larger costs to non-sparse solutions located far from the coordinate axes and thus estimates sparse solutions better than the ℓ_2 norm.

However, it is obvious that in real world experiments, the measurements can be corrupted and that is expressed by the following relation

$$\boldsymbol{y} = \boldsymbol{\Phi b} + \boldsymbol{\eta}, \tag{2.9}$$

where $\boldsymbol{\eta} \in \mathbb{R}^{\boldsymbol{D}}$ is a noise vector with bounded energy $\|\boldsymbol{\eta}\|_2 \leq \epsilon$. In such noisy environments, the reconstruction of the sparse vector $\boldsymbol{b}$ is achieved by employing an ℓ_1 minimization approach with quadratic constraints

$$\widehat{\boldsymbol{b}} = \arg\min \|\boldsymbol{b}\|_1 \;\; s.t. \;\; \|\boldsymbol{y} - \boldsymbol{\Phi b}\|_2 \leq \epsilon, \tag{2.10}$$

where ϵ is the noise level. In (2.10), we search for the estimated $\boldsymbol{b}$ such that the approximation error $\boldsymbol{y} - \boldsymbol{\Phi b}$ is within the noise level. Problem (2.10) can be solved efficiently as it can be recast as a Second Order Cone Program (SOCP)[41].

For an appropriate Lagrange multiplier λ the solution of (2.10) is precisely the solution to the following unconstrained convex problem, known as *basis pursuit denoising*

$$\widehat{\boldsymbol{b}} = \arg\min \lambda\|\boldsymbol{b}\|_1 + \frac{1}{2}\|\boldsymbol{y} - \boldsymbol{\Phi b}\|_2^2. \tag{2.11}$$

The value of λ governs the sparsity of the solution: larger values typically produce sparser results.

In cases where the measurements are corrupted by zero-mean Gaussian noise with a bounded variance, the Dantzig selector has been proposed in order to reconstruct $\boldsymbol{b}$ [42, 43]

$$\widehat{\boldsymbol{b}} = \arg\min \|\boldsymbol{b}\|_1 \;\; s.t. \;\; \|\boldsymbol{\Phi}^T(\boldsymbol{y} - \boldsymbol{\Phi b})\|_\infty \leq \gamma, \tag{2.12}$$

where γ is a specified parameter depending on the noise variance. Penalizing the correlated residual $\|\boldsymbol{\Phi}^T(\boldsymbol{y}-\boldsymbol{\Phi b})\|_\infty$ instead of $\|\boldsymbol{y}-\boldsymbol{\Phi b})\|_\infty$ results in estimations that are invariant with respect to orthogonal transformations applied to the measurement vector. This is evidence as: $(\boldsymbol{U\Phi})\times(\boldsymbol{U\Phi b}-\boldsymbol{Uy}) = \boldsymbol{U}\times(\boldsymbol{Ub}-\boldsymbol{y})$, where $\boldsymbol{U}$ is the orthogonal transformation matrix.

2.4 Conditions for sparse recovery

In this Section we consider the appropriate theoretical claims imposed on the sparse signal and on the measurement matrix in order to provide accurate signal recovery. Initially, the conditions for uniqueness of the ℓ_0 norm minimization problem (2.7) will be presented and then the conditions for the ℓ_1 problem (2.8) will follow.

2.4.1 Uniqueness of ℓ_0 minimization problem

A key property in order to identify the uniqueness of the ℓ_0 is the *spark* of the matrix $\boldsymbol{\Phi}$.

Definition 2.1 *Let a matrix $\boldsymbol{\Phi} \in \mathbb{R}^{J\times D}$. The spark of the matrix $\boldsymbol{\Phi}$, denoted by $spark(\boldsymbol{\Phi})$, is the smallest number of linearly independent columns of $\boldsymbol{\Phi}$.*

In other words, if a matrix $\boldsymbol{\Phi}$ has r linearly independent columns, but there exists a subset of $r+1$ columns that are linearly dependent then $spark(\boldsymbol{\Phi}) = r+1$. Generally, the following relation holds for the spark and the rank of a matrix $\boldsymbol{\Phi} \in \mathbb{R}^{J\times D}$, with $J \geq 2$

$$2 \leq spark(\boldsymbol{\Phi}) \leq rank(\boldsymbol{\Phi}) + 1. \tag{2.13}$$

The following theorem considers the spark quantity in order to provide the necessary and sufficient conditions of sparse solutions.

Theorem 2.2 *Consider the linear system $\boldsymbol{y} = \boldsymbol{\Phi b}$ with $\boldsymbol{\Phi} \in \mathbb{R}^{J\times D}$, $J \leq D$. If the linear system has a solution $\boldsymbol{b}$ satisfying $\|\boldsymbol{b}\|_0 \leq spark(\boldsymbol{\Phi})/2$, then this is the unique solution.*

2.4.2 Uniqueness of ℓ_1 minimization problem

The properties of the matrix $\boldsymbol{\Phi}$ plays an important role in the stability of the optimization problem presented in (2.8). Especially for compressible signals we need to ensure that the null space of $\boldsymbol{\Phi}$ does not contain any vectors that are too compressible additionally to vectors that are sparse. Thus the matrix $\boldsymbol{\Phi}$ should satisfy the so-called *null space property* (NSP). Before introducing the NSP we determine the null space of $\boldsymbol{\Phi}$ as:

$$\mathcal{N} = \mathcal{N}(\boldsymbol{\Phi}) := \{\boldsymbol{b} \in \mathbb{R}^D : \boldsymbol{\Phi b} = 0\}. \tag{2.14}$$

Definition 2.3 *Assume the matrix $\mathbf{\Phi} \in \mathbb{R}^{J\times D}$. The matrix $\mathbf{\Phi}$ has the null space property of the order k, if*

$$\forall v \in \mathcal{N}(\mathbf{\Phi}) \setminus \{0\}, \;\; \forall |T| \leq k, \;\; \|u_T\|_1 < \|u_{T^c}\|_1. \tag{2.15}$$

NSP is known as a characterization of uniqueness of problem (2.8) in cases where there is no noise.

Theorem 2.4 *Consider the linear system $\boldsymbol{y} = \mathbf{\Phi}\boldsymbol{b}$ with $\mathbf{\Phi} \in \mathbb{R}^{J\times D}$, $J \leq D$. If $\mathbf{\Phi}$ satisfies the null property of order k, then this is the unique solution.*

2.4.3 Sufficient conditions for sparse signal recovery

Effective sparse signal recovery is obtained when the optimal solution of the ℓ_0 and ℓ_1 minimization problems are unique and coincide. In this case, one says that ℓ_0-ℓ_1 equivalence holds or that the ℓ_0-solution can be recovered by the ℓ_1-solution. Restricted Isometry Property and Mutual Coherence are the most famous sufficient conditions under which the ℓ_0-ℓ_1 equivalence holds.

Restricted Isometry Property

Restricted Isometry Property (RIP) introduced by Candès and Tao in [44]. RIP measures the degree to which each submatrix consisting of k columns vectors of $\mathbf{\Phi}$ is close to being an isometry.

Definition 2.5 *A matrix $\mathbf{\Phi} \in \mathbb{R}^{J\times D}$ is said to posse a k-RIP if there exists a $\delta_k \in (0,1)$ such that*

$$\forall \boldsymbol{c} \in \mathbb{R}^k \quad (1-\delta_k)\|\boldsymbol{c}\|_2^2 \leq \|\mathbf{\Phi}\boldsymbol{c}\|_2^2 (1+\delta_k)\|\boldsymbol{c}\|_2^2. \tag{2.16}$$

Equivalent, a matrix holds the RIP if all the subsets of k columns retrieved from $\mathbf{\Phi}$ are in fact nearly orthogonal. Particularly, the ℓ_1 optimization reconstructs all the k-sparse vectors if the matrix $\mathbf{\Phi}$ satisfies $\delta_{2k} \leq 0.473$

Mutual Coherence

RIP provides guarantees for the recovery of $k$sparse vectors having the disadvantage of high computational complexity, since it demands the consideration of $\binom{D}{K}$ submatrices. On the contrary, the *coherence* property of the matrix $\mathbf{\Phi}$ provides an easily computable recovery guarantee [45],[46].

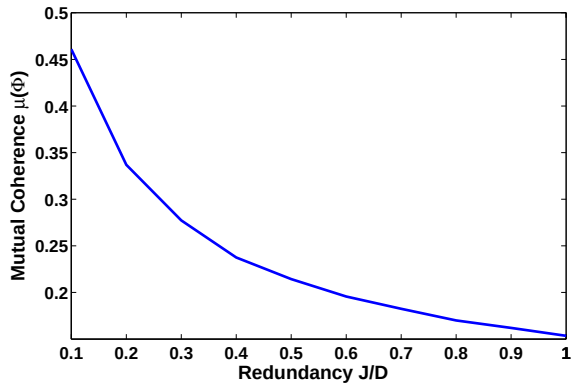

FIGURE 2.3: Coherence of a random matrix decays with the redundancy $\frac{J}{D}$. Higher coherence yields in higher lower bounds for the cardinality of the sparset solution.

Definition 2.6 *The mutual coherence of a matrix $\mathbf{\Phi}$, denoted as $\mu(\mathbf{\Phi})$, is the largest absolute inner product between different columns of the matrix:*

$$\mu(\mathbf{\Phi}) = \max_{1 \leq < j \leq D} \frac{\|\langle a_i, a_j \rangle\|}{\|a_i\|_2 \|a_j\|_2}. \tag{2.17}$$

Mutual coherence expresses the similarity between columns of $\mathbf{\Phi}$. Thus $\mu(\mathbf{\Phi}) = 0$ if the columns of $\mathbf{\Phi}$ are orthogonal to each other. Particularly, it has been shown that for full-rank matrices of size $J \times D$ has the lower bound, known as Welch bound [47]

$$\mu(\mathbf{\Phi}) \geq \sqrt{\frac{D - J}{J(D-1)}}. \tag{2.18}$$

Figure 2.3 indicates the average coherence of a random matrix over the redundancy $\frac{J}{D}$. The coherence decreases with decreased redundancy. The mutual coherence of the matrix can be imposed as a lower bound on the cardinality of the sparse vector in order to define unique solution of the ℓ_0 and ℓ_1 problems.

Theorem 2.7 *Denote $\mathbf{\Phi} \in \mathbb{R}^{J \times D}$ and let $\boldsymbol{b} \in \mathbb{R}^D \setminus \{0\}$ be a solution of the ℓ_0 problem such that: $\|\boldsymbol{b}\|_0 < \frac{1}{2}(1 + \mu(\mathbf{\Phi})^{-1})$, then this solution is necessary the sparsest possible.*

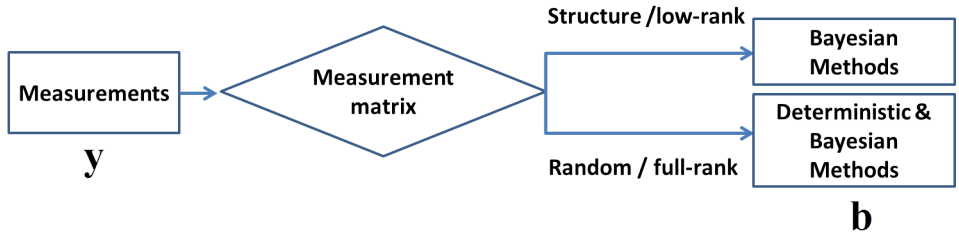

FIGURE 2.4: Sparse recovery model. Structure dictionaries fail to provide sparse solutions due to RIP violations. In these cases, emprical Bayesian reconstruction techniques successfully estimate the sparse signal. For random measurement matrices sparse signal recovery techniques provide efficient signal recovery.

2.5 Structured measurement matrices

In the previous sections we introduced the performance guarantees using ideal full rank matrices. However, structured matrices appear in a large number real time applications. For example, in applications such as model selection with correlated features, source localization and compressed sensing with constrained measurement directions, the sensing matrix is highly coherent. Unfortunately, in these situations the RIP equivalence conditions are violated, imposing that the $\ell_0 - \ell_1$ equivalence does not hold.

An alternative approach is to apply a pre-processing step where column normalization is adopted in order to standardize structured dictionaries. In most cases an ℓ_2 normalization in used in each column of the sensing matrix. This procedure ensures that no one column is implicitly favored over another during the estimation procedure. Particularly, consider the linear system of equations $\boldsymbol{y} = \boldsymbol{\Psi b}$, where $\boldsymbol{\Psi} = \tilde{\boldsymbol{\Psi}}\boldsymbol{S} + \sigma \boldsymbol{a}\boldsymbol{c}^T$, $\tilde{\boldsymbol{\Psi}}$ is an incoherent dictionary, $\boldsymbol{S}$ is a diagonal matrix, and $\sigma \boldsymbol{a}\boldsymbol{c}^T$ defines a rank one adjustment. Applying a column normalization to remove the effect of $\boldsymbol{S}$ results in a matrix $\boldsymbol{\Psi}$ dominated by the rank one factor for large σ. However, with no normalization the matrix $\boldsymbol{S}$ biases the estimation results. More ambiguous cases result when the measurement matrix is generated via $\boldsymbol{\Psi} = \tilde{\boldsymbol{\Psi}}\boldsymbol{D}$, where $\tilde{\boldsymbol{\Psi}}$ obeys the RIP, and $\boldsymbol{D}$ is low-rank. The unrestricted matrix $\boldsymbol{D}$ can introduce arbitrary structure between the columns of $\boldsymbol{\Psi}$, resulting in an low-rank matrix $\boldsymbol{\Psi}$ regardless of how well-behaved the original $\tilde{\boldsymbol{\Psi}}$ is.

In the aforementioned cases ℓ_1 fails to provide sparse solutions due to RIP violations resulting from correlations between columns of the measurement matrix. However, recent literature [48, 49] proves that empirical Bayesian estimator methods can be successful for structured dictionaries. Section 2.8 presents theoretical results that support this claim. Figure 2.4 describes the sparse recovery model for different types of measurement matrices.

2.6 Sparse signal recovery techniques

The ℓ_1 minimization problem presented in the previous section provides accurate results for sparse signal recovery. Particularly, (2.10) is a convex optimization problem for which there exist efficient and accurate numerical solvers. Interior-point methods have been developed in order to solve sparse approximation problems by convex optimization [50][51]. Interior point methods can be robust in the sense that quite rarely fail completely and their performance does not depend on the sparsity of the solution. Gradient-descent algorithms have been proposed [52],[53] having the advantage of fast convergence to the sparsest solution and being appropriate for large-scale problems.

Greedy algorithms rely on the iterative approximation of the sparse solution by successfully identifying one or more components that yield the greatest improvement in quality. Matching Pursuit (MP) belongs in this category and and has been expended by researchers. Famous extensions are the Orthogonal Matching Pursuit (OMP), Stagewise OMP (StOMP), and Compressive Sampling Matching Pursuit (CoSAMP). Greedy pursuit algorithms significantly reduce computational complexity though they present lower reconstruction quality.

Iterative thresholding algorithms [54, 55, 56], serve as an alternative to the greedy class of sparse reconstruction methods. They are fast and accurate. Additionally, they can be adopted to refine the solutions of the greedy methods and can easily incorporate additional extension criteria.

2.7 Distributed compressed sensing

The principles of sparse estimation theory and compressed sensing have been applied for signal reconstruction, detection and classification by exploiting the intra-signal structures at a single collection point (*e.g.*, a sensor). Multiple collection points usually capture related phenomena and a joint structure is expected for the signals ensemble, in addition to the intra-signal correlation between the individual measurements. Recently, the authors in [57] introduced a theory for *distributed compressed sensing* (DCS) that exploits both intra- and inter-signal correlation structures. DCS considers the joint sparsity of a signal ensemble to obtain accurate signal reconstruction.

In this section we generalize the notion of a sparse signal in a basis to the notion of an ensemble of signals being jointly sparse. Particularly, we consider three models for jointly sparse signals that can be applied in different situations.

According to the first model, all signals share a common sparse component but they have sparse innovations components that are unique to each signal.This situation arises in applications where global signal processes affect all sensors while local noise affects individual sensors.A practical situation is a group of microphones placed in a venue. The measured signals have both temporal correlations (intra-signal) and spatial (inter-signal)

correlations. Global factors, such as the music from the band, could have an effect that is both common to all microphones and structured enough to permit sparse representation. Additionally, microphones are affected from local factors that could contribute localized innovations that present a sparse structure. Consequently, this model descries measured properties of physical processes that change smoothly over time and space and thus they are highly correlated. A γ-weighted ℓ_1 formulation is applied in order to recover signals that follow the first model formulation [58].

The second model describes signals that are constructed from the same sparse set of basis vectors but with different coefficients. This is the case in our indoor positioning application where the signals are sparse in the spatial domain, yet different propagation path losses cause different attenuations among the received signals at each AP. An other useful application for the second model is MIMO-communication [59]. In this case, accurate recovery is achieved via the DCS-SOMP algorithm [60].

Finally, the third model is an extension of the first model in that the common component need not be sparse in any basis. This model describes a scenario where several sources are recorded by different sensors together with a background signal that is not sparse in any basis. A motivated example includes the compression of video data, where the innovations or differences between video frames may be sparse, regardless the fact that a single frame may not be extremely sparse. The DCS approach suggests that each video frame is encoded independently while all frames of the video sequence are decoded jointly.

2.8 Bayesian compressed sensing

Recently, the signal processing literature transferred ideas from the deterministic sparse modelling into a powerful Bayesian statistical approach for signal estimation. Bayesian learning via sparse prior holds its roots in the area of machine learning for estimating sparse solutions to regression and classification problems that utilize linear parametric models. A theoretical analysis of SBL performance can be found at [61]. Authors in [62] introduce the SBL to the CS theory indicating that the Bayesian formalism for estimating a sparse signal based on compressive-sensing measurements outperforms traditional deterministic reconstruction approaches. Recent literature focuses on developing different sparsity-including priors. Particularly, a popular sparse promoting prior model is the *spike and slab* prior [63, 64, 65]. The spike component, which concentrates its mass at values close to zero, allows shrinkage of small effects to zero, whereas the slab component has its mass spread over a wide range of plausible values indicating the non-zero components. Moreover, sparsity priors have been utilized in a hierarchical model, where a complex prior is composed of two or more simple distributions. Initially, in SBL with relevance vector machine (RVM) framework the Student-t sparsity prior is composed of a Gaussian and a gamma prior [66]. A Gaussian-gamma prior that composed the Laplace prior is introduced in [67].

The major characteristic of the Bayesian modelling is that estimates the most probable (MAP) sparse solution with different variance hyperparameters while represents the full posterior distribution on the latent variables. Thus, apart for signal estimation the uncertainty of the recovery process is captured. Practically, the Bayesian framework allows learning model parameters while adaptively determines the optimum number of measurements [65, 62].

Standard MAP estimation (the so-called Type I) involves maximizing over both the hyperparameters and the sparse coefficients. However, in the empirical Bayesian approach (the so-called Type II) the coefficients are initially marginalized and then maximized over the hyperparameters, resulting to a more amenable posterior approximation [49]. Thus, Type II techniques are of special interest as they can successfully recover sparse coefficients when the RIP is violated and the popular deterministic approaches fail to provide the sparsest solution [68]. This property is implied via the following theorem:

Theorem 2.8 *[49] Consider the sparse vector $\boldsymbol{b} \in \mathbb{R}^D$ and the structured dictionary $\boldsymbol{\Psi} \in \mathbb{R}^{J \times D}$ such that the angle between any two column vectors of $\boldsymbol{\Psi}$ is less than some $\epsilon > 0$, where ϵ is sufficient small. Reweighted ℓ_1 minimization using weights $g_i(\boldsymbol{b}; \alpha, q)$, with $q \geq 1$ and α sufficiently small will recover $\boldsymbol{b}$ exactly, given the coefficients of the dictionary $\boldsymbol{\Psi}$ do not sum to zero.*

2.9 Matrix completion problem

Matrix Completion (MC) is a recently proposed framework that has attracted a great deal of attention due to its solid mathematical formulation and numerous practical applications across disciplines. In many practical problems of interest, one would like to recover a matrix from only a small part of its entries. As a motivating example, consider the Netflix problem where we observe a few movie ratings from a large data matrix (the so-called preference matrix). The preference matrix has as many rows as the users and as many columns as the movies, and each entry indicates the rating of a user for one movie. Apparently, a small part of preferences are observed as each user rates just a few movies as opposed to the tens of thousands of the available ones. An interesting question arising at this point is the possibility to make an educated guess about the missing rating. In general, everybody would agree that it is not possible to a recover a data matrix from a subset of its entries. However, MC builds on the observation that a matrix which is low-rank or approximately low-rank can be recovered using just a subset of randomly observed data [69].

The MC problem initially appeared in the area of machine learning that applies collaborative filtering techniques. Collaborative filtering is the process of automatically predicting (filtering) the interests of a user by collecting preferences from many other users (collaborating). The matrices arising in these types of applications are low-rank as typically only a small number of factors affect the preferences of one individual. Additionally, the

MC recovery problem appears in many other applications including the global positioning problem in ad-hoc networks, the state recovery in system identification, the estimation of network correlated signals in remote sensing and many others.

2.9.1 Low-rank matrix recovery

Formally, let the matrix $\boldsymbol{\Psi} \in \mathbb{R}^{K \times D}$ be the measurements matrix we wish to recover as precisely as possible. The goal according to the MC formulation is to recover the matrix $\boldsymbol{\Psi}$ using a subset of M entries, collected by the linear operator $\mathcal{A} : \mathbb{R}^{K \times D} \rightarrow \mathbb{R}^{M}$ such that:

$$\boldsymbol{y} = \mathcal{A}(\boldsymbol{\Psi}), \tag{2.19}$$

where $\boldsymbol{y} \in \mathbb{R}^{M}$ gathers the observed measurements.

In general, the recovery of the $K \times D$ entries of the matrix $\boldsymbol{\Psi}$ is impossible from $M \ll K \times D$ measurements. This occurs as the linear system of equations described in (2.19) is underdetermined (*i.e.*, there are more unknowns than equations). However, inspired by the sparse approximation theory, we can exploit the correlations of the observations and obtain a feasible recovery of the full matrix.

Particularly, within the MC framework suck a recovery is possible, provided that the *rank* of matrix $\boldsymbol{\Psi}$ is small enough compared to its dimensions. We recall that the rank of a matrix is defined as the number of the linearly independent rows or columns. To recover an estimate $\hat{\boldsymbol{\Psi}}$ of the unknown matrix $\boldsymbol{\Psi}$ the following rank minimization problem needs to be solved:

$$\begin{aligned} \text{minimize} \quad & rank(\hat{\boldsymbol{\Psi}}) \\ \text{subject to} \quad & \mathcal{A}(\hat{\boldsymbol{\Psi}}) = \mathcal{A}(\boldsymbol{\Psi}). \end{aligned} \tag{2.20}$$

The low-rank matrix completion problem, as defined in (2.20) is NP-hard and all known algorithms which provide exact solutions require time doubly stochastic exponential in the maximum dimension D of the matrix.

Consider the singular value decomposition (SVD) of the matrix $\boldsymbol{\Psi}$:

$$\boldsymbol{\Psi} = \boldsymbol{U}\boldsymbol{\Sigma}\boldsymbol{V}^{T}, \tag{2.21}$$

where $\boldsymbol{U} \in \mathbb{R}^{J \times r}$ and $\boldsymbol{V} \in \mathbb{R}^{D \times r}$ denote the orthogonal matrices of the left and right singular vectors. The singular values are the diagonal of the matrix $\Sigma = diag(\Sigma_1, \ldots, \Sigma_r)$ and r is the rank of the matrix.

In the special case where the rank of the matrix is equal (or approximately equal) with r the matrix has exactly (or approximately exact) r nonzero singular values. Figure 2.5 indicates matrices with different rank and the associated singular values. Low rank matrices are characterized with a small number of non singular values. In other words, the rank

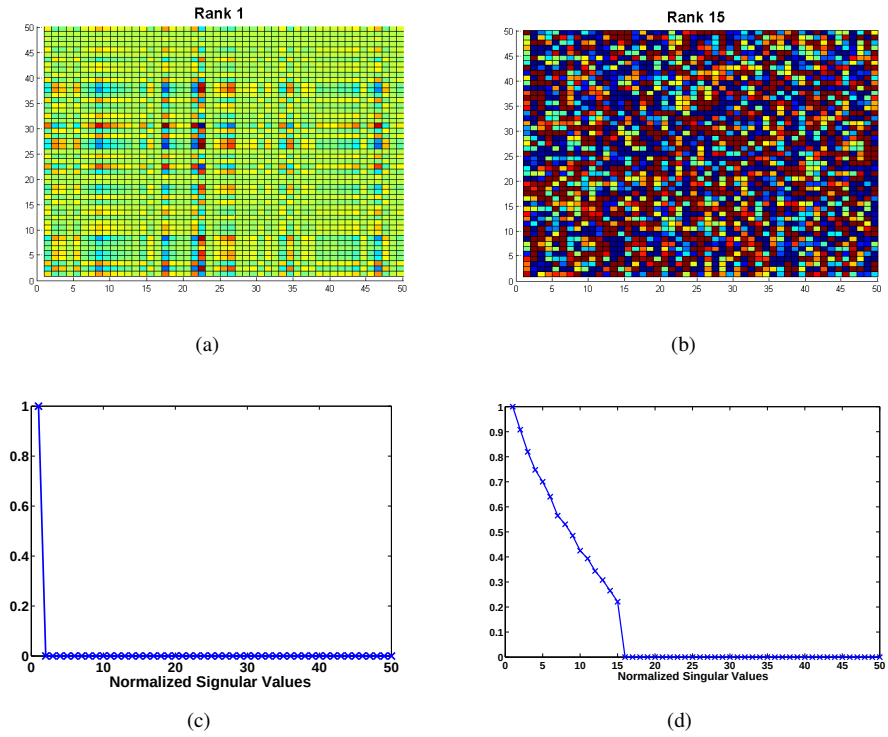

FIGURE 2.5: Matrices with the associated singular values. Observe that low-rank matrices preserve their energy only by a small number of measurements

function is simply the number of non zero singular values of $\mathbf{\Psi}$. Thus, the optimization problem in (2.20)can be replaced by nuclear norm function

$$\|\mathbf{\Psi}\|_\star = \sum_{k=1}^{K} |\sigma_k|, \tag{2.22}$$

where σ_k denotes the kth largest singular values of $\mathbf{\Psi}$. Consequently, the rank minimization problem can be approximated by the tightest convex problem:

$$\begin{aligned} \text{minimize} \quad & \|\hat{\mathbf{\Psi}}\|_\star \\ \text{subject to} \quad & \mathcal{A}(\hat{\mathbf{\Psi}}) = \mathcal{A}(\mathbf{\Psi}), \end{aligned} \tag{2.23}$$

where $\mathcal{A}(\cdot)$ denotes a linear map.

In the case where the observed measurements are corrupted by noise, the equality constraint in (2.23) can be replace with an inequality, in which case the problem is formulated

as:

$$\begin{aligned} \text{minimize} \quad & \|\boldsymbol{\Psi}\|_\star \\ \text{subject to} \quad & \|\mathcal{A}(\boldsymbol{\Psi}) - \mathcal{A}(\boldsymbol{M})\|_F^2 \leq \epsilon, \end{aligned} \tag{2.24}$$

where the *Frobenius norm* is defined as $\|\boldsymbol{\Psi}\|_F^2 = \sum_k \sigma_k^2$ and $\epsilon \geq 0$ represents the tolerance in the approximation error. The estimation of the low-rank matrix $\boldsymbol{\Psi}$ depends on the structure of the sampled measurements. Particularly, the linear map $\mathcal{A}$ should satisfy the incoherence property [70] defined in the following section.

2.9.2 Incoherence property

The low-rank assumption of the matrix $\boldsymbol{\Psi}$ is not sufficient in order to recover the unknown matrix from a small number of its sampled entries. As a motivating example, consider the extreme case of a rank one matrix $\boldsymbol{\Psi} = \boldsymbol{e}_i \boldsymbol{e}_j^T$, where $\boldsymbol{e}_i$ is the basis vector that has 1 on the ith entry and zeros everywhere else. In this case the original matrix $\boldsymbol{\Psi}$ cannot be recovered unless the (i, j) entry is sample of all its entries. Thus, to recover a matrix from a small number of sampled measurements the singular vectors must be sufficiently sparse (i.e. incoherent with the standard basis). In the following we define the incoherence property.

Definition 2.9 *Denote the matrix $\boldsymbol{\Psi} \in \mathbb{R}^{J \times D}$ with rank r and SVD $\boldsymbol{\Psi} = \boldsymbol{U}\boldsymbol{\Sigma}\boldsymbol{V}^T$, where $\boldsymbol{U}$ and $\boldsymbol{V}$ hold the left and right singular values. The matrix $\boldsymbol{\Psi}$ is μ coherent, if it satisfies the following properties:*

1. $\sum_{1 \leq k \leq r} \boldsymbol{U}_k^2 \leq \frac{\mu r}{J}$ *and* $\sum_{1 \leq k \leq r} \boldsymbol{V}_k^2 \leq \frac{\mu r}{D}$
2. $|\Psi_{ij}| \leq \frac{\mu \sqrt{r} \sigma_k(\boldsymbol{\Psi})}{\sqrt{JD}}, \forall 1 \leq i \leq J$, *and* $\forall 1 \leq j \leq D$

It has been proven that if the matrix $\boldsymbol{\Psi}$ is μ coherent the nuclear norm minimization problem (2.24) can recover the unknown low-rank matrix from a small number of measurements as indicated by the following theorem.

Theorem 2.10 *Consider the matrix $\boldsymbol{\Psi} \in \mathbb{R}^{J \times D}$ with rank r that obeys the properties 1 and 2 in 2.9 and $n = max(J, D)$. The recovery of the matrix $\boldsymbol{\Psi}$ is exact with high probability from m measurements if there exist constant C such that*

$$m \geq C n^{6/5} r \log(n). \tag{2.25}$$

2.9.3 Reconstruction algorithms

The constrained optimization problem in (2.23) can be reformulated as a semidefinite programming problem, in which case it can be solved by off-the-shelf solvers (*e.g.*, CVX [71]). A limitation of this approach is that typically these algorithms converge slowly, especially when dealing with large matrices. Recently, efficient algorithms, that take the characteristics of this specific optimization into account, have been proposed for solving the MC problem [72, 73]. Singular Value Thresholding (SVT) [73], one of earliest nuclear norm based MC techniques, is an iterative algorithm where at each iteration, a singular value decomposition step is applied first, followed by a projection onto the known elements. SVT relies on the fact that the unknown matrix at each iteration is low-rank and the auxiliary matrices that hold the observed measurements are sparse.

Authors in [74] solve the nuclear norm minimization problem via the Augmented Lagrange Multiplier (ALM) method. Particularly they propose a fast and scalable algorithm where each iteration involves computing a partial SVD of the partial observed matrix. The OptSpace algorithm presented in [75] is an efficient approach that consists of only three steps and has low complexity. The Optspace algorithm is ideal for massive data sets.

Chapter 3

Indoor Localization based on jointly compressed sensing

In this Chapter we propose two localization algorithms that exploit the spatial signal correlation structure, observed in an indoor localization environment, in order to provide position estimations by means of a limited amount of signal-strength measurements. The proposed received signal-strength localization protocol respects the limited processing power and battery capacity of the mobile device, by performing the position estimation remotely and monitoring either at a localization server or at a specific base station. Remote location estimation is advantageous since battery capacity grows slowly and power management is still a challenge in mobile computing. Exploiting the observation that the base stations receive correlated signals from the mobile devices, the introduced methods consider the joint structure of the runtime measurements in order to jointly estimate the positions precisely by minimizing the amount of measurements exchanged in the network.

Considering the above insights two algorithms are proposed, a centralized and a decentralized, that exploit the distributed compressed sensing (DCS) theory. DCS framework rests on the joint sparsity of a signal ensemble and provides effective signal recovery by jointly reconstructing all the signals [57]. According to the centralized Jointly Compressed Sensing scheme all local runtime measurements are sent to a central unit to perform sparse signal recovery. On the contrary, the decentralized scheme combines recent developments in sparse approximation and distributed consensus theory to efficiently perform decentralized localization in wireless networks. We introduce a novel decentralized technique that considers the spatial correlations among the received measurements at the base stations (BSs) to provide global accurate position estimation, while reducing significantly the amount of measurements exchanged among the BSs and required for accurate positioning. The decentralized protocol provides flexibility to the network administration since position estimations are distributed over the network and thus are accessible at each BS.

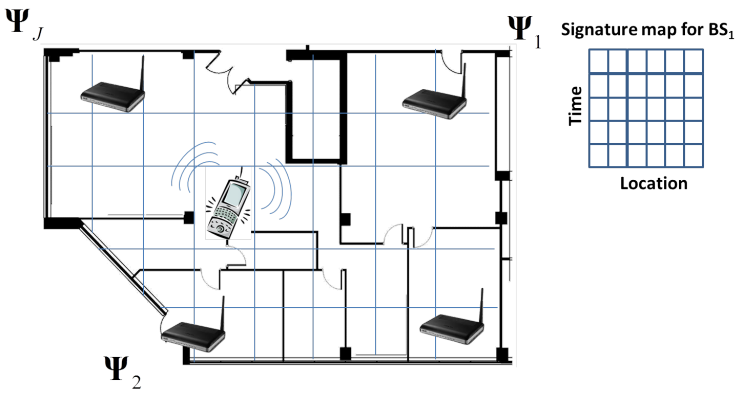

FIGURE 3.1: Training phase of the proposed centralized Jointly Detection Compressed Sensing localization framework.

3.1 Problem formulation

Consider a typical indoor WLAN scenario with one mobile device equipped with an active wireless adapter card. A BS that listens to a channel receives the packets transmitted by the mobile user at that channel and records its RSSI values. Given that the BS vendor provides the appropriate API, the RSSI information on the BS's hardware can be retrieved with high level programming.

The CS-based fingerprint method consists of two phases, the training phase and the runtime phase. During the training phase, a calibration procedure is adopted in order to create a signature map for each BS. Specifically, each BS j receives signal strength measurements from a MS that moves to various reference points (RPs) (cf. Figure 3.1). The signature basis matrix $\mathbf{\Psi}_j$ is represented as:

$$\mathbf{\Psi}_j = \begin{pmatrix} P_{1,1,j} & P_{1,2,j} & \cdots & P_{1,D,j} \\ P_{2,1,j} & P_{2,2,j} & \cdots & P_{2,D,j} \\ \vdots & \vdots & \ddots & \vdots \\ P_{D,1,j} & P_{D,2,j} & \cdots & P_{D,D,j} \end{pmatrix}. \tag{3.1}$$

Particularly, each column of $\mathbf{\Psi}_j$ corresponds to the RSSI from a MS at the corresponding RP. We denote the t-th RSSI sample the j-th BS receives from a node at location k as $P_{t,k,j}$.

To perform localization, we discretize the spatial space and therefore, we consider the finite set of cells $\mathcal{C} = \{p_1, p_2, \ldots, p_D\}$, where D is the number of RPs. The sparse vector $\boldsymbol{b} \in \mathbb{R}^D$ selects elements from $\mathcal{C}$. Particularly, a non-zero component in $\boldsymbol{b}$ at the i-th position

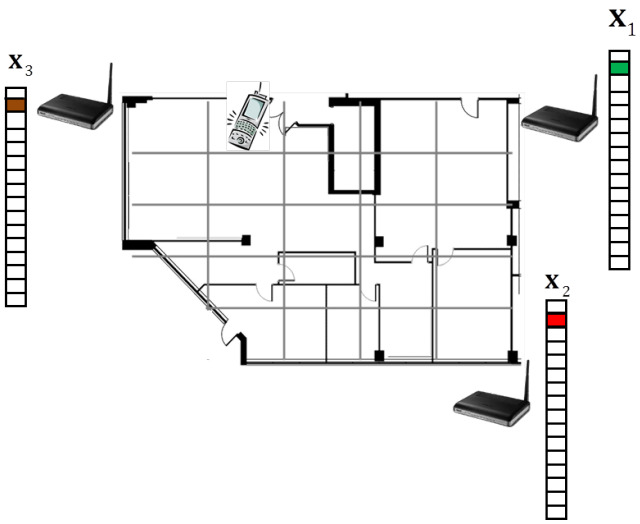

FIGURE 3.2: Common sparse support set in an indoor environment. Each BS receives signal-strength vectors $\boldsymbol{x}$ on its local grid. Each vector has non-zero coefficient at the position occupied by the MS.

indicates the presence of a mobile node at cell p_i. For instance, the vector

$$\boldsymbol{b} = [0, 0, 1, \ldots, 0]^T, \tag{3.2}$$

indicates that the node is located at cell p_3. Using the above notation, we can express the received signal strength measurements $\boldsymbol{x}_j$ received at the j-th BS as:

$$\boldsymbol{x}_j = \boldsymbol{\Psi}_j \boldsymbol{b}, \tag{3.3}$$

where $\boldsymbol{b}$ is supported on the same $\mathcal{C}' \subset \mathcal{C}$ and $|\mathcal{C}'| = 1$.

Compressed Sensing exploits sparsity in the spatial domain to acquire a signal representation without collecting D samples [35]. The main goal to efficiently perform location sensing, translates to the accurate detection of the non-zero coefficient of the sparse vector $\boldsymbol{b}$. In this work, we exploit the joint sparsity structure of the received signals $\boldsymbol{x}_j$ at the BSs (cf. Fig. 3.2) to provide accurate location estimations. The key observation is that the BSs share a common sparse support set, as each received signal $\boldsymbol{x}_j$ has non-zero coefficient at the position occupied by the MS.

The sparse coefficients of $\boldsymbol{b}$ for AP j, can be detected by considering M linear projections $y_j(m) = \langle \boldsymbol{x}_j, \boldsymbol{\phi}_{m,j}^T \rangle$ of the signal $\boldsymbol{x}_j$ into M measurement basis vectors $\{\boldsymbol{\phi}_{m,j}\}_{m=1}^M$. The symbol T denotes the transpose of the vector and $\langle \cdot, \cdot \rangle$ denotes the inner product. We can represent the measurement $y_j(m)$ in a $M \times 1$ vector $\boldsymbol{y}_j$ and the measurement basis vectors $\boldsymbol{\phi}_{m,j}^T$ as rows in a $M \times D$ matrix $\boldsymbol{\Phi}_j$. An essential requirement is that the rows

$\{\phi_{m,j}\}$ of $\mathbf{\Phi}_j$ cannot sparsely represent the columns $\{\psi_{i,j}\}$ of $\mathbf{\Psi}_j$ (incoherence property). It has been proven that independent and identically distributed (i.i.d.) Gaussian or Bernoulli vectors provide universal measurement bases that are incoherent with any basis matrix $\mathbf{\Psi}_j$ with high probability (universality property) [36].

In the proposed algorithm, each AP constructs a random measurement matrix $\mathbf{\Phi_j} \in \mathbb{R}^{M_j \times D}$, where $M_j = rD$ is the number of CS measurements, $M_j \ll D$ and r is the sampling factor. For simplicity and without loss of generality we choose $M_j = M, \forall j \in \mathcal{J}$. The measurement matrix $\mathbf{\Phi}_j$ contains i.i.d. random variables from a Gaussian probability density function with mean zero and variance 1/D in order to satisfy the property required by the CS theory.

During runtime the location estimation procedure takes place. Particularly, each AP receives M runtime RSSI measurements $\boldsymbol{y}_j = [P^R_{j,1}, \ldots, P^R_{j,M}]^T_{(1\times M)}$ from the mobile device, where $P^R_{j,i}$ indicates the i-th sample received at the j-th AP. The runtime measurements can be formulated as:

$$\boldsymbol{y}_j \;=\; \mathbf{\Phi}_j \boldsymbol{x}_j \;=\; \mathbf{\Theta}_j \boldsymbol{b}, \qquad \forall j \in \mathcal{J}, \tag{3.4}$$

where $\mathbf{\Theta}_j \;=\; \mathbf{\Phi}_j \mathbf{\Psi}_j$.

The sparsity pattern vector b can be found from the set of samples from all the APs by solving the following ℓ_1 optimization problem

$$\hat{\boldsymbol{b}} = \arg\min \|\boldsymbol{b}\|_1 \;\; s.t. \|\boldsymbol{y}_j - \mathbf{\Theta}_j \boldsymbol{b}\|_2^2 < \epsilon, \forall j \in \mathcal{J}, \tag{3.5}$$

where ϵ defines the environmental noise level.

A CS based localization protocol aims to reduce the total number of measurements needed. Considering M compressive measurements, the original sparse vector $\boldsymbol{b}$ can be recovered by a number of different approaches that solve the ℓ_1 optimization problem (3.5). Greedy sparse recovery algorithms compute the support of the signal iteratively and can be also very efficient and computationally flexible in case the signal of interest is highly sparse.

The solution of an ℓ_1- minimization problem can accurately recover a K-sparse signal with hight probability using only $M \geq K \log(D/K)$ i.i.d. Gaussian measurements [35]. The Basis Pursuit (BP) [50] algorithm formulates the reconstruction problem with equality constrains and solves it through the interior-point method. BP is precise but slow in general and thus not applicable in real world case scenarios. Additionally, algorithms such as the Orthogonal Matching Pursuit (OMP) [76, 77], identify the basis vectors that are most correlated with the signal, in a greedy way. OMP provides fast solutions, compared to BP, but it fails to converge with high probability [78]. Simultaneous Orthogonal Matching Pursuit (SOMP) [79] gives simultaneous sparse approximations by identifying one coefficient of the sparse vector at a time. Specifically, the Distributed Compressed Sensing theory [57], adopts the SOMP algorithm to recover, from incoherent measurements, an ensemble of signals sharing a common sparse structure, at a single collection point.

Algorithm 1 Centralized Localization via Jointly Compressed Sensing

Training phase

- Each BS collects RSSI fingerprints to capture the physical space via the $\mathbf{\Psi}_j$ basis matrix.
- Each BS creates a measurement matrix $\mathbf{\Phi}_j$.
- The central unit collects the projection of the RSSI fingerprints into the incoherent basis $\mathbf{\Phi}_j$, ($\mathbf{\Theta}_j = \mathbf{\Phi}_j \mathbf{\Psi}_j$).

Runtime phase

- Each BS samples locally RSSI measurements to collect $\boldsymbol{y}_j$.
- The central unit collects the runtime measurements $\boldsymbol{y}_j$ from the BS and applies the JDCS algorithms to estimate centrally the position of the MS.

The main goal, i.e., to efficiently perform location sensing, translates to the accurate detection of the non-zero coefficient of the sparse vector $\boldsymbol{b}$. In the following the centralized localization scheme based on jointly detection compressed sensing is presented.

3.2 Centralized localization scheme

In a typical localization scenario, the BS sample signals transmitted from the MS are individually sparse in a certain basis and also correlated among the BSs. The centralized CS-based localization scheme aims to exploit the spatial correlations among the measurements in order to jointly estimate the sparse coefficients in a central unit (Algorithm 1) [37].

During the training phase, each AP collects RSSI measurements for a period of time to create a signature map of the space, as it was described in (3.1). Moreover, the construction of a measurement matrix $\mathbf{\Phi}_j$ is essential in order to effectively implement the CS methodology. The corresponding measurement matrix $\mathbf{\Phi}_j$ follows the properties implied by the CS theory for accurate reconstruction (cf. Section 3.3.1). Upon completion of the signal acquisition procedure, each AP projects its signal into the incoherent basis and then transmits the resulting coefficients to the central unit.

During the runtime phase, the central unit collects the RSSI runtime measurements $\boldsymbol{y}_j$ from the APs (cf. Figure 3.3). The localization process is performed in the central unit where the location of the MS is jointly estimated via an iterative *Joint Detection Compressed Sensing* (JDCS) algorithm (Algorithm 2).

The key observation is that all $\boldsymbol{x}_j$ signals received at the APs are 1-sparse and are constructed from the same elements of the signature basis matrix $\mathbf{\Psi}_j$ but with different coefficients. Exploiting this insight, the JDCS algorithm aims to detect the sparse coefficients of vector $\boldsymbol{b}$ that correspond to the estimated position of the user based on the common sparse support set among the J APs. Particularly, in Step 1 of Algorithm 2, the sparse coefficient

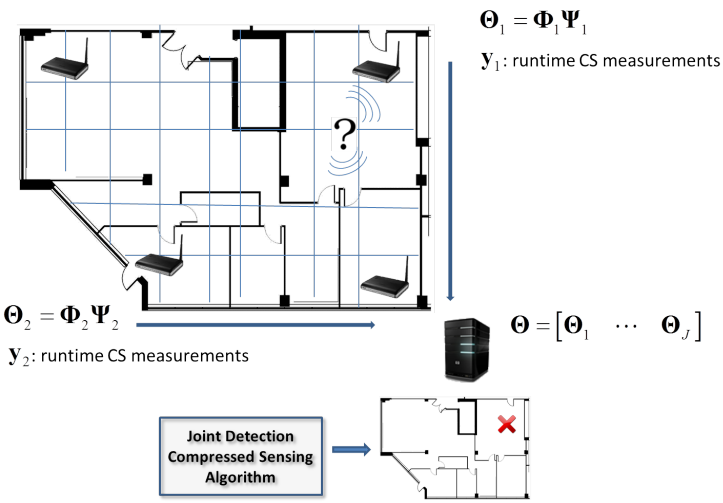

FIGURE 3.3: Runtime phase of the proposed centralized Joint Detection Compressed Sensing localization framework.

vector $\boldsymbol{b}_j$ is estimated for each AP. Because of the joint sparsity, the index of the maximum value of the $\boldsymbol{b}_j$ vectors should ideally coincide $\forall j \in \mathcal{J}$. However, in non-stationary indoor environments radio propagation suffers from dense multipath effects causing fluctuations of the received runtime measurements and thus resulting in non accurate position for each BS. To alleviate this effect, Step 2 estimates cumulatively the global energy of the sparse signal $\boldsymbol{b}$. Finally, in Step 3, the position of the MS is detected as the index that corresponds to the coefficient of the vector $\boldsymbol{b}$ that holds the maximum global energy. The localization algorithm returns the set $\mathcal{C}'$ that contains the estimated position p_i.

Algorithm 2 JDCS

Inputs: $\mathbf{\Theta}_j$, RSSI measurements $\mathbf{y}_j$, $j = 1, \ldots, J$.
Outputs: Support set $\mathcal{C}'$

1. $\mathbf{b}_j \leftarrow \mathbf{\Theta}_j^T \mathbf{y}_j, \quad \forall j \in \mathcal{J}$
2. $\mathbf{b} = \sum_{j=1}^{J} \mathbf{b}_j$
3. $p_i = \arg\max \mathbf{b}$
4. $\mathcal{C}' \leftarrow [p_l]$

return $\mathcal{C}'$

3.2.1 Experimental results

In this Section we study the effectiveness and the properties of the proposed centralized JDCS approach. As metric we consider the location error defined as the Euclidean distance between the estimated position of the mobile node and the true one. To explore the robustness of the proposed scheme we consider different RSSI variations characteristics. To this aim we collect real RSSI measurements at a laboratory area of $7m \times 12m$. For this area, a grid-based structure was considered with cells of size $55cm \times 55cm$. During the training phase, RSSI observations were recorded from 109 different cells. At each cell we record 109 samples (one sample per second). If no RSSI observations are found for a candidate location in the grid the corresponding RSSI entry in the signature map is set to -100 dBm. The experiment involved a total of 13 access points. The effectiveness of the proposed method was compared to the traditional K-nearest Neighbour localization technique that has been adopted by various localization systems [16, 12]. The 109 grid cells with prior known positions were chosen as test points. To evaluate the performance of the algorithm under different shadowing effects, we added Gaussian noise to the observation vector $\boldsymbol{x}$.[1]. Figure 3.4

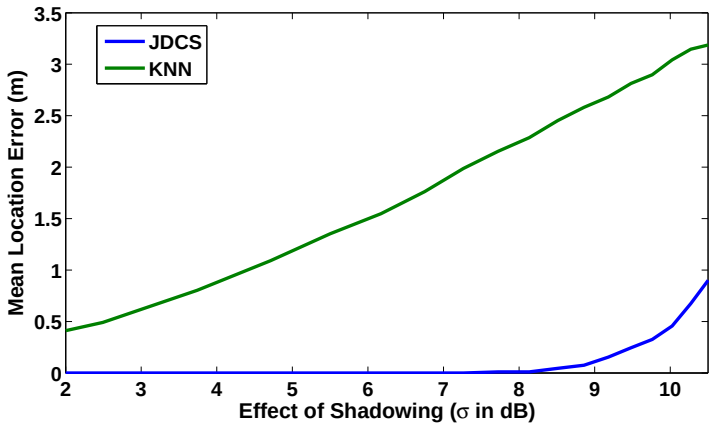

FIGURE 3.4: Mean location error for the KNN and JDCS methods under various environmental conditions. The JDCS algorithm has better performance in all cases.

indicates the effectiveness of the proposed framework when compared to the KNN method for different shadowing effects (σ in dB). Figure 3.4 shows that for a certain environmental conditions (i.e. shadowing effects), the proposed JDCS method achieves a significant reduction in the location error when compared to the KNN localization technique. Particularly, in dynamic indoor environments ($\sigma = 11$), we observe that the proposed algorithm cuts the mean location error by approximately 67% of the value corresponding to the KNN

[1] Following the channel model for signal propagation presented in [80] the shadowing variable is a zero-mean Gaussian distributed random variable (in dB) with standard deviation σ (dB)

algorithm. The ability of the JDCS algorithm to restrain the noise features is essential since non-stationary indoor environments suffer from unexpected radio propagation effects.

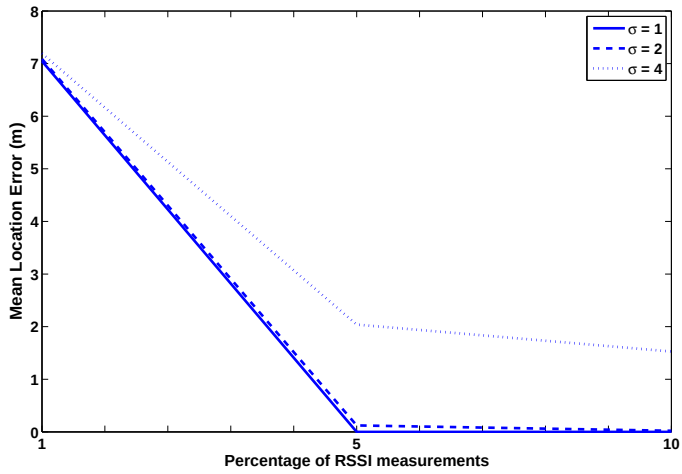

FIGURE 3.5: Mean location error for different percentage of RSSI runtime measurements for the Joint Detection Compressed Sensing localization under different shadowing effects.

The effect of the number of measurements in the estimated accuracy is further examined in terms of the mean location error under environmental conditions. Figure 3.5 indicates the corresponding mean location error as a function of available RSSI runtime measurements. We observe that the mean location error decreases as the number of measurements increases and increases with decreasing environmental noise. This behaviour is expected as the accuracy of the compressed sensing based algorithm is affected by the increase of noise level and the number of measurements. Specifically the number of measurements is highly connected with the sparsity of the signal. The localization problem presents the highest level sparsity (1-sparse vector) and thus the JDCS algorithm achieves its desired accuracy with only 5% to 10% of the runtime RSSI measurements.

Finally, Figure 3.6 illustrates the empirical CDF curves $(P(|X| \leq x))$ of the localization error for the two methods and a case of non-stationary environmental conditions (the variance of the shadowing variable for the signal propagation channel model is 10). JDCS employs 10% of the available runtime RSSI measurements. We observe that 73% of the time the location error of JDCS is almost zero. On the contrary, the median location error (*i.e.*, the value bellow which 50% of the location error fall), is 3 m for the KNN localization method.

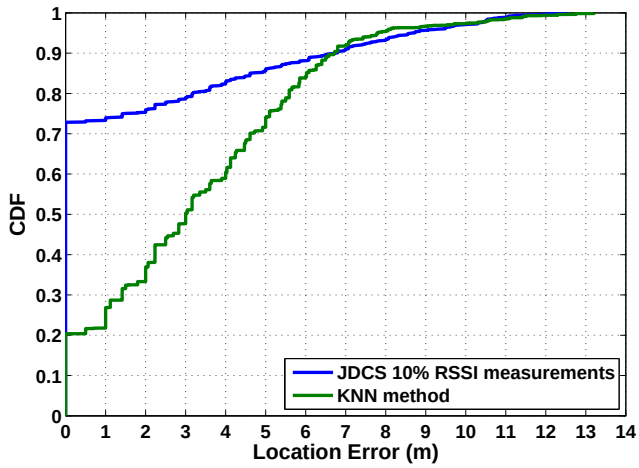

FIGURE 3.6: CDF curves ($P|X| \leq x$) for two methods for non stationary environmental conditions. JDCS considers only 10% of the available runtime RSSI measurements. Observe that the JDCS algorithm estimates precisely the true location of the user for 73% of the time.

3.3 Decentralized localization

In the previous section we introduced a centralized CS signal strength based localization scheme that considers the measurements received at the BSs and offers accurate position estimation by means of a limited amount of signal strength measurements. According to our centralized protocol all local samples are sent to a central unit to perform sparse signal recovery via JDCS.

However, centralized approaches exhibit several potential drawbacks. Specifically, they cannot handle the problem of single point failure, that is, if the central unit fails, the system becomes inoperative and location sensing impossible. Indeed, in a dynamic wireless scenario one can expect the possibility of a breakdown or the inaccessibility of the existing infrastructure and subsequently the inability of a centralized algorithm to adapt to a collapse (*e.g.*, power or network outage). Moreover, traditional fault tolerance techniques, such as server failover, are still sensitive to large-scale outages of electrical power or the wired network infrastructure.

Hence, to prevent extra cost of using additional back-up servers, we propose to exploit the available infrastructure by performing localization at the BSs which form the wireless backbone of the network (wireless mesh routers, wireless APs, sensor nodes). A decentralized localization protocol provides flexibility to the network administration since position estimations are distributed over the network and thus are accessible from each individual BS.

Considering the above observations, in this section we develop a novel *decentralized fingerprint-based CS signal strength localization* scheme that makes use of the signal correlation structures among the received measurements. In contrast to existing fingerprint based approaches, we consider both intra- and inter- signal correlation structures among the received signal strength measurements. An accurate positioning is therefore provided using only a limited amount of runtime measurements. Exploiting the joint sparsity of the signal ensemble, the proposed method builds on *gossip consensus* based approaches to distribute decision estimations in the network. Recently, gossip algorithms have received a great deal of attention in wireless networks because they possess certain desired operational attributes, such as simplicity, scalability, and robustness [81].

The proposed localization algorithm can be applied to the infrastructure network of a building, *e.g.*, a wireless distribution system (WDS) or a wireless mesh network (WMN) [82], where indoor navigation is mandatory. Our approach will be beneficial to environments where wired networks are not applicable or not easily set up, as for example in military or emergency (fire/safety/rescue) fields. On the other hand, in cases where the robustness of the location infrastructure is at stake, the decentralized version of the proposed localization protocol will allow each BS to estimate the position of the mobile user locally.

3.3.1 Proposed decentralized localization approach

Consider the network of J wirelessly connected BSs modeled by a network graph $\mathcal{G}(\mathcal{J},\mathcal{I})$ where $\mathcal{J} =: \{1,\ldots,J\}$ is the set of BSs and $\mathcal{I} = \{(j,k) : j,k \in \mathcal{J}\}$ is the set comprising the bi-directional links between the BSs. Graph $\mathcal{G}$ is assumed connected, meaning that data at any BS can become available to any other BS generally through a multi-hop path of $\mathcal{G}$.

Suppose that there is a MS equipped with an active wireless adapter card. A BS that listens to a channel, collects the packets transmitted from the MS, at that channel and records its RSSI values. Details concerning the characteristics of RSSI can be found in [83]. Given that the BS vendor provides the appropriate API, the RSSI information on the BS's hardware can be retrieved with high level programming.

The new localization scheme that we introduce in this section, exploits the spatial correlations among the measurements received at the J BSs and efficiently disseminates them throughout the network using a gossip algorithm. The goal is to allow *every BS* to have an estimation of the sparse coefficient vector when the algorithm terminates. Thus at convergence, all BSs should have knowledge of the mobile device position.

The fingerprinting-based system is characterized by two phases (Algorithm 3). During the training phase, each BS collects RSSI measurements for a period of time to create the signature map of the physical space $\mathbf{\Psi}_j \in \mathbb{R}^{D\times D}$, as it was described in (3.1). Moreover the construction of a measurement matrix $\mathbf{\Phi}_j \in \mathbb{R}^{M\times D}$ is essential in order to effectively implement the CS methodology. Each BS constructs a random measurement matrix $\mathbf{\Phi}_j \in \mathbb{R}^{M_j\times D}$, where $M_j = rD$ is the number of CS measurements, $M_j \ll D$, and r is the

Algorithm 3 Distributed Localization via CS

Training phase

- Each BS collects RSSI fingerprints in order to capture the physical space via the $\mathbf{\Psi}_j$ basis matrix.
- Each BS creates a measurement matrix $\mathbf{\Phi}_j$.

Online phase

- Each BS samples locally RSSI measurements to collect $\boldsymbol{y}_j$.

1. Each BS computes the correlations among the runtime measurements and the basis matrix $\mathbf{\Psi}_j$.
2. Update the estimations of the BSs via average consensus.
3. Upon convergence, each BS obtains the global estimation of mobile user's location.

sampling factor. For simplicity and without loss of generality, we choose $M_j = M, \forall j \in \mathcal{J}$. The measurement matrix $\mathbf{\Phi}_j$ contains i.i.d. random variables from a Gaussian probability density function with mean zero and variance 1/D in order to satisfy the property required by the CS theory. We recall that D is the number of the RPs.

During the online phase, the location estimation procedure is executed. Particularly, each BS receives M runtime RSSI measurements $\boldsymbol{y}_j = [P^R_{j,1}, \ldots, P^R_{j,M}]^T_{(1\times M)}$ from the mobile device, where $P^R_{j,i}$ indicates the i-th sample received at the j-th BS. The runtime measurements can be expressed as:

$$\boldsymbol{y}_j = \mathbf{\Phi}_j \boldsymbol{x}_j = \mathbf{\Theta}_j \boldsymbol{b}, \qquad \forall j \in \mathcal{J}, \tag{3.6}$$

where $\mathbf{\Theta}_j = \mathbf{\Phi}_j \mathbf{\Psi}_j$. Then, distributed localization is performed in three stages, namely, *initial estimation*, *decision fusion*, and *fine localization*.

3.3.2 Initial estimation

In the first stage, the joint sparsity structure of the signal ensemble is observed independently at each BS to perform an initial estimation of the sparse vector $\boldsymbol{b}$. Each BS estimates its own sparse vector $\boldsymbol{b}_j$ in order to obtain locally a first guess of the atom that contributes the most energy to the runtime signal $\boldsymbol{y}_j$, according to:

$$b_{j,i} = \frac{< \boldsymbol{y}_j, \boldsymbol{\theta}_{j,i} >}{\|\boldsymbol{\theta}_{j,i}\|_2} \quad , \quad \forall i = 1, \ldots, D \quad \textit{and} \quad \forall j = 1, \ldots, J, \tag{3.7}$$

where $b_{j,i}$ are the coefficients of the vectors $\boldsymbol{b}_j$ and $\boldsymbol{\theta}_{j,i}$ are the columns of the matrix $\mathbf{\Theta}_j = [\boldsymbol{\theta}_{j,1}, \ldots, \boldsymbol{\theta}_{1,D}]$.

3.3.3 Decision fusion

In our physical set-up, the collected sparse signals $\boldsymbol{y}_j$ are constructed from the same basis elements of the signature map $\boldsymbol{\Psi}_j$ but with arbitrarily different coefficients. By taking advantage of this property, in the second stage, an *average consensus* algorithm is adopted to iteratively update the estimations at each BS.

At each iteration t, a BS j is chosen uniformly at random from the set $\mathcal{J}$, using the asynchronous time model described in [84], and randomly selects a BS k such that $(k, j) \in \mathcal{I}$. By executing a gossip algorithm, the estimations described in (3.7) are carried out locally to obtain a global decision. Here, we propose two different gossip variants to distribute the estimations $\boldsymbol{b}_j$ in the network.

First, consider the matrix $\boldsymbol{B}(0) = [\boldsymbol{b}_1(0), \boldsymbol{b}_2(0), \ldots, \boldsymbol{b}_J(0)]^T$ that gathers the initial values of each BS. Let $\boldsymbol{B}(t)$ denote the matrix that collects the current values of the averaged estimations. Gossip algorithms update their estimates linearly at each iteration t according to an averaging matrix $\boldsymbol{W}(t)$ such that:

$$\boldsymbol{B}(t) = \boldsymbol{W}(t)\boldsymbol{B}(t-1). \tag{3.8}$$

Pairwise Gossip considers random pairs of nodes that iteratively and locally average their estimations until convergence to the global estimate. Particularly, in each gossip round only the values of two BSs j, k are averaged. Consequently, the averaging matrix $\boldsymbol{W}(t)$ is

$$\boldsymbol{W}(t) = \boldsymbol{I} - \frac{(\boldsymbol{e}_j - \boldsymbol{e}_k)(\boldsymbol{e}_j - \boldsymbol{e}_k)^T}{2}, \tag{3.9}$$

where $\boldsymbol{e}_j = [0, \ldots, 1, \ldots, 0]^T$ is the $J \times 1$ unit vector that has the j-th component equal to 1 [85, 81]. $\boldsymbol{I}$ indicates the identity matrix. It is straightforward to observe that in Pairwise Gossip, the averaging matrix $\boldsymbol{W}(t)$ is doubly stochastic as it satisfies the following properties:

$$\boldsymbol{W}(t)\mathbf{1} = \mathbf{1} \tag{3.10a}$$

$$\mathbf{1}^T\boldsymbol{W}(t) = \mathbf{1}^T, \tag{3.10b}$$

where property 3.10a ensures that the global average is acquired and property 3.10b ensures stability. $\mathbf{1}$ represents a vector of ones. The distributed linear iteration (3.8) converges to the average, for any initial vector $\boldsymbol{b}_j(0) \in \mathbb{R}$ if and only if

$$\lim_{t\to\infty} \boldsymbol{W}(t) = \frac{\mathbf{1}\mathbf{1}^T}{J}. \tag{3.11}$$

Pairwise gossip fulfils the requirements of the decentralized localization estimation and it is

a simple algorithm which does not require global knowledge.

Selective Gossip solves the average consensus problem iteratively by adaptively determining which elements are significant and which are insignificant while gossiping [86]. In order to preserve bandwidth, the algorithm computes only the entries of a vector which are above a defined threshold. Specifically, two one-hop neighbors exchange information concerning only the components that at least one of them believes to be significant, resulting in fewer transmissions of the insignificant ones. In practice, the two-neighboring nodes exchange three transmissions as to inform each other about the components that they consider significant. Let $b_{j,i}$ denote the i-th component for the j-th BS. Then BS j and k update the significant components i for which either $|b_{j,i}(t-1)| \geq \tau$ or $|b_{k,i}(t-1)| \geq \tau$ by setting

$$b_{j,i}(t) = b_{k,i}(t) = \frac{1}{2}(b_{j,i}(t-1) + b_{k,i}(t-1)). \tag{3.12}$$

For values for which $|b_{j,i}(t-1)| < \tau$ and $|b_{k,i}(t-1)| < \tau$, no changes are performed. The threshold τ is defined as the d-th value of the vector $\boldsymbol{b}_j = [b_{j,max}, \ldots, b_{j,min}]$, where $b_{j,max}$ and $b_{j,min}$ is the maximum and minimum value of the vector $\boldsymbol{b}_j$, respectively. The d-th value is defined as $d = qD$, where q indicates the percentage of the decisions that will be exchanged at each gossip round.

Selective gossip converges in a global consensus [86]. The nature of the localization problem makes selective gossiping an appropriate technique for estimating the most significant coefficients in the sparse vector $\boldsymbol{b}$. Specifically, location sensing is based on the detection of the largest coefficient of the sparse vector $\boldsymbol{b}$, as it was described in Section 3.3.1. Thus, although all coefficients contain significant information, selective gossip gives more importance to the largest coefficients of the vector $\boldsymbol{b}$ and distributes them efficiently through the network.

3.3.4 Fine localization

Upon convergence of the average consensus protocol, each column of the matrix $\boldsymbol{B}(t)$ (cf. 3.8) contains the averaged estimations $\boldsymbol{b}_{ave}$ such that:

$$\lim_{t\to\infty} \boldsymbol{b}_{ave} = \frac{1}{|\mathcal{J}|} \sum_{j=1}^{J} \boldsymbol{b}_j(0). \tag{3.13}$$

Thus, the global estimation vectors $\boldsymbol{b}_{ave}$ have been distributed in the network to efficiently allow each BS to identify the coefficients with the largest magnitude. In the fine localization stage, each BS detects the position p_i of the mobile device as the index that corresponds to the largest coefficient of vector $\boldsymbol{b}_{ave}$.

$$p_i = \arg \max_{i=1,\ldots,D} \boldsymbol{b}_{ave}. \tag{3.14}$$

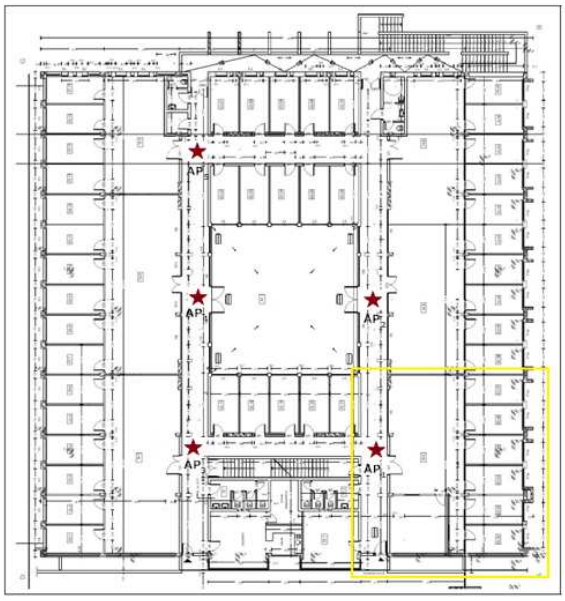

FIGURE 3.7: Experiment set up at FORTH. The stars indicate the position of the APs. The yellow block indicates the experimental area.

3.3.5 Experimental results

In this Section, we evaluate the performance of the proposed decentralized localization system. Real RSSI data were collected at the long hallway and the Telecommunications and Networks Lab (TNL) of FORTH, an area of $8.5m \times 14m$. For this area, a grid-based structure was considered with cells of size $55cm \times 55cm$. TNL is partitioned by 1.60m-height cubicle walls with hard-partioned offices and glass windows. The experiment involved a total of 5 APs (Cisco Aironet 1200 series APs, 802.11 b/g) placed on the same floor where TNL is located (Fig. 3.7).

The AP operating system, Cisco IOS, possesses a special command that enters the device in *scanner/monitor* mode. When the AP is in monitor mode, it receives packets that contain the RSSI information. In a real environment where the device is not transmitting enough packets per time unit, we trigger the device with the assistance of the infrastructure (*i.e.*, ping) to produce packet transmissions more frequently. Each AP uses the unique MAC address of the mobile device as a distinctive feature to recognize the packets of the transmitter that wants to be located. The signature maps were constructed during the training phase at various cells of the grid. Specifically, the RSSI observations were collected for a period of 20 seconds over 135 reference points ($D = 135$). The online observations were collected at a different period of time by the APs from the device at 30 unknown distinct cells in order to evaluate the performance of the system in a time-varying environment. The number of RPs and online observations is comparable to those reported in [87] and [28]. The performance

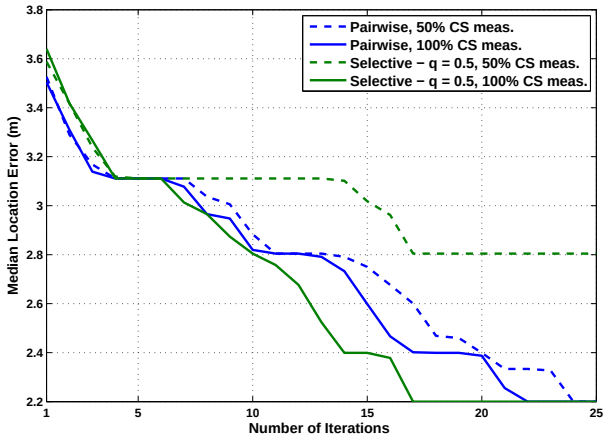

FIGURE 3.8: Median location error vs. the number of iterations for different gossip variants during decision fusion.

is evaluated in terms of the location error. The location error is defined as the Euclidean distance between the center of the estimated cell of the user location and the true cell where the mobile user was located during the runtime phase.

To evaluate the convergence of the proposed decentralized CS-based localization scheme, in Figure 3.8 we illustrate the median location error with respect to the number of iterations for the two gossip variants during decision fusion, for different number of CS measurements. It is reminded that the first iteration demonstrates the accuracy during the initial estimation while the last iteration shows the accuracy in fine localization. Figure 3.8 shows that the algorithm converges faster as the number of CS measurements increases. Selective Gossip algorithm transmits only a fraction of the decisions acquired during the initial estimation procedure, thus as the number of the exchanged values decreases the convergence time increases.

The effect of the number of CS measurements in the estimated accuracy is further examined for the Pairwise Gossip variant in terms of the location error. Figure 3.9 depicts the empirical CDF curve ($P(|X| \leq x)$) as a fraction of the number of the RSSI runtime measurements used during the fine localization phase ($M = rD$ with $r \in \{5\%, 10\%, 50\%, 100\%\}$). We observe that the location error of the decentralized scheme decreases as the number of measurements increases. This behavior is consistent with CS theory, as the accuracy of the recovery algorithm is affected by the number of CS measurements. Particularly, the 36th percentile of the location error for the CS Pairwise Gossip algorithm is almost zero with only 5% of the RSSI measurements. We note that 5% of the measurements corresponds to $M \approx 7$ which is above the minimum bound of $\log(D) \approx 7.08$, as required by the CS theory.

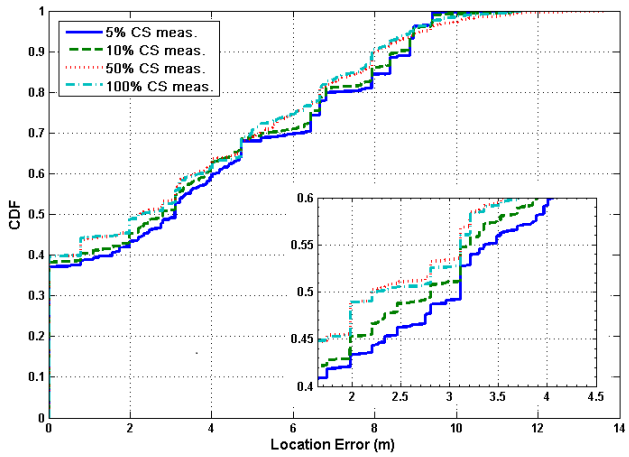

FIGURE 3.9: Empirical CDF curves of the Pairwise Gossip algorithm during the fine localization stage as a function of CS measurements.

Figure 3.10 depicts the median location error of the decentralized selective localization scheme as a function of q, the percentage of decisions exchanged at each gossip round. Varying q changes the localization accuracy. Specifically, as the number of exchanged decisions among the BSs decreases the location error increases. However, fewer transmitted values result in less energy consumption and bandwidth. Moreover, we observe that as the number of CS measurements increases the percentage of exchanged measurements among the BSs decreases.

Figure 3.11 compares the effectiveness of the proposed decentralized gossip based localization framework with two well-known localization algorithms, the KNN and the Bayesian classification methods. Only 10% of the total runtime RSSI measurements were employed by the proposed CS localization algorithm while both the KNN and the Bayesian classification methods used all the available RSSI measurements for location sensing. Figure 3.11 illustrates the empirical CDF curve for the different fingerprinting-based localization schemes. We notice that the proposed CS pairwise gossip-based algorithm leads to improvements in terms of median location error (*i.e.*, the value bellow which 50% of location errors fall) in the order of 40% for KNN and 30% for the Bayesian algorithm. It is shown that the decentralized selective-gossip algorithm provides effective location estimation, compared with the pairwise-gossip algorithm, while exchanging only 50% of the initial decisions.

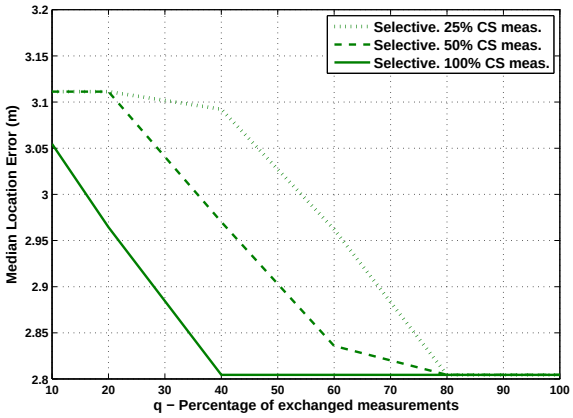

FIGURE 3.10: Median location error of the Selective Gossip algorithm during the fine localization stage as a function of transmitted estimations and for different CS measurements.

3.4 Discussion

In this Chapter, the framework of compressed sensing theory is exploited in order to perform accurate indoor localization based on received signal strength measurements, while reducing the amount of runtime measurements transmitted in the network. The key idea is that the location of the mobile station is sparse over the ground plane, *i.e* the mobile station can be in one location at each given time. Following this observation we reformulated the localization problem as a sparse approximation problem and the ℓ_1 minimization approach is exploited to recover the location of the user. The proposed fingerprint methods perform remote estimations by utilizing the RSSI measurements transmitted from the mobile station. The jointly compressed sensing localization algorithms rely on the observation that in the indoor localization problem the base stations capture signals that are sparse in the spatial domain but yet different propagation path losses cause distinct attenuations among the received measurements. According to the centralized localization protocol, all local RSSI runtime measurements are sent to a central unit to perform sparse signal recovery via jointly compressed sensing. The experimental results validated the proposed Joint Detection Compressed Sensing approach under various RSSI characteristics. Additionally we developed a novel fully decentralized cooperative CS localization scheme based on signal strength fingerprints. The localization procedure is performed at the BSs to eliminate the need for a central unit and requires a limited amount of signal-strength measurements for accurate positioning. The decentralized protocol exploits the signal correlation structures among the individual runtime measurements. Based on the joint sparsity of the signal ensemble among the BSs, it builds a gossip consensus approach to distribute decision estimations within the network. Upon convergence, all BSs have knowledge of the mobile device position. We

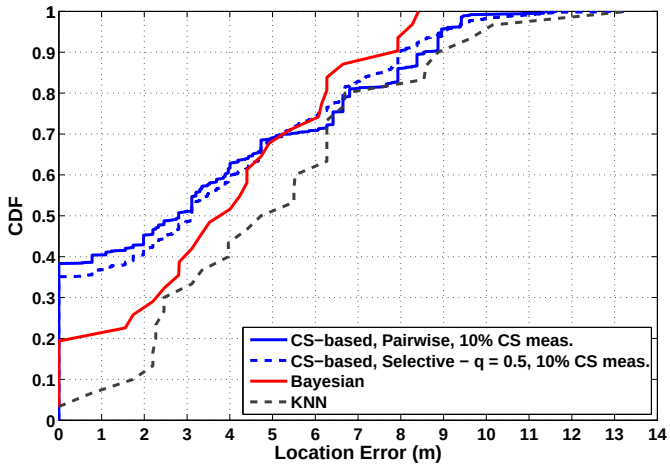

FIGURE 3.11: CDF curves for the fingerprint-based localization methods.

performed an evaluation of the decentralized localization scheme under two gossip based variants to effectively distribute the decisions in the network. The implementation results in the premises of FORTH reveal a superior performance of the proposed decentralized CS-based localization scheme when compared with related work.

Chapter 4

Localization in wireless networks via laser scanning and sparse Bayesian learning

In the previous Chapter we exploited the inherent sparsity of the user positioning in the spatial domain and we reformulated the location estimation as a sparse approximation problem. We introduced two localization algorithms that exploit the signal correlation structures among the individual runtime measurements received from the mobile user and are based on the joint sparsity of the signal ensemble among the base stations. From an application perspective, the jointly compressed sensing approaches provide accurate location estimations, compared to traditional localization methods, while minimizing significantly the number of measurements exchanged in the network during the location estimation phase.

WiFi fingerprint CS-based systems achieve high accuracy, however several issues concerning the calibration and location estimation phase can potentially limit the accuracy and scalability of these systems. Initially, effective location sensing requires the collection of a large number of representative training data to increase the localization accuracy, a task that demands substantial cost and labour. Furthermore, manual fingerprinting techniques that split the indoor environment into pre-defined grids are implicitly bounding the maximum achievable localization accuracy. Additionally, estimating the location of the user via sparsity seeking provides accurate estimations with the expense of creating a random measurement matrix required to provide the incoherent property with the signature space map. While Gaussian random matrices ensure sparse recovery, from an application point of view they can be limited used as no fast matrix multiplications are available and thus make them not desirable for large scale localization problems.

In this Chapter we address the aforementioned major issues by presenting WoLF, a Wireless localization and Laser-scanner assisted Fingerprinting system that provides autonomous signature map generation during the calibration phase. Additionally, we show

that WiFi localization on the generated high resolution maps can be performed by sparse reconstruction which exploits the peculiarities imposed by the physical characteristics of indoor environments. Specifically, a sparse Bayesian learning (SBL) approach is adopted in order to find the position of the mobile user and dynamically determine the sufficient number of access points (APs) required for accurate positioning. SBL employs a Bayesian formalism in order to robustly identify the location of the mobile station by solving an under-determined system of equations that arises during the location estimation phase. Compared to traditional deterministic sparse recovery techniques, the Bayesian framework presents desirable invariance properties leading to accurate estimations, without the need of a random Gaussian measurement matrix, especially for localization problems where where the spatial transform domain representation is highly structured [48],[49].

4.1 System overview

WoLF, the proposed localization system, provides an *automatic training phase* by employing a handheld laser-scanner based simultaneous localization and mapping (SLAM) system [88] combined with consumer-grade WiFi cards. During training, WoLF automatically gathers a map of the physical environment, localizes the user on this map and scans the WiFi channels in parallel. Based on the gathered fingerprint map, WoLF employs a Bayesian Compressed Sensing WiFi localization algorithm to localize a user during runtime. WoLF is also adaptive as it introduces a novel dynamic access point selection algorithm that determines the optimum number of APs required for localization. The automated training phase diminishes the practical barriers of state-of-art fingerprint based systems, while the sparse approximation approach to estimate the user location ensures an improved position detection accuracy.

Consider a typical WLAN scenario of J connected APs and one mobile station (MS), equipped with a wireless adapter card, which is carried by a person to be located. WoLF is based on the RSSI measurements transmitted from the APs and consists of two distinct phases.

4.1.1 Training phase

The goal of the training phase is to establish a mapping between the current user's position and the RSSI measurements on the wireless channel. To establish this mapping we used the hardware shown in Fig. 4.1. This hardware runs a SLAM-approach [88], in which the laser scans are stabilized with the included IMU. This returns the position and the map of the current environment at $40Hz$. The consumer-grade WiFi modules passively scan the surrounding WiFi networks, i.e. they constantly listen for beacon frames sent by the APs on a specified channel. This allows to gather a fingerprint map in a fine-grained spatial resolution ($5cm$), in the user's most natural movement patterns.

FIGURE 4.1: The handheld laser-scanner hardware comprising a low-cost MEMS Inertial Measurement Unit (IMU), an UTM-30LX LIDAR system and four commercial WiFi cards.

Since the sampling rate of the user's position is much higher than the achievable sampling rate of the WiFi networks, we decided to follow passive scanning approach. An active WiFi scan works by sending a beacon request on one of the 35 WiFi channels on the 2.4 and $5GHz$ bands and then listening on this channel for roughly $100 - 200ms$. It should be noted that, due to security reasons, most APs are not reacting to this beacon request and only send out beacon frames periodically. A full spectrum scan then takes between $3.5 - 7sec$. An average human has walked almost $11m$ in such a timespan, which would result in a low spatial resolution for the WiFi scans. To counteract this problem, we simply set the WiFi cards into passive mode on four fixed channels and only report the RSSI values of the periodically sent beacons of the APs. The period of these beacons is typically between $200ms$ and $1sec$ and we achieved sampling rates in our environment of $60 - 100Hz$ by passively scanning the WiFi network.

Even though the sampling rate is increased by the passive scanning approach, we still face the problem of incomplete RSSI measurement vectors. This is due to the fact that our position estimation is not synchronized with the WiFi scanning, i.e. the RSSI measurement vectors do not include all reachable APs at a certain location. To solve this problem the area is discretized into a finite set of cells of equivalent size and all measurement vectors in the same cell are gathered into vector $\mathbf{\Psi}_i = [P^t_{i,1}, \ldots, P^t_{i,J}]^T \in \mathbb{R}^J$. $P^t_{i,j}$ corresponds to the mean value of RSSI samples received from the j-th AP at grid point i during training. This reduces the spatial resolution of the fingerprint map, but allows for systems that assume a complete RSSI measurement vector at each position. The fingerprint map is represented by the matrix $\mathbf{\Psi} = [\mathbf{\Psi}_1 \ldots \mathbf{\Psi}_D]_{J \times D}$ where D is the number of the grid points. The localization server collects the fingerprint map in order to perform location sensing.

4.1.2 Runtime phase

During the runtime the MS scans the available channels to collect the runtime RSSI measurements. The MS creates the runtime measurement vector $\boldsymbol{y} = [P_1^r, \ldots, P_J^r]^T \in \mathbb{R}^{J\times 1}$, where P_j^r is the mean value of the RSSI measurements from the j-th AP during runtime.

The main goal is to determine the location of the user by identifying the cell in which he is located. We define the sparse vector $\boldsymbol{b} \in \mathbb{R}^D$ that has the dimensions of the physical space and a non-zero component in the corresponding occupied location. Consequently, we can express the set of the runtime measurements $\boldsymbol{y}$ as:

$$\boldsymbol{y} = \boldsymbol{\Psi}\boldsymbol{b} + \boldsymbol{\epsilon} \tag{4.1}$$

where $\boldsymbol{\Psi} \in \mathbb{R}^{J\times D}$. Indoor radio propagation is affected by multipath effects, a fact that results in differences between the training and runtime fingerprints corresponding to the same grid point. Particularly, the errors $\boldsymbol{\epsilon} \in \mathbb{R}^D$ are modelled probabilistically as independent zero-mean Gaussian, with variance σ^2, $p(\boldsymbol{\epsilon}) = \prod_{j=1}^{J} N(\epsilon_j|0, \sigma^2)$ and the parameter σ^2 can be estimated form the runtime measurements. Therefore, the following multivariate Gaussian likelihood model is implied:

$$p(\boldsymbol{y}|\boldsymbol{b}, \sigma^2) = (2\pi\sigma^2)^{-J/2} \exp\Big(-\frac{1}{2\sigma^2}\|\boldsymbol{y} - \boldsymbol{\Psi}\boldsymbol{b}\|^2\Big). \tag{4.2}$$

4.1.3 Location estimation via SBL

Estimating the location of the user translates to solving a linear regression problem with a sparsity prior on $\boldsymbol{b}$. The main objective, via the SBL approach, is to find a posterior density function for each location in the area of interest. To control the strength of the prior over each position a set of independent hyperparameters $\boldsymbol{\alpha} = (\alpha_1, \ldots, \alpha_D)^T$ is defined. Thus, the sparse prior of the vector $\boldsymbol{b}$ is expressed as:

$$p(\boldsymbol{b}|\boldsymbol{\alpha}) = (2\pi)^{-D/2} \prod_{i=1}^{D} \alpha_i^{1/2} \exp\Big(-\frac{\alpha_i b_i^2}{2}\Big). \tag{4.3}$$

The posterior distribution of the sparse vector $\boldsymbol{b}$ is expressed as a multivariate Gaussian distribution with mean and covariance:

$$\boldsymbol{\mu} = \alpha_0 \boldsymbol{\Sigma}\boldsymbol{\Psi}^T\boldsymbol{b} \tag{4.4}$$

$$\boldsymbol{\Sigma} = (\alpha_0 \boldsymbol{\Psi}^T\boldsymbol{\Psi} + \boldsymbol{A})^{-1} \tag{4.5}$$

where α_0 is the inverse of the noise variance σ^2 and $\boldsymbol{A} = diag(\alpha_1, \ldots, \alpha_D)$.

Thus, estimating the posterior distribution of the sparse vector requires the estimation of the hyperparameters $\boldsymbol{\alpha}$. A most probable point estimation α_{MP} is found via the Type II

maximum likelihood procedure. Type II techniques are of special interest as they can successfully recover sparse coefficients when the RIP is violated and the popular deterministic approaches fail to provide the sparsest solution [68]. The sparse Bayesian learning is formulated as the maximization with respect to α of the logarithm of the marginal likelihood:

$$\begin{aligned}\mathcal{L}(\boldsymbol{\alpha}) &= \log p(\boldsymbol{y}|\boldsymbol{\alpha}, \sigma^2) \\ &= \log \int_{-\infty}^{+\infty} p(\boldsymbol{y}|\boldsymbol{b}, \sigma^2) p(\boldsymbol{b}|\alpha) d\boldsymbol{b} \\ &= -\frac{1}{2}[N \log 2\pi + \log |\boldsymbol{C}| + \boldsymbol{y}^T \boldsymbol{C}^{-1} \boldsymbol{y}] \end{aligned} \tag{4.6}$$

where the matrix $\boldsymbol{C}$ is defined as:

$$\boldsymbol{C} = \sigma^2 \boldsymbol{I} + \boldsymbol{\Psi} \boldsymbol{A} \boldsymbol{\Psi}^T. \tag{4.7}$$

A critical observation is that after a number of iterations the values of many hyperparameters are infinite, resulting to a parameter posterior infinitely peaked at zero for a large number of locations. Consequently, the estimated location of the mobile user is the cell g that corresponds to the maximum component of $\boldsymbol{b}$ (*i.e.*, to the smallest a_i)

$$g = \arg\max \boldsymbol{b} = \arg\max p(\boldsymbol{y}|\boldsymbol{b}, \boldsymbol{a}, \sigma^2). \tag{4.8}$$

In order to solve eq. (4.6) the fast relevant vector machine (RMV) algorithm is developed. Fast RMV algorithm analyses the properties of the logarithm of the marginal likelihood. Particularly, it applies an efficient sequential addition and deletion of the candidate locations in the area of interest and monotonically maximizes the marginal likelihood. The algorithm operates in a constructive manner until the most probable location has been selected. Additionally, the inverse operation of the matrix Σ (eq. 4.5) is performed in a reduced complexity way. The complexity of the localization algorithm is proportional to the dimension of the space, i.e. $\mathcal{O}(D)$.

4.1.4 Dynamic AP selection via SBL

The server employs the proposed iterative Dynamic AP selection via SBL algorithm (Algorithm 4) in order to estimate the location of the MS and dynamically determine the sufficient number of APs required for localization. Particularly, it collects the runtime measurements $\boldsymbol{y}$ from the MS and estimates the sparsity pattern of the vector $\boldsymbol{b}$ from the fingerprint map $\boldsymbol{\Psi}$ by solving the following ℓ_1 minimization problem

$$\hat{\boldsymbol{b}} = \arg\min_{\boldsymbol{b}} (\|\boldsymbol{b}\|_1 + \rho \|\boldsymbol{y} - \boldsymbol{\Psi}\boldsymbol{b}\|_2^2) \tag{4.9}$$

where the factor ρ controls the sparseness of the signal (first term) and the relative impor-

Algorithm 4 Dynamic Access Point Selection via SBL

Input: fingerprint map $\boldsymbol{\Psi}$, runtime measurements $\boldsymbol{y}$, minimum number of APs k, threshold h.

Output: Optimum number of APs J_{opt}, estimated cell c

1. Apply the SBL reconstruction method to estimate $\hat{\boldsymbol{b}}$ via (4.9)

if $|\sqrt{diag(\boldsymbol{\Sigma})} - h| \leq \eta$ **then**

  $J_{opt} \leftarrow k$; $c = \arg\max \hat{\mathbf{b}}$;

else

  $k = k + 1$; go to 1;

end if

return J_{opt}, c;

tance of the reconstruction error (second term). The Bayesian framework is adopted in order to solve the optimization problem (4.9).

The SBL approach provides confidence intervals that benefit the construction of stopping criteria that determine the optimum number of APs, *i.e.* the number of measurements. Particularly, the optimum number of APs is defined dynamically when the absolute difference of the variance of the recovered vector $\hat{\boldsymbol{b}}$ from the predefined threshold h does not exceed a positive constant η. The variance of the recovered vector is defined as the square root of the diagonal elements of the covariance matrix (eq. 4.5). The estimated cell is detected as the index that corresponds to the largest coefficient of vector $\boldsymbol{b}$.

4.2 Experimental results

The effectiveness of proposed WoLF localization system employing the SBL approach is studied via real time experiments performed at the floor of TU Darmstadt, spanning an area of $100m \times 12m$ (c.f Figure 4.2).

The purpose of the experiment is to evaluate the accuracy of the proposed system under different environmental parameters. During the training phase, we performed two random walks in order to collect RSSI observations via the laser mapping (cf. Fig 4.1). From the 10755 measurement points, we extracted 206 different location cells. In total 64 APs were involved. We compare our proposed approach with the KNN localization method under different parameters, and define the location error as the Euclidean distance between the center of the estimated cell and the position measured by the laser mapping system.

The laser mapping utilized during the training phase provides a dense training map. We validated the accuracy of the proposed SBL localization method under various cells sizes. Figure 4.3 demonstrates the mean location error for the SBL and KNN techniques as a function of the grid size. We observe that as the grid spacing increases, the localization

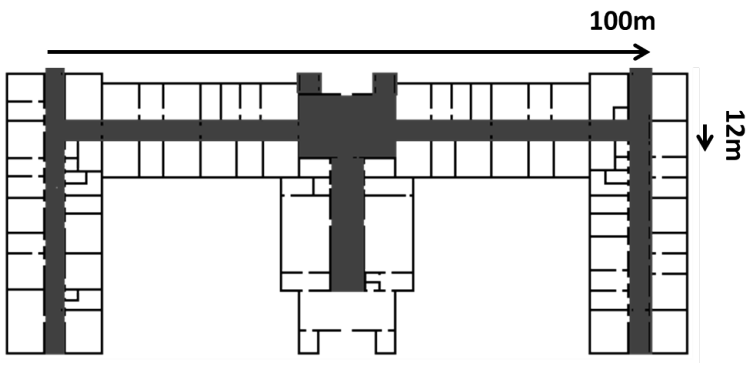

FIGURE 4.2: Experiment set up at Technical University of Darmstadt. The grey corridors indicate the experimental area.

accuracy decreases. This behaviour is expected since by increasing the discretization of the physical space, the distance between the center of the estimated cell and the real location of the user decreases, given that the localization system has high accuracy. We observe the robustness of the proposed SBL localization approach under the different resolution levels for the physical space. One should keep in mind that high space resolution increases the computational complexity as the dimension of space increases.

Figure 4.4 indicates the mean localization error for the SBL and the KNN algorithms as a function of the number of APs and for grid space equal to one meter. The localization error decreases as the number of APs increases. Interestingly, the localization performance is not affected after a certain number of APs (6 in our experiment). The proposed SBL algorithm identifies the optimum number of APs by adopting the dynamic AP selection algorithm. Particularly, when the average error bars reach the required threshold, the number of APs is enough in order to achieve the desired accuracy. Table 1 indicates the average error bars as a function of the number of APs. As the number of APs increases, the variance decreases.

Number of APs	3	4	5	6	7
Mean error bars	0.073	0.064	0.062	**0.0523**	0.0521

TABLE 4.1: Mean error bars vs. the number of APs

Figure 4.5 presents the performance in terms of localization error CDF curve $(P|X| \leq x)$ for the two positioning techniques. The proposed SBL dynamic AP selection algorithm stops at the iteration when the average error bar reaches as low as the threshold $h = 0.052$. On the contrary, the KNN algorithm utilizes all the available APs. The average number of detectable APs per cell is 24. The proposed dynamic AP selection algorithm utilizes on

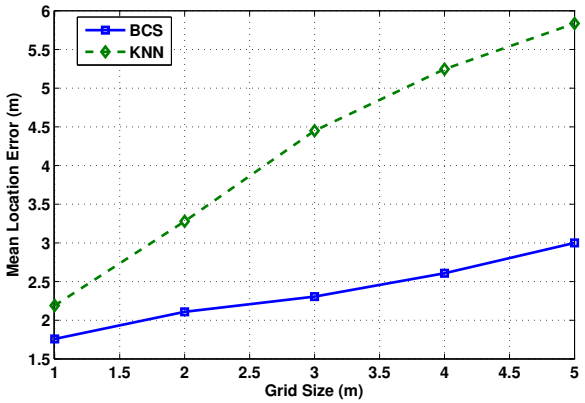

FIGURE 4.3: Location error for the SBL and the KNN localization techniques as a function of the grid size.

average 25% of the available APs. We observe that the median location error (*i.e.* the value below which 50% of the location errors fall) is $1.4m$ for the SBL algorithm vs. $2.7m$ for the KNN approach.

4.3 Discussion

In this Chapter we proposed WoLF, a combination of a handheld laser-based simultaneous localization, mapping (SLAM), and WiFi localization system based on Bayesian Compressed Sensing. WoLF allows to accelerate the cumbersome procedure of spatially sampling the WiFi RSSI signal (i.e. building fingerprint maps) while also retaining a high spatial resolution concerning the user's position. We argued that discretizing an indoor environment into predefined grids, as usually done for evaluating RSSI localization systems, bounds the maximum achievable localization accuracy.

For accurate location estimation, we proposed a SBL approach. The proposed localization approach can handle the correlation features presented in the computed signals while is able to select the most significant APs, thus decreasing the overall localization error. The results revealed the superiority of the proposed technique over the KNN localization method in the experimental setup.

However, WoLF is not without limitations. Currently only maps with a fixed height can be mapped, i.e. only single floors. Additionally, one major problem is the comparatively slow WiFi scanning procedure. In a standard environment with no access to the WiFi access points the security hardening, i.e. sending beacons only periodically, cannot be solved. Access to the provided WiFi network is mandatory to achieve a high rate of RSSI measure-

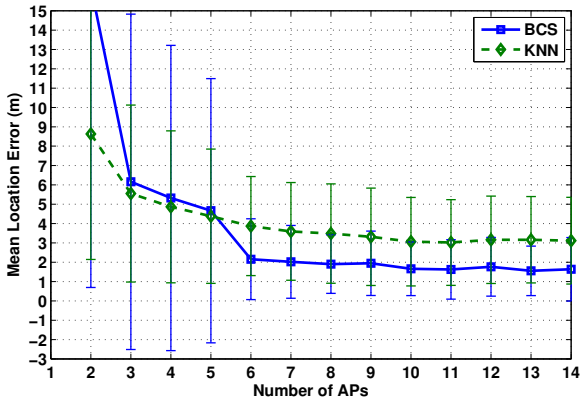

FIGURE 4.4: Impact of the number of APs on the localization error for the SBL and the KNN localization algorithms.

ments. This would ultimately lead to a handheld system which can map, localize and collect fingerprints of a building in a single run with high precision.

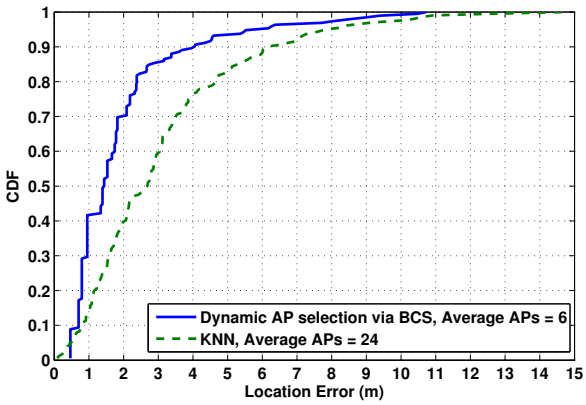

FIGURE 4.5: CDF of localization error for the SBL and KNN algorithms. The proposed Dynamic Access Point selection algorithm utilizes on average 25% of the APs.

Chapter 5

Efficient multi-channel signal strength based localization via matrix completion and Bayesian sparse learning

Fingerprint-based location sensing techniques play an increasingly important role in pervasive computing applications since they require minimal modifications to the existing wireless infrastructure. However, typical fingerprint-based schemes implicitly assume that communication occurs over the same frequency channel during the training and the runtime phases. When this assumption is violated, the mismatches between training and runtime fingerprints can significantly deteriorate the localization performance. Additionally, the exhaustive calibration procedure required during training limits the scalability of this class of methods. In this Chapter, we propose a novel, scalable, multi-channel fingerprint-based indoor localization system that employs modern mathematical concepts based on the Sparse Representations and Matrix Completion theories. The contribution of our work is threefold. First, we investigate the impact of channel changes on the fingerprint characteristics and the effects of channel mismatch on state-of-the-art localization schemes. Second, we propose a novel fingerprint collection technique without the need of additional hardware that significantly reduces the calibration time by formulating the map construction as an instance of the Matrix Completion problem. Third, we propose the use of sparse Bayesian learning to achieve accurate location estimation. Experimental evaluation on real data highlights the superior performance of the proposed framework in terms of reconstruction error and localization accuracy.

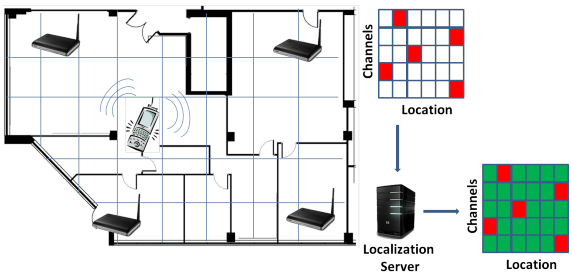

FIGURE 5.1: A visual illustration of the fingerprint collection process during the training phase. Each Access Point (AP) records packets transmitted from the mobile device from multiple locations and at different channels. The incomplete signature maps are sent to the Localization Server which performs the MC based reconstruction to complete the missing entries. Note that the incomplete matrix shown in the figure corresponds to a single AP.

5.1 Overview of the proposed scheme

Our proposed multi-channel localization scheme consists of two phases: the training phase and the runtime phase. We propose a reduced effort training phase where random channel sub-sampling is performed in order to collect RSS measurements on a grid of reference points, from a subset of the available channels. The LS takes the partial signature maps and applies the proposed Matrix Completion (MC)-based recovery technique in order to estimate the unobserved measurements and to build the complete channel-set signature map. A visual illustration of the training process is shown in Figure 5.1.

During the runtime phase, the APs collect RSS measurements from the MS operating at a specific frequency, and location estimation is performed using the part of the signature map associated to that frequency. A major contribution of this work is that we introduce for the first time a frequency-aware fingerprint-based localization system. Although the selected channel during runtime may be different from the one used during training, our MC approach provides the appropriate matching RSS measurements for localization. Furthermore, we propose a sparse Bayesian learning technique where localization estimates are obtained by searching for the sparsest solution of an underdetermined system of equations. An illustrative example of the runtime process is shown in Figure 5.2.

The proposed multi-channel localization scheme was evaluated on real RSS measurements collected at the Institute of Computer Science (ICS) of the Foundation for Research and Technology-Hellas (FORTH).

Our proposed localization scheme offers many advantages over current state-of-the-art techniques. In short, the main contributions of our system are:

- We explore the effect of multiple wireless frequency channels on RSS based fingerprint localization. This marks a significant departure from typical localization

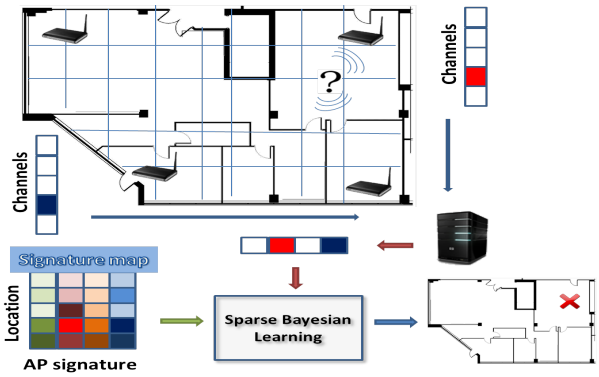

FIGURE 5.2: A visual illustration of the localization process. Only the second (top right) and the fourth (bottom left) APs are in the same channel as the MS and collect runtime RSS measurements. The runtime measurements and the dictionary corresponding to the active channel are utilized by the SBL algorithm to identify the unknown location of the MS.

schemes that do not consider channel mismatch between the training and the runtime phase.

- We propose a novel training scheme, based on Matrix Completion, for efficiently generating a complete (across space and frequency) training signature map by randomly sub-sampling the available channels at various locations. The proposed training scheme substantially reduces the effort and time spent during training.
- Motivated by the inherent sparsity of indoor localization, we propose a novel location sensing technique based on Sparse Bayesian Learning (SBL). SBL is able to robustly identify the MS location by solving an under-determined system of equations arising from the recovered measurements.
- We experimentally validate our claims on real data collected from an active indoor office area. These experimental data allow the quantification of the effects of multiple channels on both state-of-art and the proposed technique.

5.2 Motivation

In this section, we present illustrative examples that highlight two major issues that affect multi-channel fingerprint based positioning. First, we discuss the effect of channel frequency changes on the RSS measured values and the implication of this phenomenon on localization systems. Second, we describe the spatio-frequency correlations of the RSS measurements and we provide motivation for utilizing these correlations to reduce the time and effort of the training procedure.

5.2.1 Multichannel RSS model

Efficient channel assignment in IEEE 802.11 WLANs is critical in order to minimize the interference degradation between adjacent APs. Dynamic channel allocation strategies consider the temporary stochastic variations in traffic demand to provide optimal network coverage [89, 90]. Consequently, the associated channel per AP changes over time in order to successfully manage various network parameters such as mobility, user population, and demand of service.

We consider a typical WLAN positioning scenario where a set of APs are connected and a user carries an MS equipped with a wireless network card. An AP that listens to a *specific* channel, collects the packets transmitted from the MS at that channel, and records the corresponding RSS values using the appropriate high level programming APIs. Wireless APs that support fingerprint-based positioning systems receive RSS measurements from a specific channel to generate statistical fingerprints for a position, called signature maps. During the location estimation phase, runtime RSS measurements transmitted from the MS are collected and compared with the fingerprints obtained during the training phase.

As a consequence of the existence of multiple communication channels, in a real world scenario it is possible that fingerprints received during the runtime phase are compared with training fingerprints obtained from a different channel. Specifically, the radio frequency band of IEEE 802.11b/g is in 2.4 GHz, which is divided into 13 overlapping channels spaced 20MHz apart. Furthermore, for Cognitive Radios (CR) technology systems, where opportunistic spectrum sharing among primary and secondary users takes place, fingerprint based localization techniques will be strongly affected as the radios change their transmission and reception parameters, automatically.

Multipath fading is the random variation of channel quality in time, frequency and space which result in performance degradation of wireless communications. Specifically, multipath in the dynamic indoor environments is caused by multiple signal reflections from various objects (i.e walls, ceilings, furniture). Received power is a function of frequency because of frequency selective fading. In non-stationary indoor environments frequency selective fading causes several variations in dBs that vary with location. To demonstrate the impact of different frequency (communication channel) while performing dynamic channel on the received RSS fingerprints, Figures 5.4 5.5 illustrate the mean RSS values collected over 20 seconds (in dBm) from channels 1, 5, 9 and 13, as a function of distance from each AP. The real RSS measurements collected in the corridors of a laboratory area during midnight in order to ensure a stable environment. Figure 5.3 shows the floor map of the experimental area along with the locations of some of the APs.

These plots reveal some very interesting characteristics regarding the relationship between distance and channel (frequency). Overall, we observe that as the distance increases, the RSS values generally tend to decrease. This is expected since the power of the received signal is highly dependent on the distance. However, this decrease does not follow a smooth linear trend, *e.g.*, observe in Figure 5.4 that the mean RSS value for the AP 1 in channel 1

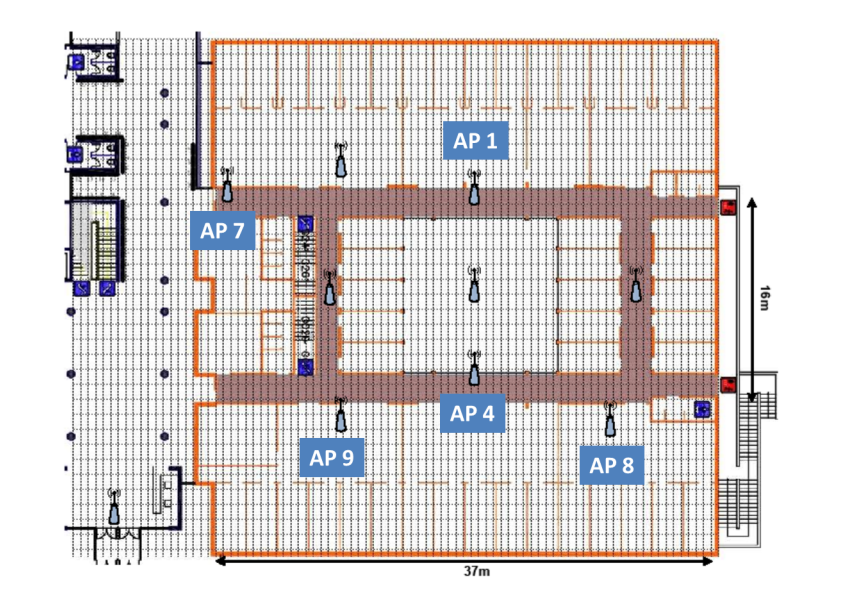

FIGURE 5.3: Experimental set up at FORTH. The experiments were performed within the brown-colored area.

is higher 3.6 meters away than it is 1.2 meter away from the AP. Apparently, this effect is more pronounced for the AP 7; located in the corner of the corridor, and the received signal suffers from various amounts of shadowing and multipath phenomena.

Furthermore, each channel is affected differently due to frequency related effects in radio propagation including multipath fading with propagation delays. From a localization perspective, Figures 5.4 and 5.5 reveal the sensitive relationship between location (distance) and channel (frequency) and that errors may result when this relationship is not taken into account.

For example, an RSS measurement of -40dBm received from the AP 1 (c.f. Figure 5.4), may correspond to a 2.4 meter distance for channel 2 or to a 4.8 meter distance for channel 1. As a result, a fingerprint based location scheme can produce an error of 2.2 meters when it compares the training fingerprint from channel 1 with the runtime fingerprint from channel 2. Similar effects can also be observed for a signal power equal to -60dBm that corresponds to a distance of 13.2 meters for channel 1 or 20.4 meters for channel 13. Interestingly enough, intense multipath phenomena in various frequencies appear for the APs located in particular positions in the area of interest (i.e AP 7) and especially for APs that do not satisfy the desirable line-of-sight conditions (i.e. APs 8 and 9).

The aforementioned illustrative examples suggest that a channel-unaware fingerprint comparison can lead to considerable location estimation errors. In order to provide accurate

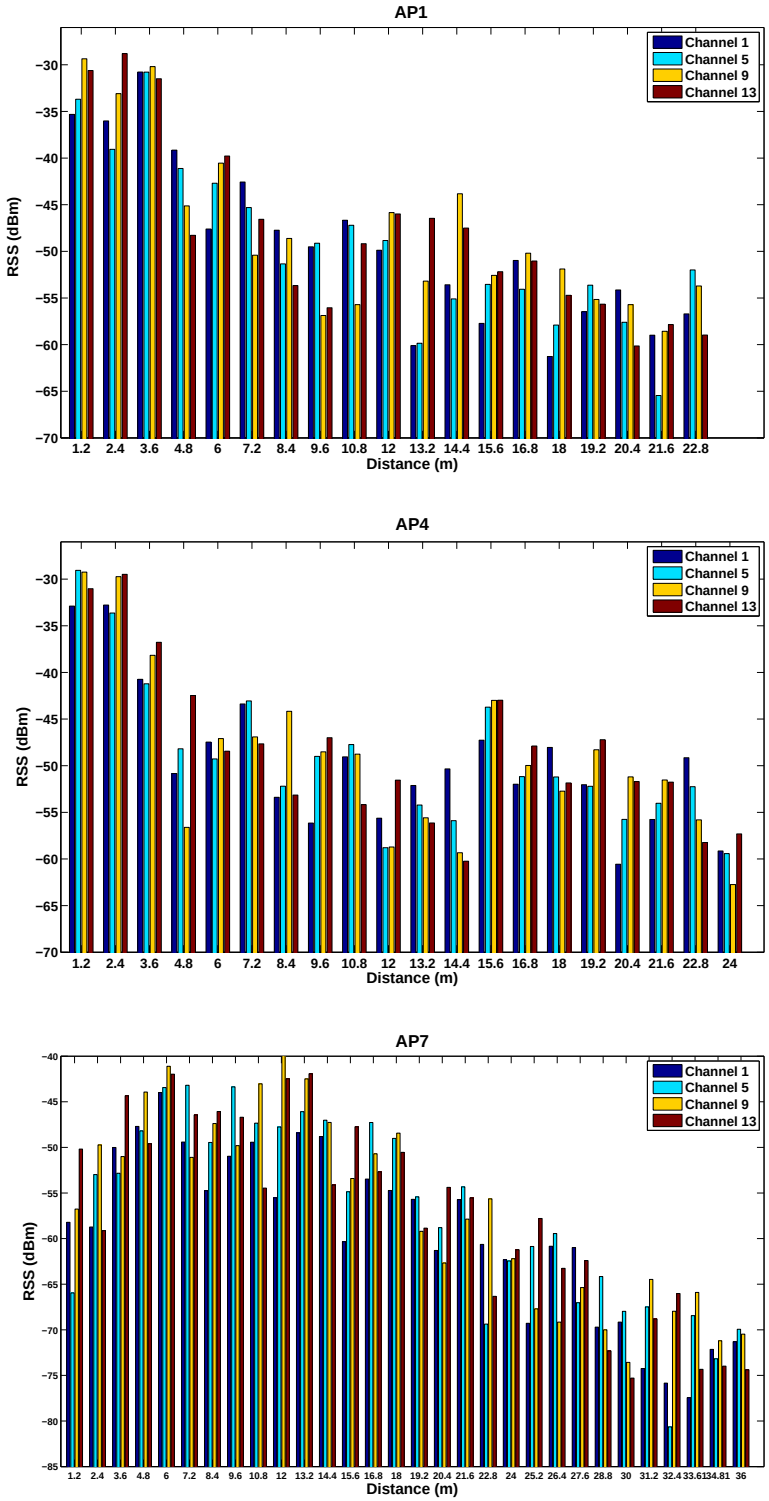

Figure 5.4: The RSS value variation as a function of the distance for 3 different APs placed at the corridors of the experimental area. Each colorbar corresponds to the mean RSS measurements of a specific channel at a certain distance.

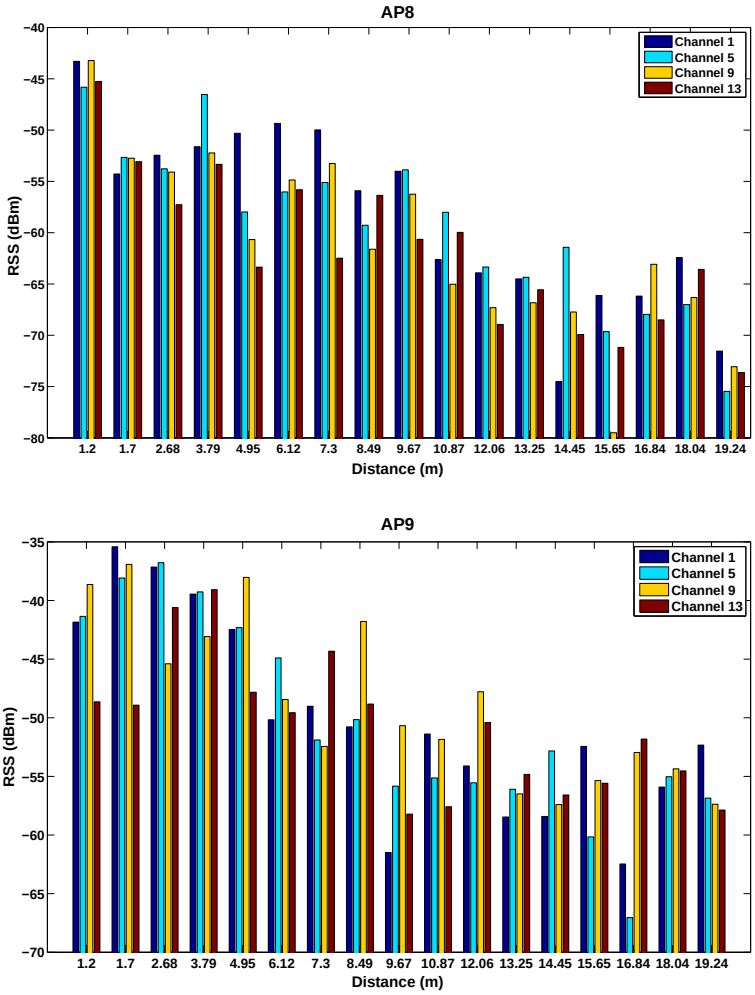

FIGURE 5.5: The RSS value variation as a function of the distance for 2 APs placed in the laboratory rooms. Each colorbar corresponds to the mean RSS measurements of a specific channel at a certain distance.

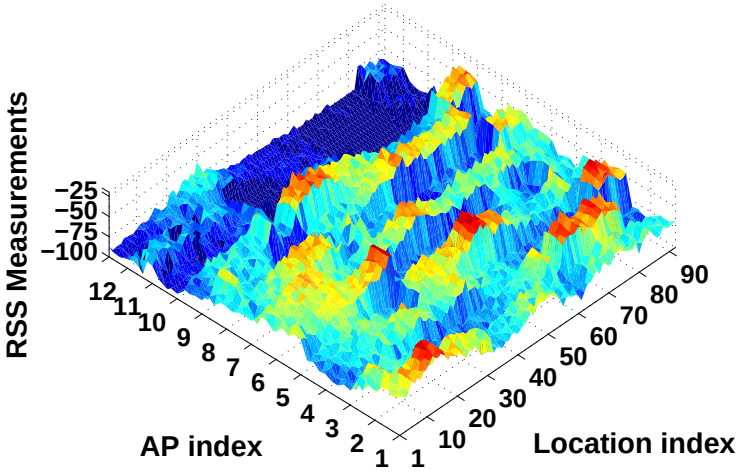

FIGURE 5.6: Signature map of recorded RSS signatures from 12 APs for 4 channels at 91 different positions.

positioning, it is thus necessary to take into consideration the dynamic channel assignment during the training and the runtime phases and to account for the different channels and the corresponding changes in RSS characteristics.

5.2.2 RSS correlation model

One of the major shortcomings of fingerprint-based systems is the exhaustive survey which is necessary for creating the signature map, a task that requires substantial cost and labour. To address this problem, we propose to exploit the characteristics of the RSS measurements in order to significantly reduce time and effort spent to create the map. One fundamental characteristic is the existence of spatio-temporal correlations.

In this work, we argue that spatio-temporal correlations are prevalent in RSS measurements collected by a densely deployed AP infrastructure. To illustrate this behavior, we investigate the spatial and frequency correlations of RSS measurements collected from various APs at different channels and locations. More specifically, we consider the real RSS fingerprints encoded in a matrix, the signature map, shown in Figure 5.6. Each element of this matrix indicates the average RSS measurements from a specific AP, at a given channel and at a certain location. In this figure, we observe that APs, closely placed in space, tend to produce similar RSS values. This behavior is expected, since signal attenuation due to path loss is highly dependent on the distance between the transmitter and the receiver. Furthermore, we observe that measurements from the same location but from different channels are also highly correlated due to the frequency invariant features of the RSS fingerprints.

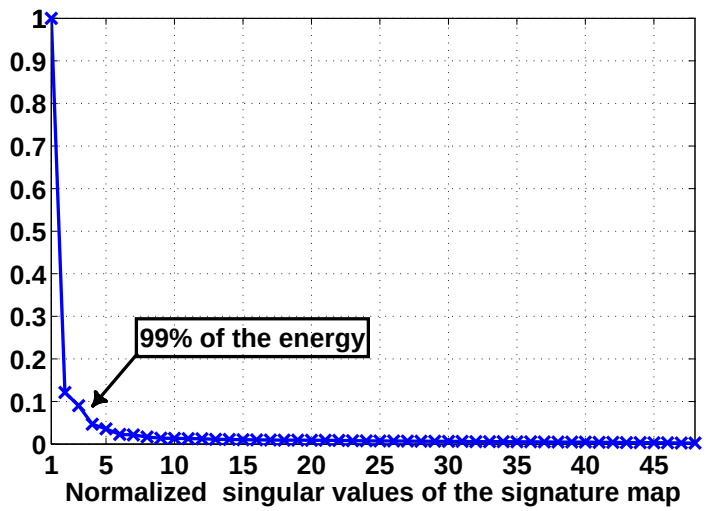

FIGURE 5.7: Normalized singular values of the signature map. The rank of the signature map equals the number of non-zero singular values.

The correlations of the measurements imply that the degrees of freedom of this matrix are much lower than its dimensions. The limited number of degrees of freedom results in a matrix that exhibits a rank much lower than its dimension. The low rank nature of the signature map can be observed in Figure 5.7 which shows the normalized singular values of the signature map.

The gathered training map is characterized as low rank, while noise-like phenomena result in additional singular values that exhibit much lower energy. The recently proposed framework of Matrix Completion asserts that it is possible to recover a large number of missing RSS entries from this low-rank map matrix by solving a simple convex optimization problem. In the following sections, we present the theoretical framework and its application on multi-channel localization.

5.3 Multi-channel based localization

In this Section, we describe our proposed multi-channel fingerprint based WLAN localization method. We consider a grid partition of the physical space into fixed structured cells. The proposed system is characterized by two phases; the *training* phase and the *runtime* phase.

5.3.1 Training phase

Under the traditional fingerprint-based localization paradigm, during the training phase, RSS measurements have to be collected from the MS at each possible reference point, termed cell, and each individual channel. In addition to the time and effort required in order to collect such a set of RSS measurements, physical constraints could even make such process unfeasible, since APs may not change channel during the collection of the training data. In order to minimize the duration of the calibration phase and overcome the limitations of traditional training, we propose to perform random sampling of the RF environment, where the APs collect RSS measurements from a randomly selected channel at each cell.

More specifically, during the calibration procedure of the training phase, each AP receives signal strength measurements from a MS that moves to the cells that define the area of interest. These measurements are stored at the local signature map of each AP. The local signature map $\mathbf{\Psi}_j \in \mathcal{R}^{C\times D}$ for the j-th AP is defined as

$$\mathbf{\Psi}_j = \begin{pmatrix} P_{1,1} & P_{1,2} & \cdots & P_{1,D} \\ P_{2,1} & P_{2,2} & \cdots & P_{2,D} \\ \vdots & \vdots & \ddots & \vdots \\ P_{C,1} & P_{C,2} & \cdots & P_{C,D} \end{pmatrix}_{C\times D}, \tag{5.1}$$

where $P_{c,i}$ corresponds to the time averaged RSS measurements received from channel c at location i. C represents the total number of channels and D is the number of cells in the area of interest. Hence, the c-th row of $\mathbf{\Psi}_j$ is the vector of RSS measurements that the j-th AP receives at frequency c from all D reference points.

The MC formulation is able to recover a matrix by making no assumption about the process that generates the matrix, except that it is low rank. In the proposed method, each AP, instead of sensing all C available channels, randomly selects C' channels. Once the selection is performed, the RSS measurements received from C' channels ($C' < C$) are recorded. It is obvious that sub-sampling over channels at each cell of the grid will result in an overall reduction of calibration time.

The LS receives $\mathbf{\Psi}_j$ from each AP$_j \in \{1, ..., J\}$, in order to create the signature map $\mathbf{\Psi} = [\mathbf{\Psi}_1; \ldots; \mathbf{\Psi}_J]_{C\cdot J\times D}$. The process of channel sub-sampling results in an incomplete signature map. The observed training signature map contains a subset $\Omega \subseteq [CJ] \times [D]$ of $\mathbf{\Psi}$'s entries, where $|\Omega| = \frac{C'}{C}(CJ \times D)$. Furthermore, the specific sampling pattern is defined by the sampling operator $\mathcal{A}$:

$$[\mathcal{A}_\Omega(\boldsymbol{M})] = \begin{cases} P_{c,i}, & (c,i) \in \Omega \\ 0, & \text{otherwise.} \end{cases} \tag{5.2}$$

The LS collects the incomplete matrix $\mathbf{\Psi}$ (cf. Fig. 5.1 - Training phase) that satisfies the low-rank property required by the MC theory. Effective location sensing requires the recovery

of the complete signature map $\hat{\boldsymbol{\Psi}}$ that will be used during the runtime phase. Recovery of the unobserved RSS measurements can be achieved by solving the following optimization problem

$$\min\{\|\hat{\boldsymbol{\Psi}}\|_\star \;\; : \;\; \|\mathcal{A}_\Omega(\hat{\boldsymbol{\Psi}}) - \mathcal{A}_\Omega(\boldsymbol{M})\|_F^2 < \epsilon\}, \tag{5.3}$$

where $\hat{\boldsymbol{\Psi}}$ is the recovered signature map, ϵ is the noise level, and $\|\cdot\|_F$ denotes the *Frobenius* norm. The optimization problem in (5.3) can be solved using the methods presented in Section 2.

5.3.2 Runtime phase

The new multi-channel localization scheme that we introduce in this work, considers the impact of frequency on the RSS propagation and utilizes this information during the estimation of the mobile user's location. A critical insight regarding the position of a MS is that the associated location vector is inherently sparse when considering a discretized physical space [34].

Particularly, we consider the sparse vector $\boldsymbol{b} \in \mathbb{R}^D$ where a non-zero component at the i-th position indicates the presence of the MS at cell g_i. For instance, the vector

$$\boldsymbol{b} = [0, 1, 0, \ldots, 0]^T, \tag{5.4}$$

indicates that the MS is located at the second cell.

During the runtime phase, the MS broadcasts on all available channels and each AP, associated to a specific channel k, collects runtime RSS measurements from the MS at that channel. The localization process is performed in the LS where the runtime measurements $\boldsymbol{y}_j$ from each AP are collected into the runtime fingerprint

$$\boldsymbol{y} = [y_1^{(c_1)}, y_2^{(c_2)}, \ldots, y_J^{(c_J)}]^T_{J\times 1} \tag{5.5}$$

where J is the number of APs and $y_j^{(c_j)} = \frac{1}{N}\sum_{t=1}^{N} P_j^{(c_j)}(t)$ is the average value of RSS runtime measurements over time from AP$_j$ from channel c_j. The channel information is acquired from the packet's channel information element transmitted from the mobile device.

Contrary to currently employed localization methods, the proposed multi-channel localization scheme considers the channel information of the runtime measurements. For-

mally, the concept of AP channel selection can be expressed in the following form:

$$y_j^{(c_j)} = \overbrace{\underset{1\times C}{[0\ 1\ \dots\ 0]}}^{\boldsymbol{\phi}_j} \cdot \overbrace{\underset{C\times D}{\begin{pmatrix} P_{1,1} & P_{1,2} & \cdots & P_{1,D} \\ P_{2,1} & P_{2,2} & \cdots & P_{2,D} \\ \vdots & \vdots & \ddots & \vdots \\ P_{C,1} & P_{C,2} & \cdots & P_{C,D} \end{pmatrix}}}^{\boldsymbol{\Psi}_j} \cdot \overbrace{\underset{D\times 1}{\begin{pmatrix} b_1 \\ b_2 \\ \vdots \\ b_D \end{pmatrix}}}^{\boldsymbol{b}}. \tag{5.6}$$

The unit vector $\boldsymbol{\phi}_j$ has all elements equal to zero except $\phi(c_j) = 1$, and c_j is the index of the channel where AP$_j$ received runtime measurements.

Exploiting the sparsity in the spatial domain, efficient location sensing translates to the accurate detection of the non-zero coefficient of the sparse vector $\boldsymbol{b}$. The signal ensemble can be expressed as:

$$\boldsymbol{y} = \boldsymbol{\Phi}\boldsymbol{\Psi}\boldsymbol{b} \overset{\boldsymbol{\Theta}=\boldsymbol{\Phi}\boldsymbol{\Psi}}{=} \boldsymbol{\Theta}\boldsymbol{b} + \boldsymbol{\epsilon}, \tag{5.7}$$

where $\boldsymbol{\Phi} = [\boldsymbol{\phi}_1, \dots, \boldsymbol{\phi}_J]$, $\boldsymbol{\Theta}$ is a submatrix of $\boldsymbol{\Psi}$ that collects training fingerprints from the APs of the runtime frequency and $\boldsymbol{\epsilon}$ is the noise vector.

The matrix $\boldsymbol{\Theta}$ is a structured low-rank dictionary as it obeys the property $rank(\boldsymbol{\Theta}) = rank(\boldsymbol{\Phi}\boldsymbol{\Psi}) \leq min(rank(\boldsymbol{\Phi}), rank(\boldsymbol{\Psi}))$, where $\boldsymbol{\Phi}$ is a full-rank matrix and $\boldsymbol{\Psi}$ is low-rank (cf. Section 6.1).

Exploiting the low-rank and sparsity properties of the model in (5.7), we employ at the LS a sparse Bayesian learning with relevance vector machine (RVM) approach to obtain the localization of the mobile user. The Bayesian framework associated with RVM, given a dictionary-dependent sparsity penalty, presents invariance properties leading to accurate sparse signal estimation, especially for structured dictionaries [91, 48]. Given the runtime measurements $\boldsymbol{y}$ and a prior belief that $\boldsymbol{b}$ is sparse in basis $\boldsymbol{\Psi}$, the main objective is to formulate a posterior probability distribution for $\boldsymbol{b}$. The adopted probabilistic framework introduces a prior over the sparse vector regularized by a set of hyperparameters α_i associated with each position in the area of interest that mitigate the prior. The hyperparameters individually control the strength of the prior over its associated weight.

Sparse Bayesian learning defines a zero-mean Gaussian prior with precision a_i (inverse-variance) on each element of the sparse vector $\boldsymbol{b}$:

$$p(\boldsymbol{b}|\boldsymbol{\alpha}) = \prod_{i=1}^{D} \mathcal{N}(b_i|0, a_i^{-1}). \tag{5.8}$$

The measurement vector $\boldsymbol{y}$ is modeled using a Gaussian distribution with variance σ_0^2,

$$p(\boldsymbol{y}|\boldsymbol{b}, a_0) = (2\pi\sigma_0^2)^{-\frac{J}{2}} \exp\Big(-\frac{\|\boldsymbol{y} - \boldsymbol{\Theta}\boldsymbol{b}\|^2}{2\sigma_0^2}\Big). \tag{5.9}$$

By employing Bayes' rule and the Gaussian likelihood model, the posterior probability for the sparse vector $\boldsymbol{b}$ is defined as:

$$p(\boldsymbol{b}|\boldsymbol{y},\boldsymbol{a},a_0) = \frac{p(\boldsymbol{y}|\boldsymbol{b},a_0)p(\boldsymbol{b}|\boldsymbol{a})}{p(\boldsymbol{y}|\boldsymbol{a},a_0)}$$
$$= (2\pi)^{-\frac{D}{2}}|\boldsymbol{\Sigma}|^{-\frac{1}{2}}\exp\Big(-\frac{1}{2}(\boldsymbol{b}-\boldsymbol{\mu})^T\boldsymbol{\Sigma}^{-1}(\boldsymbol{b}-\boldsymbol{\mu})\Big), \tag{5.10}$$

where $|\cdot|$ denotes the determinant of a matrix. The posterior mean $\boldsymbol{\mu}$ and the covariance matrix $\boldsymbol{\Sigma}$ are given by:

$$\boldsymbol{\Sigma} = (\boldsymbol{A} + a_0\boldsymbol{\Theta}\boldsymbol{\Theta}^T)^{-1}\ ,\ \ \boldsymbol{\mu} = a_0\boldsymbol{\Sigma}\boldsymbol{\Theta}^T\boldsymbol{b} \tag{5.11}$$

and $\boldsymbol{A} = diag(a_1,\ldots,a_D)$. The vector $\boldsymbol{a}$ defines the hyperparameters over each component of the estimated sparse vector given the prior [92]. The diagonal elements of the covariance matrix provide confidence intervals (*i.e.*, error bars) on the accuracy of the estimated components of the sparse vector $\boldsymbol{b}$. Consequently, estimating the sparse vector $\boldsymbol{b}$ translates in estimating the unknown variables $\boldsymbol{a}$, $\boldsymbol{\mu}$ and $\boldsymbol{\Sigma}$.

The hyperparameters are estimated by marginalizing them over the sparse vector $\boldsymbol{b}$. This is an iterative process where each iteration estimates $\boldsymbol{a}$ and a_0 that maximize the marginal likelihood

$$\mathcal{L}(\boldsymbol{a},a_0) = \log p(\boldsymbol{y}|\boldsymbol{a},a_0)$$
$$= -\frac{1}{2}[J\log 2\pi + \log|\boldsymbol{C}| + \boldsymbol{y}^T\boldsymbol{C}^{-1}\boldsymbol{y}], \tag{5.12}$$

with $\boldsymbol{C} = \sigma_0^2\boldsymbol{I} + \boldsymbol{\Theta}\boldsymbol{A}^{-1}\boldsymbol{\Theta}^T$. After a number of iterations, a small fraction of a_i remains relatively small indicating the non-zero components of the sparse vector $\boldsymbol{b}$. Consequently, the estimated location of the mobile user is the cell g that corresponds to the maximum component of $\boldsymbol{b}$ (*i.e.*, to the smallest a_i)

$$g = \arg\max \boldsymbol{b} = \arg\max p(\boldsymbol{y}|\boldsymbol{b},\boldsymbol{a},a_0). \tag{5.13}$$

The runtime localization algorithm via SBL is summarized in Algorithm (5).

5.4 Experimental results

In this Section, we test and evaluate the proposed multi-channel fingerprint based localization technique in an indoor WLAN environment. Real RSS data were collected in the corridors of the Institute of Computer Science (ICS) of the Foundation for Research and Technology Hellas (FORTH), an area of approximately $37m \times 16m$. For this area, a grid-based structure was considered with a cell of size $1.2m \times 1.2m$ (cf. Fig. 5.3). The experi-

Algorithm 5 Localization via SBL

Input: runtime measurements $\boldsymbol{y}$.
Output: estimated location g

1. Determine prior distribution per each cell (eq. 5.8).
2. Estimate the posterior probability of the sparse vector $\boldsymbol{b}$ from Bayes' rule (eq. 5.10).
   (a) Estimate the hyperparameters via maximizing (eq. 5.12).
3. Estimate the location via (eq. 5.13).

ment involved a total of 12 IEEE 802.11b/g APs ($J = 12$), 10 of which were placed on the same floor and 2 were located on a different floor.

During the training phase, the signature map was constructed as follows. RSS observations were collected for a period of 20 seconds for each of 4 channels ($C = 4$) of IEEE 802.11 b/g (channels 1, 5, 9 and 13) over 92 cells ($D = 92$). The four partially overlapping channels where chosen in order to achieve higher spectrum utilization with minimum interference. The amount of calibration effort can be defined as:

$$\text{Time} = T_s \times C \times J \times D + T_{cs} \times C \times D + T_w \times D, \tag{5.14}$$

where $T_s = 20s$ is the sensing period, $T_{cs} = 140ms$ is the time required for an AP to change communication channel, and $T_w = 0.8s$ defines the average time for a mobile user to change cell. Thus, in our setting, complete channel sensing requires $24.5h$.

The systems are evaluated by their ability to identify the correct location, out of 46 distinct cells. The runtime dataset was collected on a typical weekday afternoon. We note here that the number of cells and online observations is comparable to those reported in [18] and [28].

The objectives of the experiments are twofold. First, we are interested in exploring and quantifying the effects that multiple channels have on the localization performance. This is a critical test, since localization algorithms typically assume a single communications channel. Second, we are aiming at identifying the benefits of using the proposed localization system, both in training and runtime phase. The accuracy of the reconstruction versus the number of measurements clearly describes the tradeoff between performance and time complexity during the training phase and localization accuracy during runtime.

5.4.1 Effects of dynamic channel assignment on state-of-the-art localization techniques

In this Section, we investigate the effects of frequency mismatch during training and runtime on the localization error of two state-of-the-art fingerprint based systems, the Radar [12] and the Horus [26]. In order to analyze the impact of dynamic channel assignment (DCA)

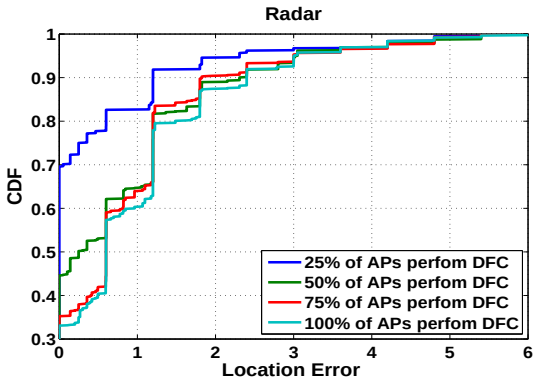

FIGURE 5.8: CDF curves of the location error for the Radar system as a function of the number of APs that perform DCA, *i.e.*, APs that may change the selected communications channel between training and runtime phase. The plot clearly indicates that changes of the RSS characteristics between training and testing have a profound effect on fingerprint matching and localization accuracy.

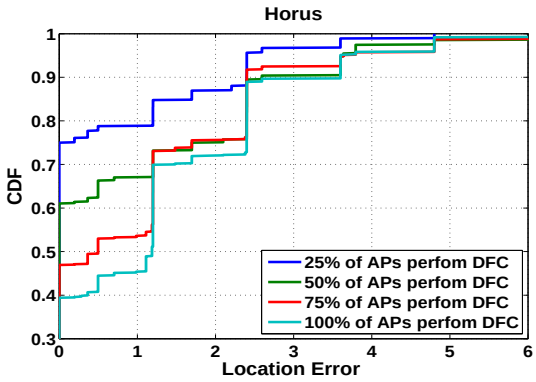

FIGURE 5.9: CDF curves of the location error for the Horus system as a function of the number of APs that perform DCA. We observe that Horus exhibits a similar behavior to Radar with respect to the number of APs that may change channels between phases, demonstrating the additional localization error due to channel mismatch.

in location error, for this experiment only, we consider runtime measurements received in a stable environment, *i.e.*, during midnight. We selected this setup since a stable environment minimizes the errors introduced by unexpected multipath and shadowing effects (*i.e*, from moving people and objects). We implemented the Radar positioning system by employing the nearest neighbor in signal space (NNSS) localization technique, while we implemented the Horus system by maximizing the posterior probabilities with respect to each possible position in the area of interest.

Figures 5.8 and 5.9 show the CDF curves ($P|X| \leq x$) of the location error as a function of the number of APs that adopt DCA for the Radar and the Horus systems, respectively. In each run we choose randomly the indexes of APs that perform DCA while each curve in the graph is the average of 20 Monte-Carlo runs. The random channel assignment will lead to runtime RSS observations which are compared with RSS data observed at different frequencies and therefore different fingerprints.

We observe in the plots that as the number of APs that adopt DCA increases, the achieved localization accuracy decreases. Furthermore, frequency mismatch affects the location error for both systems, quite significantly. Particularly, in the case where only 25% of the APs perform DCA, the 90th percentile, (*i.e.*, the value below which the 90% of the location error falls) is more than 1m, for both systems. Comparing the two systems, we observe that Horus is slightly more robust to the changes in channels compared to Radar.

Different channel assignment strategies cause different effects. Specifically, the correlation between adjacent channels affects differently the localization accuracy. Table 5.1 indicates the position error statistics when all the APs perform DCA in adjacent and non-adjacent channels. We define as adjacent channels the partially overlapping channels of IEEE802.11b/g and as non-adjacent the non-overlapping channels. We observe that adjacent communication channels result in higher localization accuracy for both systems. The highly correlated RSS measurements between the training and runtime measurements in adjacent channels produces a much smaller location error compared to the non-overlapping case.

	Radar		**Horus**	
	Mean	std	Mean	std
Adjacent Channels	1.31	1.16	1.24	1.53
Non-adjacent Channels	1.66	1.43	1.51	1.61

TABLE 5.1: Location error statistics in meters for Radar and Horus when the DCA assigns to the APs adjacent and non-adjacent channels. Observe that adjacent channel assignment results in lower mean location errors for both systems.

This section highlights the need for considering the actual communications channels that are employed during both the training and the runtime phases. In the next section, we compare the proposed channel aware-sparse Bayesian learning localization system with state-of-the-art methods when fingerprints from all the available channels are available.

5.4.2 Localization via sparse Bayesian learning

In the previous section, we presented experimental results on real data that reveal the influence of frequency mismatch on localization accuracy. In this section, we turn our attention

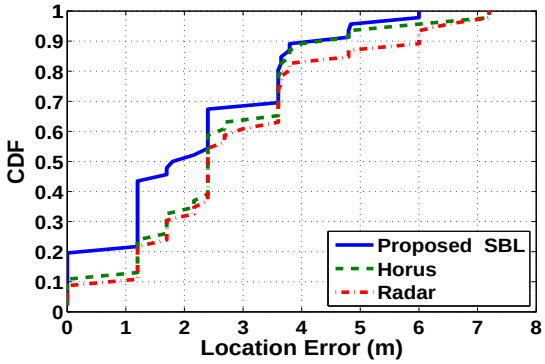

FIGURE 5.10: The CDF of location error for the sparse Bayesian learning method, the Horus, and the Radar. During training, we perform full channel sampling.

to the evaluation of the proposed multi-channel localization and compare its performance to the multi-frequency extension of the state-of-the-art Radar and Horus systems. We perform full frequency sensing during training while during runtime the correct channel information is considered via the matrix $\mathbf{\Phi}$ as it was described in Section 5.3.2.

The CDF curves ($P|X| \leq x$) in Figure 5.10 illustrate the performance of the proposed sparse Bayesian learning localization method compared to channel-aware Radar and Horus. Observe that the 40% percentile (*i.e.*, the number below which 40% of location errors falls) is 1.2m for the proposed method, while for the Radar and Horus is 2.4m.

Figure 5.11 illustrates the impact of the available infrastructure (*i.e.*, number of APs) on the system's accuracy. The bigger the number of APs, the higher the localization accuracy. We observe that the proposed technique achieves a lower mean location error compared to the other fingerprint-based systems. For instance, in the case of only 3 APs the mean location error of the proposed technique is $3.7m$ while for the Horus and Radar is $5m$ and $5.7m$, respectively. Interestingly enough, it appears that there is a critical number of APs required after which the accuracy of the system increases marginally (7 in our experiment).

In the aforementioned localization systems, the training fingerprints were collected from all channels at each location. However, as discussed in the previous sections, this leads to a significant increase in labor and time that is required during the training phase. Next, we experimentally assert how spatio-frequency correlations can be exploited in order to significantly reduce the training time.

5.4.3 Signature map estimation via matrix completion

The performance gain in utilizing the appropriate channel during the localization process, motivates the need for an efficient estimation of the complete set of RSS fingerprints. The

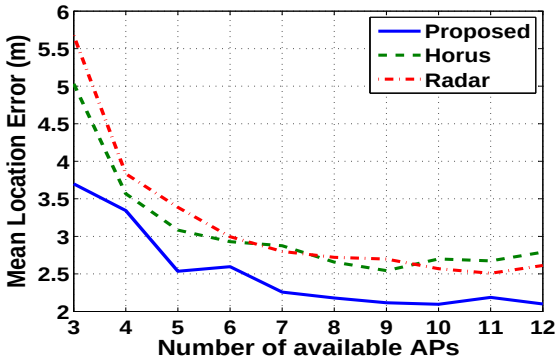

FIGURE 5.11: Mean location error for various localization systems as a function of the number of available APs.

effectiveness of the proposed MC training technique is compared to the traditional Interpolation technique that serves as a baseline. The reconstruction problem presented in (5.3) is solved using the convex programming package *CVX* and the optimization approach SVT [1]. We evaluated the performance of the proposed scheme with respect to both the reconstruction quality of the signature map and the corresponding localization error. The reconstruction error between the full signature map Ψ and the estimated map $\hat{\Psi}$ is defined as:

$$RE = \|\hat{\mathbf{\Psi}} - \mathbf{\Psi}\|_F / \|\mathbf{\Psi}\|_F. \tag{5.15}$$

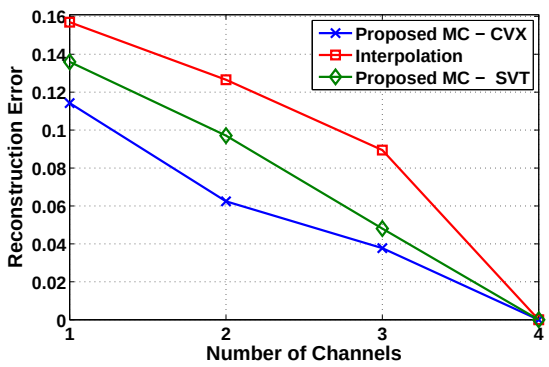

FIGURE 5.12: The reconstruction error during the training phase as a function of the number of sensed channels. The experiment involves a total of 12 APs. We observe that MC with CVX achieves the lowest reconstruction error, half that of interpolation for the case of 2 sensed channels.

[1]For the implementation of MC and methods CVX and SVT we used the MATLAB codes included in the packages: `http://cvxr.com/cvx/`, `http://svt.stanford.edu/index.html`

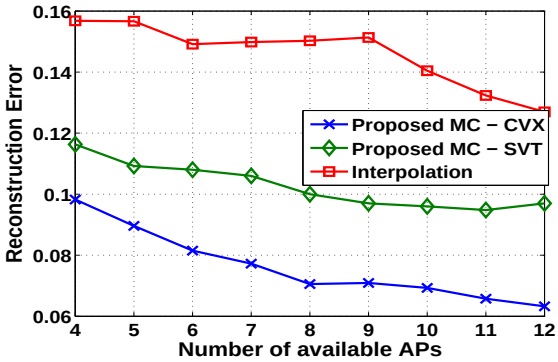

FIGURE 5.13: Signature map reconstruction error during training phase as a function of the total number of available APs. In this experiment, the APs receive measurements only from 2 channels. The number of APs defines the structure of the signature map.

First, the proposed MC-based RSS recovery technique is evaluated with respect to the number of sensed channels when training fingerprints are received from all 12 APs. Figure 5.12 shows the recovery of the signature map as a function of the number of sensed channels. We observe that the performance of the proposed technique improves, as the number of sensed channels increases. Furthermore, the proposed approach is able to achieve lower reconstruction error compared to the interpolation technique.

Figure 5.13 illustrates the performance of our technique as a function of the total number of available APs, when the APs receive RSS measurements only from two channels (*i.e.*, reducing calibration effort by half). Notice that the total number of available APs affects the structure of the signature map. Particularly, as the number of APs increases, more correlated RSS measurements are produced, thus the signature map exhibits a lower rank relative to its dimensions, which leads to a lower reconstruction error.

It is apparent that the MC-based approach provides lower reconstruction errors when compared to the Interpolation method for equivalent calibration effort. The proposed channel sub-sampling training approach can be adopted from various fingerprinting localization techniques in order to minimize the exhaustive calibration phase.

5.4.4 Localization performance with recovered signature maps

In this Section, we evaluate the effect of the proposed training technique during the runtime phase on various fingerprint based localization systems. Particularly, we are interested in determining how the errors in the reconstruction of the signature maps affect the localization performance.

Figure 5.14 illustrates the CDF curves ($P|X| \leq x$) of the proposed sparse Bayesian learning (SBL) location method. As the number of sensed channels used during training

increases, the performance of the proposed SBL technique improves. This behaviour is expected due to the fact that lower reconstruction errors during training result in lower localization errors during runtime. Particularly, we observe that the accuracy increases only slightly when sensing more than two channels. This behavior is consistent with the theoretical foundation of MC theory since the number of observed measurements required for accurate matrix recovery is indicated by the rank (r) of the matrix. We note that sensing 2 channels (*i.e.*, sensing 50% of the measurements in 12h and 18min) corresponds to $M = 2208$ ($0.5 \cdot CJD$, C = 4, J = 12, D = 92) measurements which is above the minimum bound of $cD^{6/5}rlog(D) \approx 1785$ measurements required by the theory of MC.

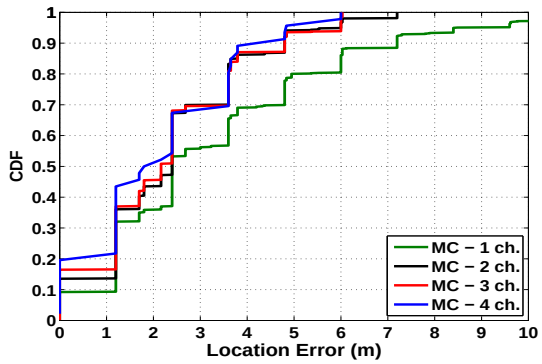

FIGURE 5.14: The CDF curves of the location error for the proposed sparse Bayesian learning algorithm using the MC-based technique as a function of the number of sensed channels during training.

Figures 5.15-5.16 illustrate the performance of the SBL, Horus, and Radar systems when one channel is sensed during the training phase. In Figure 5.15, all three systems adopt the MC-CVX strategy during training while in Figure 5.16 the interpolation technique is used to construct the signature map.

It is clear that the proposed MC-based approach results in lower location errors when compared with the Interpolation method. Observe that the MC-based approach leads to improvements of the median location error (*i.e.*, the values below which 50% of the location errors falls) in the order of 36% (1.4m), 21% (1m) and 25% (1.2m) for the SBL, the Horus, and Radar methods, respectively, over the Interpolation method. Moreover, the proposed MC-based approach results in lower maximum location errors for all three systems.

Table 5.2 summarizes the mean location error of the three localization systems over different training techniques as a function of the number of sensed channels. As it can be seen, the proposed location sensing system outperforms the Radar and Horus systems in terms of location error. In contrast to other localization systems, the proposed SBL approach marginalizes the noise variance. Consequently, even in the presence of reconstruction noise introduced during the training phase, the proposed localization algorithm results in lower

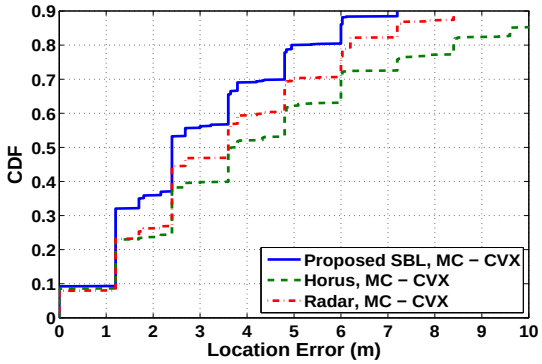

FIGURE 5.15: The CDF curves of the location error for SBL, Horus, and Radar when the proposed MC-based technique is applied. One channel is sensed during training phase.

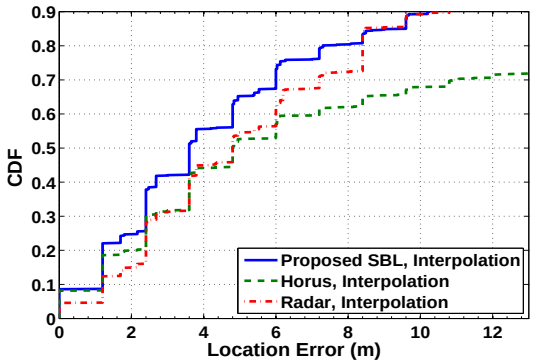

FIGURE 5.16: The CDF curves of the location error for SBL, Horus, and Radar when the Interpolation method is applied. One channel is sensed during training phase.

mean location errors for both training techniques.

5.4.5 Resources utilization analysis

Table 5.3 summarizes the time calibration effort for performing random subsampling, as suggested in our approach, as a function of the number of sensed channels. The collected training RSS fingerprints are given to estimate the full signature map. The number of received fingerprints (third row) is a function of the number of sensed channels, the number of APs, and the dimensions of the space. Table 5.3 also provides the achieved estimation accuracy for the proposed MC and the interpolation methods. Observe that the proposed MC-approach, for a calibration time of 6 hours and 9 minutes (i.e., for one sensed channel) leads to improvements of 26% over the reconstruction error achieved by the interpolation method.

	MC (Proposed)			Interpolation			FS
# Channels	**1**	**2**	**3**	**1**	**2**	**3**	**4**
Radar	4	3.2	2.9	5.7	3.4	3	2.8
Horus	5.2	3.5	3.1	8.5	5.8	3.9	2.6
SBL (Proposed)	3.3	2.3	2.2	4.8	3.2	2.8	2

TABLE 5.2: Average location error in meters for the SBL, Horus, and Radar systems and the MC and Interpolation training techniques as a function of the number of sensed channels during training. The FS (full sensing) column indicates the performance corresponding to full frequency sensing during training.

# Channels	1	2	3	FS
Calibration time	6h 9m	12h 18m	18h 26m	24h 32m
# Fingerpr.	1104	2208	3312	4416
Int. error	0.157	0.126	0.089	0
MC error	0.114	0.062	0.038	0

TABLE 5.3: Calibration effort during training time as a function of sensed channels. The last rows indicate the reconstruction error of the proposed MC technique and the Interpolation method. The FS column indicates the time effort for full frequency sensing.

Although the power consumption of packet transmission and reception is highly hardware depended, studies indicate that in general, power consumption follows a linear trend with respect to the number of transmitted packets. For example, in [93] the authors proposed a linear function relating the percentage of energy consumption as a function of transmission time, x, given by $y = 21.24x + 2.68$. A similar model was also developed in [94] where the power consumption (in Joules) for the download of x bytes of data corresponds to $0.007(x) + 5.9$, plus some overhead. Under the linearity assumption, transmission of packets over one out of four channels will result in close to 75% reduction in power consumption due to WiFi communications and will have a profound effect on the lifetime of the mobile device.

From a practical perspective of view, on-line applications of the localization algorithm impose constrains on the execution time. The proposed sparse Bayesian learning algorithm operates in a constructive manner until the most probable location has been selected. The complexity of the localization algorithm is proportional to the dimension of the space, i.e. $\mathcal{O}(D)$. Specifically, for the specific experimental set-up the execution time for estimating the location of the user is 0.015 seconds. Considering that the moving walking pattern of an average person is $1.3m/s$ (i.e approximately one cell per second) the proposed localization algorithm can be adopted in real-time scenarios.

5.5 Discussion

Indoor localization is an exciting research field, with numerous applications. RSS based fingerprint methods offer high accuracy with minimal hardware interventions at the expense of a time consuming calibration process. Furthermore, in dynamic environments, frequent re-calibration is deemed necessary in order to maintain high localization accuracy, while dynamic channel assignments can lead to significant performance loss. In this work, we address these issues by proposing a novel multi-channel fingerprint-based indoor localization technique.

According to our proposed scheme, estimation of the complete multi-channel signature map can be achieved from a small number of measurements over space and frequency (channel) by leveraging the power of Matrix Completion. Furthermore, the Sparse Bayesian Learning paradigm is introduced for the precise localization during the runtime phase.

To validate the merits of the proposed scheme, an extensive set of experiments was carried our in the premises of a research institute and a comparative analysis with state-of-the-art localization scheme was performed. Experimental results suggest that the proposed MC-based training technique can reliably estimate the signature map from partial information while sparse Bayesian learning outperforms traditional runtime localization systems.

Chapter 6

Efficient recalibration via dynamic matrix completion

Fingerprint-based localization techniques have witnessed significant progress as they provide highly accurate location estimation with minimal hardware interventions. However, the required calibration phase is time and labour consuming. In the previous chapter we exploited the spatio-frequency correlation structures received during the training phase in order to introduce a reduced effort calibration phase for fingerprint based systems. In this Chapter, we propose a novel recalibration procedure that dynamically adapts to the environmental changes while minimizing the recalibration effort. Our key observation is that in non-stationary indoor environments, the training fingerprints are constantly changing over time while the subsequent measurements may explicitly depend on past observations. Thus, we exploit the spatio-temporal correlations of the training fingerprints to reduce the training phase effort by reconstructing the signature map from fewer measurements. The recovery of partial fingerprints is formulated as an instance of a Dynamic Matrix Completion problem where we exploit the spatio-temporal correlations among the fingerprints. Analytical studies and simulations are provided to evaluate the performance of the proposed technique in terms of reconstruction and location error.

6.1 Motivation

One of the major shortcomings of fingerprint-based systems is the exhaustive survey and maintenance of the signature map, a task that requires substantial cost and labor. To address this problem, we use a grid representation of the space and we propose to perform random sampling, where the mobile device (MD) collects RSS measurements from pseudo-randomly selected cells in the area of interest. Sub-sampling in the space domain reduces the calibration effort and consequently energy consumption at the MD. While random sensing

has numerous benefits, recovering unobserved measurements is feasible if spatio-temporal correlations between the RSS fingerprints exist.

In indoor environments, signal strength measurements are affected by path loss and shadowing effects which represent the signal degradation due to the distance traveled and the obstacles, respectively. Thus, a key observation is that training fingerprints are spatially correlated in the sense that training locations in proximity have similar feature vectors. To support this claim, we created RSS fingerprints from 15 APs at 144 different positions. For this purpose we adopt the multi-wall path loss model for signal propagation in [95]. Observe in Figure 6.3 that only a small number of the singular values are actually dominant, indicating the low rank property of the signature map.

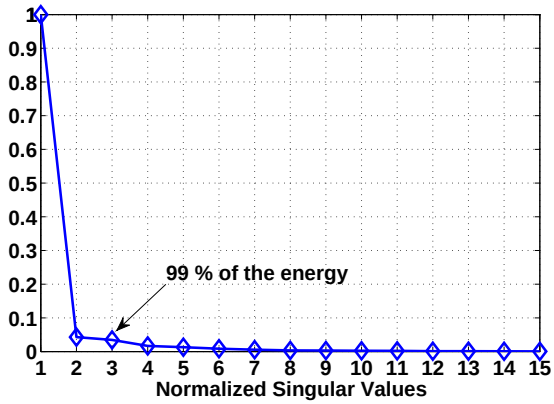

FIGURE 6.1: Singular values of the signature map at a random time instance. The rank of the signature map equals the number of non-zero singular values.

Additionally, in dynamic indoor environments the signal strength fingerprints change over time, even at fixed positions, due to multipath phenomena. Signal fluctuations resulting from environmental dynamics, such as the presence of obstacles, walls, and doors, remains the main challenge for fingerprint based systems. The degree of correlation between RSS measurements over different time instances varies according to the temporal variation characteristics of the dynamic phenomena. To indicate the temporal correlation of the fingerprint signatures received in a stochastically dynamic indoor environment we created RSS fingerprints at fixed positions under various indoor characteristics. To this aim the multi-wall path loss model [95] is adopted and at each time instance t we introduced a new thin wall into the area of interest(i.e at time 1 one wall is introduced, at time 2 two walls are introduced e.t.c). Figure (6.2) indicates the average temporal correlation coefficients with 95% confidence intervals over 20 positions for the different environmental conditions for the same experimental area. We interestingly observe that a strong temporal correlation, corresponding to smaller confidence intervals, is present for the fingerprints received in close time instances. Compared to the state-of-the-art recalibration techniques, our work is the first that exploits

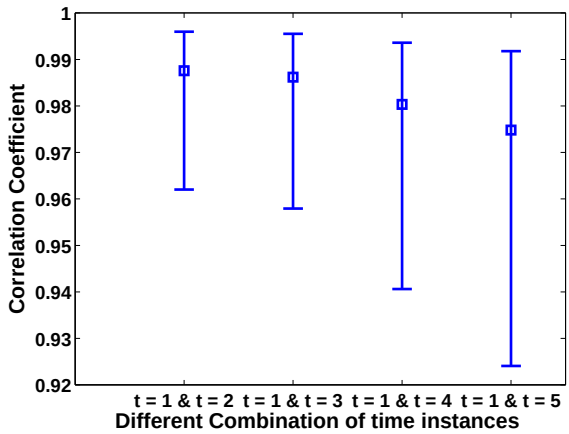

FIGURE 6.2: Correlation coefficients with 95% confidence interval for different environmental conditions. Observe that a strong temporal correlation is present for the fingerprints received in close time instances.

the spatio-temporal correlations of the RSS fingerprints in order to recover the unobserved measurements.

6.2 Proposed dynamic recalibration technique

In this chapter, we describe our proposed recalibration approach, which considers the spatio-temporal correlations of the RSS fingerprints among the APs. Consider a typical WLAN scenario with a MD equipped with an active wireless adapter card. The MD connected to a channel, periodically receives beacons sent by the APs at that channel and records its RSS value. Moreover, we consider a Location Server that is wireless connected with the MD.

Fingerprint-based techniques discretize the spatial space into a finite set of D equivalent size cells, where each cell of the grid corresponds to a physical position. During recalibration at time t, the MD moves to the various cells and collects signal strength measurements from the J APs that cover the area of interest. This procedure results in the generation of the *signature map* $\mathbf{\Psi}_t$ represented as:

$$\mathbf{\Psi}_t = \begin{pmatrix} P_{1,1,t} & P_{1,2,t} & \cdots & P_{1,D,t} \\ P_{2,1,t} & P_{2,2,t} & \cdots & P_{2,D,t} \\ \vdots & \vdots & \ddots & \vdots \\ P_{J,1,t} & P_{J,2,t} & \cdots & P_{J,D,t} \end{pmatrix}_{J \times D}, \tag{6.1}$$

where $P_{j,i,t}$ corresponds to the mean value of RSS measurements received from the jth AP

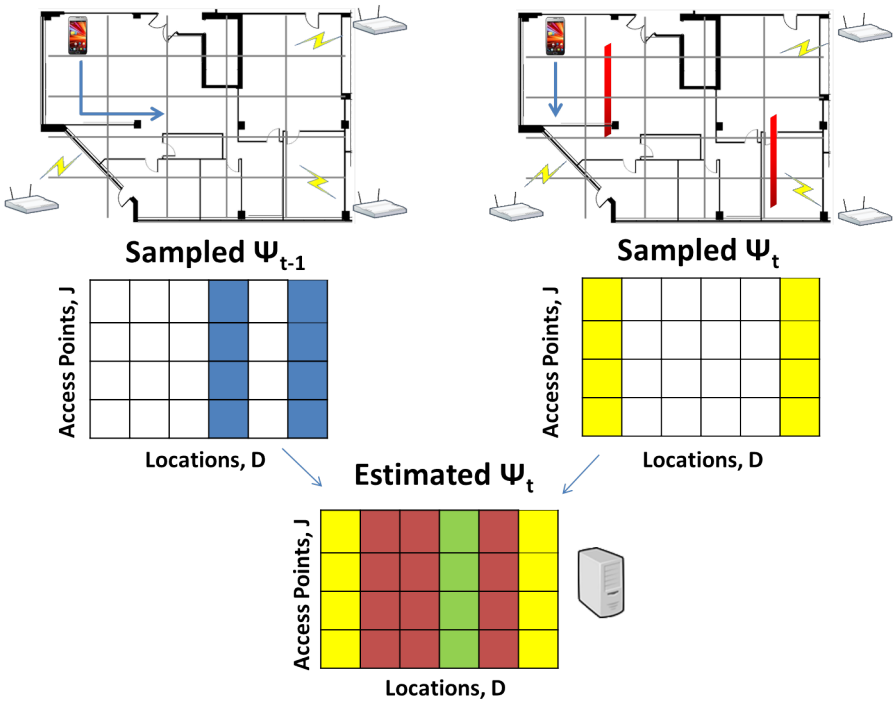

FIGURE 6.3: A visual illustration of the proposed recalibration technique during the training phase. The MD randomly selects locations at time t, i.e. cells of grid here, to create RSS fingerprints from the packets transmitted from APs. The Location Server performs the Dynamic Matrix Completion to complete the missing fingerprints.

at location i at time t.

In dynamic indoor environments, the RSS fingerprints suffer from large variations over time, even in fixed positions, caused by multipath phenomena. The relationship of RSS measurements between path-loss and distance over time can be expressed by the following linear relation as:

$$\boldsymbol{y}_t = \boldsymbol{C}\boldsymbol{y}_{t-1} + \boldsymbol{\epsilon}, \tag{6.2}$$

where $\boldsymbol{y}_t, \boldsymbol{y}_{t-1} \in \mathbb{R}^{J\times 1}$ represent the measured RSS at time t and $t-1$ respectively received at a fixed position [96]. $\boldsymbol{C} \in \mathbb{R}^{J\times J}$ expresses the temporal correlation of the path-loss for specific distances, while ϵ indicates the environmental noise.

Efficient calibration of the signature map translates to periodically sensing the area of interest in order to capture the dynamic indoor propagation phenomena. The proposed Dynamic Matrix Completion framework is able to recover the unknown matrix at time t under the assumption that the matrix is low-rank and follows a random sampling process. During training, the MD instead of visiting the whole workspace at time t, randomly, with

equal probability, selects K cells, where $K < D$. Once the selection is performed, the MD creates training fingerprints only for a subset of the area. It is obvious that spatial sub-sampling will result in an overall reduction of the calibration time.

Minimizing the number of visiting cells results in the incomplete signature map $\mathbf{\Psi}_t$. Particularly, the MD receives a subset $\Omega_t \subseteq [J] \times [D]$ of $\mathbf{\Psi}_t$'s entries, where $|\Omega|_t = K \times J$. Let $\mathcal{A}_t$ be the sampling operator defined by

$$[\mathcal{A}_t(\mathbf{\Psi})]_{j,i} = \begin{cases} P_{j,i}, & (j,i) \in \Omega_t \\ 0, & \text{otherwise.} \end{cases} \tag{6.3}$$

Ω_t is a subset of the complete set of entries $[J] \times [D]$. Moreover, $\Omega_t \cup \Omega_t^C = [J] \times [D]$. The complementary sampling operator $A_t^C(\mathbf{\Psi}_t)$ collects the unobserved measurements at time t. Additionally, we define the sampling operator $A^I = A_{t-1} \cap A_t^C$ as the intersection of the training measurements of the cells visited at time $t-1$ and not at time t.

Effective location estimation requires the recovery of the signature map (6.1) that will be used during the runtime phase. In order to recover the signature map, we exploit the RSS samples received on previous time instances. Consequently, the Localization Server recovers the signature map at time t based on the current partial measurements while also incorporating the information of the measurements obtained in the past (*i.e.* at time $t-1$). The proposed Dynamic MC problem searches for the matrix $\mathbf{\Psi}_t$ that has the minimum nuclear norm, subject to the values of $\mathbf{\Psi}_t \in \Omega_t$ being equal to the observed measurements at time t, and the sampled values at time $t-1$ being correlated with values at time t via the matrix $\boldsymbol{C}$ (eq. 6.2).

To enforce this constraint, the original matrix $\mathbf{\Psi}_t$ can be recovered as the solution of the following optimization problem:

$$\begin{aligned} \text{argmin} \quad & \|\hat{\mathbf{\Psi}}_t\|_\star \\ \text{subject to} \quad & \|\mathcal{A}_t(\hat{\mathbf{\Psi}}_t - \mathbf{\Psi}_t)\|_F^2 \leq \epsilon_1 \\ & \|\mathcal{A}^I(\hat{\mathbf{\Psi}}_t - \boldsymbol{C} \cdot \mathbf{\Psi}_{t-1})\|_F^2 \leq \epsilon_2, \end{aligned} \tag{6.4}$$

where $\hat{\mathbf{\Psi}}_t$ is the recovered signature map at time t, $\epsilon_1, \epsilon_2 \geq 0$ represent the tolerance in approximation error and $\|\cdot\|_F$ denotes the *Frobenious* norm. T matrix $\boldsymbol{C}$ expresses the relationship between the values of $\mathbf{\Psi}_t \in \Omega_t^C \cap \Omega_{t-1}$. Particularly, $\boldsymbol{C}$ is changing as the number of the common training cells at time $t-1$ and t increases. The more orthogonal the sampling operators are over time the more accurate the matrix $\boldsymbol{C}$ is.

The problem in (6.4) is a general convex optimization problem and can be solved by an off-the-shelf interior point solver, such as CVX.

6.3 Experimental results

The benefits and characteristics of the proposed recalibration technique based on Dynamic Matrix Completion are studied and analyzed through simulations. Two different performance metrics are considered, namely, the reconstruction quality of the recovered signature map with respect to the original one and the corresponding localization error. The effectiveness of the proposed scheme is investigated in various environments and network characteristics. We compare the proposed technique with the traditional MC approach that serves as a baseline. Regarding the reconstruction quality, the error was measured as $\|\hat{\mathbf{\Psi}}_t - \mathbf{\Psi}_t\|_F / \|\mathbf{\Psi}_t\|_F$. To evaluate the impact of the proposed technique in location estimation, the Nearest Neighbor in Signal Space (NNSS) algorithm was employed [16, 12].

According to the multi-wall path loss model [95], the received power at the *i*th position from the *j*th AP is given by

$$P_r = Pt - L_0 - 10nlog(d_{ij}) - \sum_{w=1}^{W} k_w \cdot L_w - s_i \tag{6.5}$$

where L_0 is the path loss at distance 1m, n denotes the path loss exponent, d_{ij} is the Euclidean distance between the jth and the ith cell. k_w and L_w are the number and loss coefficients due to the obstacles while s_i describes the shadowing effect. We chose $L_0 = 37.5dBm$, $n = 3$ for NLOS, and $L_w = 3.4dB$ for light walls/obstacles. The shadowing variable is a zero-mean Gaussian random variable (in dB) with standard deviation $\sigma = 2dB$. P_t is the AP transmit power, which is fixed at 15dBm for IEEE 802.11b based WLANs. We considered an $144m^2$-wide area and a $1m \times 1m$ grid-spacing ($D = 144$), covered by 15 APs ($J = 15$). Each data point in the results is averaged over 20 independent trials.

For the next experiment, we create changing conditions over time by introducing one obstacle in the middle of the room. Figures 6.4-6.5 indicate the recovery of the signature map based on (6.4) and the corresponding location error as a function of the number of visiting cells. We observe that the performance of the proposed dynamic recalibration scheme is improved both in reconstruction and location error, as the number of visiting cells increases. Observe that the dynamic approach is able to achieve lower reconstruction and location error as compared to the MC approach, especially for small sampling ratios. Particularly, for the NSSS, dynamic MC leads to improvements of 42% (*i.e.* 2 m) over the location error achieved by the MC approach for sampling 10% of the total number of cells.

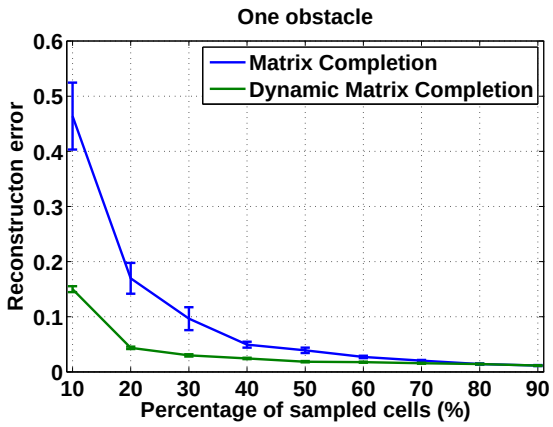

FIGURE 6.4: The reconstruction error of the signature map as a function of the number of visiting cells. The experiment involves 15 available APs. Dynamic MC achieves the lowest reconstruction error especially for a small number of visiting cells.

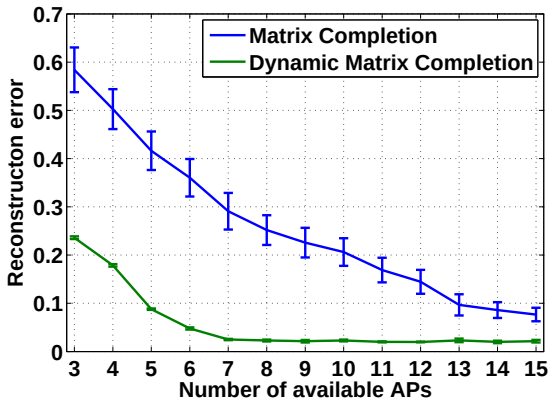

FIGURE 6.6: Signature map reconstruction, during training phase, as a function of the total number of available APs covering the area of interest. In this experiment, we visit 30% of the cells in the testbed area. The number of APs defines the structure of the signature map.

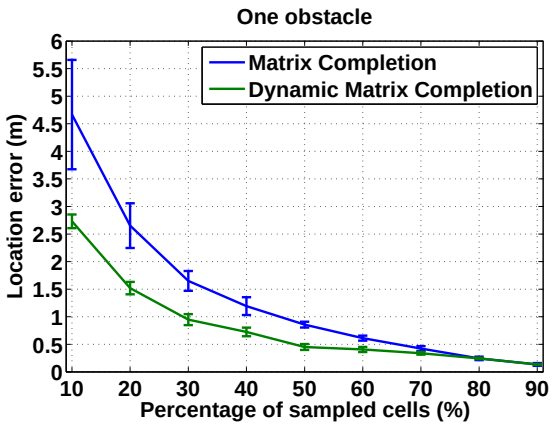

FIGURE 6.5: The location error, during runtime, for 15 APs as a function of the number of visiting cells. Observe that the proposed recalibration technique results in lower location errors.

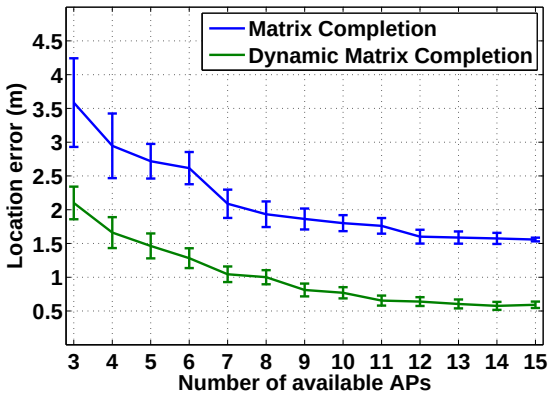

FIGURE 6.7: Location error, during runtime phase, as a function of the total number of available APs. In this experiment, we visit 30% of the cells in the testbed area.

Figures 6.6-6.7 illustrate the performance of the proposed method as a function of the total number of available APs, when the sampling ratio of the received RSS fingerprints is 0.3. The total number of APs that cover the workplace affects the structure of the signature map. Specifically, as the number of APs increases, the accuracy of the proposed technique increases. Indeed, as the number of available APs increases, more correlated RSS fingerprints are produced resulting in a signature map that has an even lower rank relative to its dimensions. Interestingly, the localization performance is not highly affected after a curtain number of APs. Observe that the dynamic MC framework converges faster to the optimum

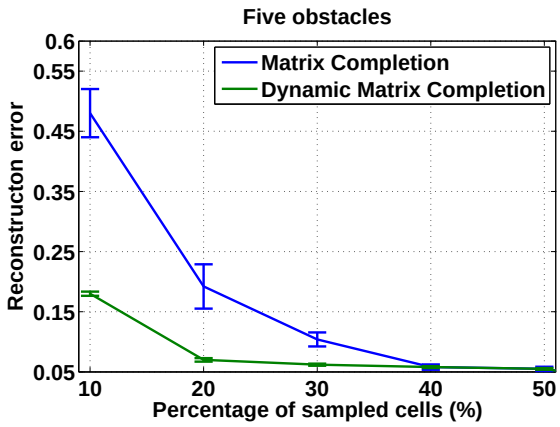

FIGURE 6.8: Reconstruction error as a function of the number of visiting cells in the extreme case scenario of introducing five obstacles at time t. The experiment involves 15 APs. The proposed Dynamic MC results in lower reconstruction errors even in complicated scenarios.

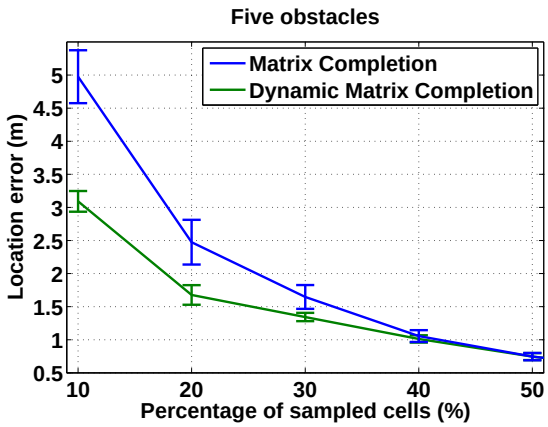

FIGURE 6.9: Location error as a function of the number of visiting cells in the extreme case scenario of introducing five obstacles at time t. The experiment involves 15 APs.

number of APs.

Finally, we investigated the robustness of the proposed recalibration technique under different environmental conditions. For this purpose, we introduced five obstacles in the workspace at time t. Figures 6.8-6.9 demonstrate the reconstruction and the location error, respectively. In this setup, we considered 15 available APs. It is clear that, for complicated scenarios, the dynamic approach results in lower reconstruction and location errors, especially for small sampling ratios. The dynamic MC is affected by the increased noise.

Particularly, we observe that after a certain sampling ratio, the prior information slightly increases the reconstruction accuracy. This behavior is expected in adaptive systems, where previous information becomes less reliable as the noise increases.

6.4 Discussion

In this Chapter, we presented a novel recalibration procedure for RSS fingerprint-based localization systems. The proposed technique, based on space sub-sampling, exploits the inherent spatial correlation structure among the RSS fingerprints, while considering prior information from RSS measurements collected in the past. We relaxed the acquisition and communication requirements while the time required for recalibration was significantly reduced. We adopted a Dynamic Matrix Completion approach to recover the original signature map just from visiting a subset of cells in the area of interest. The experimental results indicated that our Dynamic MC reconstruction method can achieve superior performance when compared to a straight MC technique, in terms of reconstruction error and localization accuracy.

Chapter 7

Conclusions

The purpose of this thesis was to answer a critical question in the exciting field of indoor localization: can we provide efficient localization in non-stationary environments while reducing the network exchanged data both in calibration and location estimation phase. This thesis compromises a study on received signal strength fingerprint based localization techniques as to provide accurate location estimation while reducing the expensive in time and resources calibration phase. Specifically, we focused on sparsity-aware signal processing methods. Sparse recovery is an emerging field that has attracted considerable research interest over the last years and has become a key concept in various areas of computer science. As a consequence, Matrix completion methods attracted our attention in order to recover the partial observed signal strength signatures. Low-rank matrix recovery is a field in its infancy and abounding with interesting and open questions at the information questions at the information-theoretic, the computational and the application level.

Taking advantage of the inherent sparsity appeared of the user's position in the ground plane we reformulated the location estimation as a sparse-approximation problem. Following this formulation we introduced a centralized compressed sensing (CS) signal strength based scheme that considers the runtime signal strength measurements received at the base stations. According to our centralized protocol, all local samples are sent to a central unit to perform sparse signal recovery via the JDCS algorithm. Nevertheless, the centralized JDCS algorithm requires global knowledge of the projection matrices and the runtime measurements and thus is not amenable to distributed implementation. Thus, to eliminate the need of a central unit we proposed a novel fully decentralized cooperative CS localization scheme. The decentralized protocol is based on the joint sparsity of the signal ensemble among the base stations and builds a gossip consensus approach to distribute the location estimation of the mobile user over the network. The centralized and decentralized CS approaches were evaluated on real data collected in the premises of a research institute and revealed a superior performance in terms of localization accuracy at a fraction of the measurements needed by current state of the art methods.

To accelerate the cumbersome procedure of spatially sampling the WiFi RSSI signal during the calibration phase we proposed a combination of a handheld laser-based simultaneous localization, mapping (SLAM), and WiFi localization system based on Sparse Bayesian Learning. Compared to related work the proposed system adopts an automated calibration phase and eliminates the need of projection matrices that were a requisite by the Compressed Sensing localization approaches. However, utilizing a robot in order to minimize the calibration phase is not the most efficient approach for several reasons. Initially, the need of extra hardware introduces additional costs and the applied kinematic metric is sensitive to the presence of people. To overcome these difficulties we introduced an efficient multi-channel localization scheme that exploits the already existed infrastructure and is robust to networking conditions that can cause significant mismatch between training and runtime fingerprints. The proposed multi-channel system eases the acquisition and communication requirements while reducing the time required for calibration. Exploiting the low-rank property of the signature map, the Matrix Completion framework is used to recover the original map from a subset of received training fingerprints. The proposed multi-channel reduced effort calibration technique forms a better signature map from partial information and can be adopted by various fingerprint based localization systems. Concluding this thesis we presented a novel reduced recalibration technique for fingerprint based systems that exploits the spatio-temporal correlation structures of the training signatures and recovers the unobserved measurements via the proposed Dynamic Matrix Completion framework.

This work resulted in several publications:

- S. Nikitaki, G. Tsagatakis and P. Tsakalides, " Efficient Multi-Channel Signal Strength based Localization via Matrix Completion and Bayesian Sparse Learning," IEEE Transactions on Mobile Computing 2013, under revision.
- S. Nikitaki, G. Tsagatakis and P. Tsakalides, "Efficient Recalibration via Dynamic Matrix Completion," to appear in Proc. 23th IEEE International Workshop on Machine Learning for Signal Processing (MLSP2013) , Southampton, UK, Sept. 22-25, 2013.
- S.Nikitaki, P. M.Scholl, K. Van Laerhoven and P.Tsakalides, "Localization in Wireless Networks via Laser Scanning and Bayesian Compressed Sensing," in Proc. 14th IEEE Workshop on Signal Processing Advances in Wireless Communications (SPAWC '13), Darmstadt, Germany, June 16-19, 2013.
- S. Nikitaki and P. Tsakalides, "Decentralized Indoor Wireless Localization Using Compressed Sensing of Signal-Strength Fingerprints," in Proc. 7th ACM Workshop on Performance Monitoring and Measurement of Heterogeneous Wireless and Wired Networks (PM^2HW^2N 2012), Paphos, Cyprus, October 21-25, 2012.
- S. Nikitaki, G. Tsagkatakis, and P. Tsakalides, "Efficient Training for Fingerprint Based Positioning Using Matrix Completion," in Proc. 20th European Signal Processing Conference (EUSIPCO '12),Boucharest, Romania, August 27-31, 2012.
- S. Nikitaki and P. Tsakalides, “Localization in Wireless Networks based on Jointly Compressed Sensing,” in Proc. 19th European Signal Processing Conference (EU-

SIPCO '11), Barcelona, Spain, August 29- September 2, 2011.

- S. Nikitaki and P. Tsakalides, "Localization in Wireless Networks via Spatial Sparsity", in 44th Asilomar Conference on Signals, Systems and Computers, Pacific Grove, CA, November 1-7, 2010.

Chapter 8

Future Work

Indoor localization has empowered a vast number of mobile and pervasive applications. Fingerprint-based methods have gained a lot of attention as they provide accurate estimations by relying on the uniqueness of the signal fingerprints with respect to location. The majority of existing localization techniques rely on Received Signal Strength of wireless signals in order to infer position estimations. However, a vast variety of distributed data sources are common today and generate a wealth of information (*i.e.* surveillance-cameras, proximity sensors, microphones). To this aim, future work will focus on extending our RSS fingerprint approach and incorporating different modalities in order to improve accuracy by means of creating a multi-fingerprint indoor localization system.

Exploiting the spatial sparsity of the user's location compressed sensing localization techniques could be applied in order to minimize the number of measurements exchanged in the network. Incorporating a CS based multimodal localization technique will be beneficial especially in large wireless networks where a great amount of data needs to be exchanged. Additionally, multimodal sensing involves intensive costs on manpower and time, limiting the applicability of a multimodal system especially in large buildings. Thus, in order to encounter this challenge the dynamic matrix completion technique could be extended in a multimodal aspect by exploring the spatio-temporal correlations arising in a non-stationary indoor environment. The key challenge under this scope is to investigate the interdependencies appeared in a heterogeneous network over time. Furthermore, under this framework, future work includes the investigation of the proposed scheme on novel communication protocols that utilize a much larger number of channels in order to increase the communication efficiency.

Next-generation computing paradigms based on multimodal sensing involves the acquisition of massive amount of data that change dynamically over time. Under this framework several challenges need to be addressed including the dynamic data collection and management from multiple sources with the objective to minimize acquisition costs and data recovery in real running time. Additionally, intelligent respond to changing circum-

stances in a non-stationary environment should be implemented in order to deliver online information with minimum latency.

Supporting the real-time intelligent framework, the dynamic matrix completion problem could be accessed in an online version where the entries of the matrix of interest are observed gradually. The objective of online learning is to predict data based on currently received measurements. The key characteristic of on-line learning is that after the prediction is made, the true measurement is discovered. Thus, observing this information could be beneficial to redefine the prediction hypothesis of the proposed technique. Precisely, this involves the extension of our dynamic approach to the sequential prediction context based on the measurements received in the past. Consider the case of online measurements received in a multimodal wireless network. The online dynamic matrix completion approach, based on a small number of observed measurements sensed could perform online prediction based on the most representative measurements from the past.

Bibliography

[1] K. Zickuhr, "Three-quarters of smartphone owners use location-based services," http://www.pewinternet.org/Reports/2012/Location-based-services.aspx/, 2012.

[2] "The global positioning system," *IEEE Transactions on Microwave Theory and Techniques*, vol. 50, no. 3, pp. 645–652, 2002. [Online]. Available: http://ieeexplore.ieee.org/stamp/stamp.jsp?arnumber=989949

[3] Y.-S. Huang and M.-L. Tsai, "The impact of compass/beidou-2 on future gnss: A perspective from asia," in *Proceedings of the 21st International Technical Meeting of the Satellite Division of The Institute of Navigation (ION GNSS 2008)*, 2001, pp. 2227–2238.

[4] G. Lindström and G. Gasparini, *The Galileo satellite system and its security implications*. European Union, Institute for Security Studies, 2003.

[5] K. Chintalapudi, A. P. Iyer, and V. N. Padmanabhan, "Indoor localization without the pain," in *Proc. 16th Int. Conf. Mobile Comput. and Netw.*, Chicago, Illinois, 2010, pp. 173–184.

[6] H. Liu, H. Darabi, P. Banerjee, and J. Liu, "Survey of wireless indoor positioning techniques and systems," *IEEE Trans. Syst. Man Cybern. C, pl. Rev.*, vol. 37, pp. 1067–1080, November 2007.

[7] S. Papadakis and A. Traganitis, "Wireless positioning using the signal strength difference on arrival," in *Proc. IEEE 7th Int. Conf. Mobile Adhoc Sensor Syst.*, San Francisco, CA, 2010, pp. 674–681.

[8] D. Niculescu and B. Nath, "Ad hoc positioning system (aps)," in *Proc. IEEE Global Telecommun. Conf.*, San Antonio, TX, 2001, pp. 2926–2931.

[9] Y. Chen, W. Trappe, and R. Martin, "Attack detection in wireless localization," in *Proc. 26th IEEE Int. Conf. Comput. Commun.*, Anchorage, AK, 2007, pp. 1964–1972.

[10] J. Yang and Y. Chen, "Indoor localization using improved rss-based lateration methods," in *Proc. IEEE Global Telecommun. Conf.*, Honolulu, Hawaii 2009, pp. 1–6.

[11] K. Kaemarungsi and P. Krishnamurthy, "Modeling of indoor positioning systems based on location fingerprinting," in *Proc. 23th IEEE Int.l Conf. Comput. Commun.*, Hong Kong, 2004, pp. 1012–1022.

[12] P. Bahl and V. N. Padmanabhan, "Radar: an in-building rf-based user location and tracking system," in *Proc. IEEE 19th Ann. Conf. Comput. Commun. Soc.*, Tel Aviv, 2000, pp. 775–784.

[13] Y. Ji, S. Biaz, S. Pandey, and P. Agrawal, "Ariadne: a dynamic indoor signal map construction and localization system," in *Proc. ACM MobiSys '06*, Uppsala, Sweden, June 2006.

[14] S. Nikitaki, G. Tsagkatakis, and P. Tsakalides, "Efficient training for fingerprint based positioning using matrix completion," in *Proc. 19th IEEE European Signal Process. Conf.*, Boucharest, 2012, pp. 195–199.

[15] A. H. *et al.*, "Practical robust localization over large-scale 802.11 wireless networks," in *Proc. 10th Ann. Int. Conf. Mobile Comput. Netw.*, 2004, pp. 70–84.

[16] B. Li, J. Salter, A. G. Dempster, and C. Rizos, "Indoor positioning techniques based on wireless lan," in *Proc. 1st IEEE Int. Conf. Wireless Broadband Ultra Wideband Commun.*, Sydney, 2006, pp. 13–16.

[17] X. Chai and Q. Yang, "Reducing the calibration effort for probabilistic indoor location estimation," *IEEE Trans. Mobile Comput.*, vol. 6, pp. 649–662, June 2007.

[18] C. Feng, W. Au, S. Valaee, and Z. Tan, "Received signal strength based indoor positioning using compressive sensing," *IEEE Trans. Mobile Comput*, vol. 11, pp. 1983–1993, December 2012.

[19] M. Atia, A. Noureldin, and M. Korenberg, "Dynamic online-calibrated radio maps for indoor positioning in wireless local area networks," *IEEE Trans. Mobile Comput.*, vol. 99, no. PrePrints, 2012.

[20] R. W. O. *et al.*, "Indoor location estimation with reduced calibration exploiting unlabeled data via hybrid generative/discriminative learning," *IEEE Trans. Mobile Comput.*, vol. 11, pp. 1613–1626, November 2012.

[21] A. Rai, K. Chintalapudi, V. Padmanabhan, and R. Sen, "Zee: Zero-effort crowdsourcing for indoor localization," in *Proc. of the 18th Ann. Int. Conf. on Mobile Comput. and Netw.*, New York, NY, 2012, pp. 293–304.

[22] *Cooperative location-sensing for wireless networks*, 2004.

[23] A. Ladd, K. Bekris, A. Rudys, D. Wallach, and L. Kavraki, "On the feasibility of using wireless ethernet for indoor localization," no. 3, June 2004, pp. 555–559.

[24] F. Seco, A. Jimenez, C. Prieto, J. Roa, and K. Koutsou, "A survey of mathematical methods for indoor localization," in *Intelligent Signal Processing, 2009. WISP 2009. IEEE International Symposium on*, aug. 2009, pp. 9 –14.

[25] T. King, S. Kopf, T. Haenselmann, C. Lubberger, and W. Effelsberg, "Compass: A probabilistic indoor positioning system based on 802.11 and digital compasses," in *Proc. 1st Int. Workshop Wirel. Netw. testbeds, experimental evaluation and characterization*, Los Angeles, CA, 2006, pp. 34–40.

[26] M. Youssef and A. Agrawala, "The horus location determination system," *Wireless Netw.*, vol. 14, pp. 357–374, June 2008.

[27] D. M. *et al.*, "Bayesian indoor positioning systems," in *Proc. IEEE 24th . Int. Conf. Comput. Commun.*, Miami, FL,2005, pp. 1217–1227.

[28] H. S. Fang and T. Lin, "Principal component localization in indoor wlan environments," *IEEE Trans. Mobile Comput.*, vol. 11, pp. 100–110, January 2012.

[29] M. Rabbat, R. Nowak, and J. Bucklew, "Robust decentralized source localization via averaging," in *Proc. IEEE ICASSP '05*, Philadelphia, PA, March 2005.

[30] U. A. Khan, S. Kar, and J. M. F. Moura, "Distributed sensor localization in random environments using minimal number of anchor nodes," *IEE Transactions Signal Processing*, vol. 57, May 2009.

[31] B. Blywis, M. GuÂ¨ andnes, F. Juraschek, and S. Gliech, "A localization framework for wireless mesh networks - anchor-free distributed localization in the des-testbed," in *Indoor Positioning and Indoor Navigation (IPIN), 2010 International Conference on*, sept. 2010, pp. 1 –10.

[32] `http://mesh.nowwireless.com/index.htm`.

[33] X. Zheng, H. Liu, J. Yang, Y. Chen, J. Francisco, R. Martin, and X. Li, "Characterizing the impact of multi-frequency and multi-power on localization accuracy," in *Proc. IEEE 7th Int. Conf. on Mobile Adhoc and Sensor Syst.*, Wuhan, 2010, pp. 156–165.

[34] S. Nikitaki and P. Tsakalides, "Localization in wireless networks via spatial sparsity," in *Proc. 44th Annu. Asilomar Conf. Signals, Syst., Comput.*, Pacific Grove, CA, 2010, pp. 236–239.

[35] E. Candès, J. Romberg, and T. Tao, "Robust uncertainty principles: Exact signal reconstruction from highly incomplete frequency information," vol. 52, no. 2, pp. 489–509, Feb. 2006.

[36] D. Donoho, "Compressed sensing," vol. 52, no. 4, pp. 1289–1306, Apr. 2006.

[37] S. Nikitaki and P. Tsakalides, "Localization in wireless networks based on jointly compressed sensing," in *Proc. 19th IEEE European Signal Process. Conf.*, Barcelona, 2011.

[38] D. M. et al., "Low-dimensional signal-strength fingerprint-based positioning in wireless lans," *Ad Hoc Netw. 2012*.

[39] t. . Elad. M.

[40] B. K. Natarajan, "Sparse approximate solutions to linear systems," *SIAM Journal on Computing*, vol. 24, no. 2, pp. 227–234, Apr. 1995.

[41] F. Alizadeh, F. Alizadeh, D. Goldfarb, and D. Goldfarb, "Second-order cone programming," *Mathematical Programming*, vol. 95, pp. 3–51, 2001.

[42] *On the LASSO and Dantzig selector equivalence*, 2010.

[43] *The Dantzig selector and generalized thresholding*, 2008.

[44] "Decoding by linear programming," vol. 51, no. 12, pp. 4203–4215, 2005. [Online]. Available: http://ieeexplore.ieee.org/stamp/stamp.jsp?arnumber=1542412

[45] D. L. Donoho and M. Elad, "Optimally sparse representation in general (nonorthogonal) dictionaries via 1 minimization," *Proceedings of the National Academy of Sciences*, vol. 100, no. 5, pp. 2197–2202, 2003. [Online]. Available: http://www.pnas.org/content/100/5/2197.short

[46] J. A. Tropp and A. C. Gilbert, "Signal recovery from random measurements via orthogonal matching pursuit," *Information Theory, IEEE Transactions on*, vol. 53, no. 12, pp. 4655–4666, 2007. [Online]. Available: http://ieeexplore.ieee.org/xpls/abs_all.jsp?arnumber=4385788

[47] T. Strohmer and R. W. Heath, "Grassmannian frames with applications to coding and communication," *Applied and computational harmonic analysis*, vol. 14, no. 3, pp. 257–275, 2003.

[48] D. P. Wipf, "Sparse estimation with structured dictionaries," in *Advances in Neural Information Processing Systems 24*, 2011, pp. 2016–2024.

[49] D. Wipf and Y. Wu, "Dual-space analysis of the sparse linear model," *arXiv preprint arXiv:1207.2422*, 2012. [Online]. Available: http://arxiv.org/abs/1207.2422

[50] S. Chen, D. Donoho, and M. Saunders, "Atomic decomposition by basis pursuit," *SIAM Journal Scientific Comput.*, vol. 20, pp. 33–61, 1998.

[51] C. E. and R. J. (2005) ℓ^1-magic : Recovery of sparse signals via convex programming,. [Online]. Available: http://www.acm.caltech.edu/l1magic/

[52] P. L. Combettes and V. R. Wajs, "Signal recovery by proximal forward-backward splitting," *SIAM MMS*, vol. 4, no. 4, pp. 1168–1200, 2005.

[53] E. T. Hale, W. Yin, and Y. Zhang, "A Fixed-Point Continuation Method for l1 -Regularized Minimization with Applications to Compressed Sensing," Rice University, Tech. Rep., Jul. 2007.

[54] T. Blumensath and M. E. Davies, "Gradient pursuits," *IEEE Trans. Signal Proc.*, vol. 56, no. 6, pp. 2370–2382, Junne 2007.

[55] F. M. and R. H., "Iterative thresholding algorithms," *Appl. Comput. Harmon. Anal*, vol. 25, no. 2, p. 187–208, 2008.

[56] T. Blumensath and M. E. Davies, "Iterative thresholding for sparse approximations," *J. of Fourier Anal. and Appl.*, vol. 14, no. 5, p. 629–654, Dec. 2008.

[57] D. Baron, M. b. Wakin, M. F. Duarte, S. Sarvotham, and R. G. Baraniuk, "Distributed compressed sensing," [On-line: www.ee.technion.ac.il/people/drorb/pdf/ DCS012009.pdf].

[58] D. Baron, M. F. Duarte, S. Sarvotham, M. B. Wakin, and R. G. Baraniuk, "An information-theoretic approach to distributed compressed sensing," in *Proc. 45rd Conference on Communication, Control, and Computing*, 2005.

[59] J. A. Tropp, A. C. Gilbert, and M. J. Strauss, "Simultaneous sparse approximation via greedy pursuit," in *Acoustics, Speech, and Signal Processing, 2005. Proceedings.(ICASSP'05). IEEE International Conference on*, vol. 5. IEEE, 2005, pp. v–721. [Online]. Available: http://ieeexplore.ieee.org/xpls/abs_all.jsp?arnumber=1416405

[60] M. F. Duarte, S. Sarvotham, D. Baron, M. B. Wakin, and R. G. Baraniuk, "Distributed compressed sensing of jointly sparse signals," in *Asilomar Conf. Signals, Sys., Comput*, 2005, pp. 1537–1541.

[61] D. P. Wipf and B. D. Rao, "Sparse bayesian learning for basis selection," *Signal Processing, IEEE Transactions on*, vol. 52, no. 8, pp. 2153–2164, 2004. [Online]. Available: http://ieeexplore.ieee.org/xpls/abs_all.jsp?arnumber=1315936

[62] S. Ji, Y. Xue, and L. Carin, "Bayesian compressive sensing," *Signal Processing, IEEE Transactions on*, vol. 56, no. 6, pp. 2346–2356, 2008. [Online]. Available: http://ieeexplore.ieee.org/xpls/abs_all.jsp?arnumber=4524050

[63] L. He and L. Carin, "Exploiting structure in wavelet-based bayesian compressive sensing," *Signal Processing, IEEE Transactions on*, vol. 57, no. 9, pp. 3488–3497, 2009. [Online]. Available: http://ieeexplore.ieee.org/xpls/abs_all.jsp?arnumber=4907073

[64] H. Ishwaran and J. S. Rao, "Spike and slab variable selection: frequentist and bayesian strategies," *Annals of Statistics*, pp. 730–773, 2005. [Online]. Available: http://www.jstor.org/stable/10.2307/3448605

[65] L. Yu, H. Sun, J.-P. Barbot, and G. Zheng, "Bayesian compressive sensing for cluster structured sparse signals," *Signal Processing*, vol. 92, no. 1, pp. 259–269, 2012. [Online]. Available: http://www.sciencedirect.com/science/article/pii/S0165168411002490

[66] M. E. Tipping, "Sparse bayesian learning and the relevance vector machine," *The Journal of Machine Learning Research*, vol. 1, pp. 211–244, 2001. [Online]. Available: http://dl.acm.org/citation.cfm?id=944741

[67] N. Lovmand Pedersen, D. Shutin, C. Navarro Manchón, and B. H. Fleury, "Sparse estimation using bayesian hierarchical prior modeling for real and complex models," 2011. [Online]. Available: http://adsabs.harvard.edu/abs/2011arXiv1108.4324L

[68] D. P. Wipf, "Sparse estimation with structured dictionaries." in *NIPS*, J. Shawe-Taylor, R. S. Zemel, P. L. Bartlett, F. C. N. Pereira, and K. Q. Weinberger, Eds., pp. 2016–2024. [Online]. Available: http://dblp.uni-trier.de/db/conf/nips/nips2011.html#Wipf11

[69] E. Candès and B. Recht, "Exact matrix completion via convex optimization," *ACM Commun.*, vol. 55, no. 6, pp. 111–119, 2012. [Online]. Available: http://doi.acm.org/10.1145/2184319.2184343

[70] B. Recht, M. Fazel, and P. Parrilo, "Guaranteed minimum-rank solutions of linear matrix equations via nuclear norm minimization," *SIAM Rev.*, vol. 52, no. 3, pp. 471–501, August 2010.

[71] M. Grant and S. Boyd, "CVX: Matlab software for disciplined convex programming, version 1.21," 2011.

[72] R. Keshavan, A. Montanari, and S. Oh, "Matrix completion from a few entries," *IEEE Trans. Inf. Theory*, vol. 56, pp. 2980–2998, June 2010.

[73] J. Cai, E. Candès, and Z. Shen, "A singular value thresholding algorithm for matrix completion," *SIAM J. on Optimization*, vol. 20, no. 4, pp. 1956–1982, January 2010.

[74] W. L. Lin Z., Chen M. and M. Y., "The augmented lagrange multiplier method for exact recovery of corrupted low-rank matrices," University of Illinois at Urbana-Champaign, Urbana Champaign, IL, Tech. Rep., 2013.

[75] M. A. Keshavan R. H. and O. S., *Matrix completion from a few entries*. [Online]. Available: arXiv:0901.3150

[76] J. A. Tropp, Anna, and C. Gilbert, "Signal recovery from random measurements via orthogonal matching pursuit," *IEEE Trans. Inform. Theory*, vol. 53, pp. 4655–4666, 2007.

[77] D. Donoho, Y. Tsaig, I. Drori, and J.-L. Starck, "Sparse solution of underdetermined linear equations by stagewise orthogonal matching pursuit."

[78] A. M. Bruckstein, D. L. Donoho, and M. Elad, "From sparse solutions of systems of equations to sparse modeling of signals and images," 2007.

[79] J. Tropp, A. Gilbert, and M. Strauss, "Simultaneous sparse approximation via greedy pursuit," in *Proc. IEEE ICASSP '05*, Philadelphia, PA, March 2005.

[80] T. Rappaport, *Wireless Communications: Principles and Practice*, 2nd ed. Upper Saddle River, NJ, USA: Prentice Hall PTR, 2001.

[81] A. G. Dimakis, S. Kar, J. M. F. Moura, M. G. Rabbat, and A. Scaglione, "Gossip algorithms for distributed signal processing," *CoRR*, 2010.

[82] I. F. Akyildiz, X. Wang, and W. Wang, "Wireless mesh networks: a survey," *Computer Networks*, vol. 47, no. 4, pp. 445 – 487, 2005. [Online]. Available: http://www.sciencedirect.com/science/article/pii/S1389128604003457

[83] K. Kaemarungsi and P. Krishnamurthy, "Properties of indoor received signal strength for wlan location fingerprinting," in *Proc. MOBIQUITOUS '04*, Boston, Massachusetts, August 2004.

[84] D. Bertsekas and J. Tsitsiklis, "Parallel and distributed computation: Numerical methods," Belmont, MA: Athena Scientific, 1997.

[85] S. Boyd, A. Ghosh, B. Prabhakar, and D. Shah, "Randomized gossip algorithms," *Information Theory, IEEE Transactions on*, vol. 52, no. 6, pp. 2508–2530, June 2006.

[86] D. Ustebay, R. Castro, and M. Rabbat, "Efficient decentralized approximation via selective gossip," *IEEE Journal of Selected Topics in Signal Processing*, vol. 5, no. 4, pp. 805–816, August 2011.

[87] S. V. C. Feng, W.S.A. Au and Z. Tan, "Compressive sensing based positioning using rss of wlan access points," in *Proc. IEEE INFOCOM '10*, San diego, CA, March 2010.

[88] S. Kohlbrecher, J. Meyer, O. von Stryk, and U. Klingauf, "A flexible and scalable SLAM system with full 3D motion estimation," in *International Symposium on Safety, Security and Rescue Robotics (SSRR)*, 2011.

[89] M. Boulmalf, T. Aouam, and H. Harroud, "Dynamic channel assignment in ieee 802.11g," in *Int. Wireless Commun. Mobile Comput. Conf.*, Crete, 2008, pp. 864–868.

[90] S. Chieochan, E. Hossain, and J. Diamond, "Channel assignment schemes for infrastructure-based 802.11 wlans: A survey," *IEEE Commun. Surveys Tutorials*, vol. 12, pp. 124–136, 2010.

[91] M. E. Tipping and A. Smola, "Sparse bayesian learning and the relevance vector machine," *Journal of Machine Learning Research*, vol. 1, pp. 211–244, 2001.

[92] M. Tipping, E. and F. A., "Fast marginal likelihood maximisation for sparse bayesian models," in *Proc. of 9th Int. Workshop on Artificial Intell. and Stat.*, Key West, FL, 2003, pp. 3–6.

[93] G. Kalic, I. Bojic, and M. Kusek, "Energy consumption in android phones when using wireless communication technologies," in *Proc. MIPRO International Convention*. IEEE, 2012, pp. 754–759.

[94] N. Balasubramanian, A. Balasubramanian, and A. Venkataramani, "Energy consumption in mobile phones: a measurement study and implications for network applications," in *Proc. ACM SIGCOMM conf. on Internet Measurements*. ACM, 2009, pp. 280–293.

[95] M. Lott and I. Forkel, "A multi-wall-and-floor model for indoor radio propagation," in *Proc. IEEE 54th Vehicular Techn. Conf.*, Atlantic City, 2001, pp. 464–468.

[96] C.-C. Lo, L.-Y. Hsu, and Y.-C. Tseng, "Adaptive radio maps for pattern-matching localization via inter-beacon co-calibration," *Journal on Pervasive Mob. Comput.*, vol. 8, no. 2, pp. 282–291, 2012.